


Attachment 1

Comparison of TN-B1 R1 SAR with RAJ-II R7 SAR Identifying the Changes in the TN-B1 SAR

Section	Changes from RAJ-II R7 SAR
Title Page	GNF RAJ-II changed to AREVA TN-B1; Docket Number changed from 71-9309 to 71-9372; and date changed from 05/04/2009 to FS1-0014159 release date.
Throughout	Changed RAJ-II to TN-B1 where appropriate.
Section 1.1	New first paragraph added to indicate that the only difference between the TN-B1 and the RAJ-II (future state) will be the allowed contents. Fourth paragraph, added complete name of Table 6-2 which was missing in RAJ-II SAR R7.
Section 1.2.3.4.7	Last sentence. Changed Table 6-2 to Section 7.1.2 to correct error. (Table 6-2 does not list quantities, only Section 7.1.2 does).
Section 1.4.1.1	Drawing list changed to list AREVA drawings 02-9162717 and 02-9162722 in place of GNF drawings 105E3744 and 105E3749.
Section 2.0	Added next to last sentence: Since the RAJ-II and TN-B1 structural designs are identical, the RAJ-II tests are completely applicable to the TN-B1 package.
Section 2.6.9	Last equation, added lb units to 3,050 in the parentheses. (Units missing in RAJ-II SAR R7)
Section 2.7.1.4 & 2.7.3	Removed reference to Supplement 1. (AREVA does not have Supplement 1 in its possession and reference to it was removed in RAJ-II SAR R8 by GNF.)
Section 8.1.2	Removed second sentence which applied to the first 10 RAJ-II production units.

IDENTIFICATION	REVISION	AREVA Front End BG Fuel BU 
FS1-0014159	1.0	
TOTAL NUMBER OF PAGES: 400		

**AREVA TN-B1
Docket No. 71-9372
Safety Analysis Report**

ADDITIONAL INFORMATION:

PROJECT	HANDLING	CATEGORY	STATUS	DISTRIBUTION TO	PURPOSE OF DISTRIBUTION
	None	TEP - Technical Report		Larry Tupper Mary Heilman	

ROLES	NAMES	DATES	ORGANIZATIONS	SIGNATURES
AUTHOR	DAVIS James			
REVIEWER	HEINEMAN Jason			
APPROVER	LINK Robert			

RELEASE DATA:

SAFETY RELATED DOCUMENT: Y

CHANGE CONTROL RECORDS: France: N
 This document, when revised, must be reviewed or approved by the following regions: USA: Y
 Germany: N

Exportkennzeichnung AL: N ECCN: 0E001
 Die mit "AL ungleich N" gekennzeichneten Güter unterliegen bei der Ausfuhr aus der EU bzw. innergemeinschaftlichen Verbringung der europäischen bzw. deutschen Ausfuhr genehmigungspflicht. Die mit "ECCN ungleich N" gekennzeichneten Güter unterliegen der US-Reexportgenehmigungspflicht. Auch ohne Kennzeichen, bzw. bei Kennzeichen "AL: N" oder "ECCN: N", kann sich eine Genehmigungspflicht, unter anderem durch den Endverbleib und Verwendungszweck der Güter, ergeben.

Export classification AL: N ECCN: 0E001
 Goods labeled with "AL not equal to N" are subject to European or German export authorization when being exported within or out of the EU. Goods labeled with "ECCN not equal to N" are subject to US reexport authorization. Even without a label, or with label "AL: N" or "ECCN: N", authorization may be required due to the final whereabouts and purpose for which the goods are to be used.



REVISIONS

REVISION	DATE	EXPLANATORY NOTES
1.0	See 1 st page release date	New document

TABLE OF CONTENTS

1.	GENERAL INFORMATION	16
1.1.	INTRODUCTION	16
1.2.	PACKAGE DESCRIPTION	21
1.2.1.	PACKAGING	21
1.2.2.	CONTAINMENT SYSTEM.....	26
1.2.3.	CONTENTS	27
1.2.4.	OPERATIONAL FEATURES	35
1.3.	GENERAL REQUIREMENTS FOR ALL PACKAGES	35
1.3.1.	MINIMUM PACKAGE SIZE	35
1.3.2.	TAMPER-INDICATING FEATURE.....	35
1.4.	APPENDIX	35
1.4.1.	TN-B1 GENERAL ARRANGEMENT DRAWINGS.....	35
2.	STRUCTURAL EVALUATION	55
2.1.	DESCRIPTION OF STRUCTURAL DESIGN	55
2.1.1.	DISCUSSION	55
2.1.2.	DESIGN CRITERIA	56
2.1.3.	WEIGHTS AND CENTERS OF GRAVITY	59
2.1.4.	IDENTIFICATION OF CODES AND STANDARDS FOR PACKAGE DESIGN	59
2.2.	MATERIALS	64
2.2.1.	MATERIAL PROPERTIES AND SPECIFICATIONS.....	64
2.2.2.	CHEMICAL, GALVANIC, OR OTHER REACTIONS.....	67
2.2.3.	EFFECTS OF RADIATION ON MATERIALS.....	68
2.3.	FABRICATION AND EXAMINATION	68
2.3.1.	FABRICATION.....	68
2.3.2.	EXAMINATION	68
2.4.	LIFTING AND TIE-DOWN STANDARDS FOR ALL PACKAGES.....	68
2.4.1.	LIFTING DEVICES	70
2.4.2.	TIE-DOWN DEVICES.....	82
2.5.	GENERAL CONSIDERATIONS	95
2.5.1.	EVALUATION BY TEST.....	95
2.5.2.	EVALUATION BY ANALYSIS	95
2.6.	NORMAL CONDITIONS OF TRANSPORT	96
2.6.1.	HEAT	97
2.6.2.	COLD.....	100
2.6.3.	REDUCED EXTERNAL PRESSURE	100



2.6.4.	INCREASED EXTERNAL PRESSURE.....	101
2.6.5.	VIBRATION	101
2.6.6.	WATER SPRAY.....	101
2.6.7.	FREE DROP.....	101
2.6.8.	CORNER DROP.....	102
2.6.9.	COMPRESSION.....	102
2.6.10.	PENETRATION.....	107
2.7.	HYPOTHETICAL ACCIDENT CONDITIONS.....	109
2.7.1.	FREE DROP.....	109
2.7.2.	CRUSH.....	112
2.7.3.	PUNCTURE.....	112
2.7.4.	THERMAL.....	113
2.7.5.	IMMERSION – FISSILE MATERIAL.....	114
2.7.6.	IMMERSION – ALL PACKAGES.....	114
2.7.7.	DEEP WATER IMMERSION TEST (FOR TYPE B PACKAGES CONTAINING MORE THAN 105 A2).....	114
2.7.8.	SUMMARY OF DAMAGE.....	115
2.8.	ACCIDENT CONDITIONS FOR AIR TRANSPORT OF PLUTONIUM.....	118
2.9.	ACCIDENT CONDITIONS FOR FISSILE MATERIAL PACKAGES FOR AIR TRANSPORT.....	118
2.10.	SPECIAL FORM.....	118
2.11.	FUEL RODS.....	118
2.12.	APPENDIX.....	118
2.12.1.	CERTIFICATION TEST.....	118
2.12.2.	GNF-J CERTIFICATION TESTS.....	137
2.12.3.	OUTER CONTAINER GASKET SEALING CAPABILITY.....	146
3.	THERMAL EVALUATION.....	149
3.1.	DESCRIPTION OF THERMAL DESIGN.....	149
3.1.1.	DESIGN FEATURES.....	149
3.1.2.	CONTENT'S DECAY HEAT.....	150
3.1.3.	SUMMARY TABLES OF TEMPERATURES.....	150
3.1.4.	SUMMARY TABLES OF MAXIMUM PRESSURES.....	150
3.2.	MATERIAL PROPERTIES AND COMPONENT SPECIFICATIONS.....	153
3.2.1.	MATERIAL PROPERTIES.....	153
3.2.2.	COMPONENT SPECIFICATIONS.....	156
3.3.	GENERAL CONSIDERATIONS.....	156
3.3.1.	EVALUATION BY ANALYSIS.....	156
3.3.2.	EVALUATION BY TEST.....	156
3.3.3.	MARGINS OF SAFETY.....	157
3.4.	THERMAL EVALUATION UNDER NORMAL CONDITIONS OF TRANSPORT.....	157
3.4.1.	HEAT AND COLD.....	157

	3.4.2.	MAXIMUM NORMAL OPERATING PRESSURE.....	158
	3.4.3.	MAXIMUM THERMAL STRESSES.....	158
3.5.		THERMAL EVALUATION UNDER HYPOTHETICAL ACCIDENT CONDITIONS.....	159
	3.5.1.	INITIAL CONDITIONS.....	159
	3.5.2.	FIRE TEST CONDITIONS.....	160
	3.5.3.	MAXIMUM TEMPERATURES AND PRESSURE.....	163
	3.5.4.	ACCIDENT CONDITIONS FOR FISSILE MATERIAL PACKAGES FOR AIR TRANSPORT.....	164
3.6.		APPENDIX.....	171
	3.6.1.	REFERENCES.....	171
	3.6.2.	ANSYS INPUT FILE LISTING.....	172
	3.6.3.	NCT TRANSIENT ANALYSIS.....	191
4.		CONTAINMENT.....	198
	4.1.	DESCRIPTION OF THE CONTAINMENT SYSTEM.....	198
		4.1.1. CONTAINMENT BOUNDARY.....	198
		4.1.2. SPECIAL REQUIREMENTS FOR PLUTONIUM.....	198
	4.2.	GENERAL CONSIDERATIONS.....	198
		4.2.1. TYPE A FISSILE PACKAGES.....	198
		4.2.2. TYPE B PACKAGES.....	198
	4.3.	CONTAINMENT UNDER NORMAL CONDITIONS OF TRANSPORT (TYPE B PACKAGES).....	199
	4.4.	CONTAINMENT UNDER FOR HYPOTHETICAL ACCIDENT CONDITIONS (TYPE B PACKAGES).....	199
	4.5.	LEAKAGE RATE TESTS FOR TYPE B PACKAGES.....	200
	4.6.	APPENDIX.....	200
5.		SHIELDING EVALUATION.....	201
6.		CRITICALITY EVALUATION.....	202
	6.1.	DESCRIPTION OF CRITICALITY DESIGN.....	202
		6.1.1. DESIGN FEATURES.....	205
		6.1.2. SUMMARY TABLE OF CRITICALITY EVALUATION.....	206
		6.1.3. CRITICALITY SAFETY INDEX.....	209
	6.2.	FISSILE MATERIAL CONTENTS.....	209
	6.3.	GENERAL CONSIDERATIONS.....	210
		6.3.1. MODEL CONFIGURATION.....	210
		6.3.2. MATERIAL PROPERTIES.....	240
		6.3.3. COMPUTER CODES AND CROSS-SECTION LIBRARIES.....	248
		6.3.4. DEMONSTRATION OF MAXIMUM REACTIVITY.....	249
	6.4.	SINGLE PACKAGE EVALUATION.....	297
		6.4.1. CONFIGURATION.....	297
		6.4.2. SINGLE PACKAGE RESULTS.....	297

6.5.	EVALUATION OF PACKAGE ARRAYS UNDER NORMAL CONDITIONS OF TRANSPORT	299
6.5.1.	CONFIGURATION.....	299
6.5.2.	PACKAGE ARRAY NCT RESULTS	300
6.6.	PACKAGE ARRAYS UNDER HYPOTHETICAL ACCIDENT CONDITIONS	301
6.6.1.	CONFIGURATION.....	301
6.6.2.	PACKAGE ARRAY HAC RESULTS.....	301
6.7.	FUEL ROD TRANSPORT IN THE TN-B1	303
6.7.1.	LOOSE FUEL ROD STUDY	303
6.7.2.	FUEL RODS BUNDLED TOGETHER.....	306
6.7.3.	FUEL RODS TRANSPORTED IN 5-INCH STAINLESS STEEL PIPE	306
6.7.4.	FUEL RODS TRANSPORTED IN STAINLESS STEEL PROTECTIVE CASE.....	310
6.7.5.	SINGLE PACKAGE FUEL ROD TRANSPORT EVALUATION.....	311
6.7.6.	EVALUATION OF PACKAGE ARRAYS WITH FUEL RODS UNDER NORMAL CONDITIONS OF TRANSPORT	313
6.7.7.	FUEL ROD TRANSPORT PACKAGE ARRAYS UNDER HYPOTHETICAL ACCIDENT CONDITIONS.....	315
6.8.	FISSILE MATERIAL PACKAGES FOR AIR TRANSPORT	317
6.9.	CONCLUSION	317
6.10.	BENCHMARK EVALUATIONS	317
6.10.1.	APPLICABILITY OF BENCHMARK EXPERIMENTS	317
6.10.2.	BIAS DETERMINATION.....	318
6.11.	APPENDIX	322
6.11.1.	SINGLE PACKAGE NORMAL CONDITIONS OF TRANSPORT INPUT	322
6.11.2.	SINGLE PACKAGE HYPOTHETICAL ACCIDENT CONDITIONS INPUT	326
6.11.3.	PACKAGE ARRAY NORMAL CONDITIONS OF TRANSPORT INPUT	330
6.11.4.	PACKAGE ARRAY HYPOTHETICAL ACCIDENT CONDITIONS INPUT	334
6.11.5.	SINGLE PACKAGE LOOSE RODS NORMAL CONDITIONS OF TRANSPORT INPUT.....	338
6.11.6.	SINGLE PACKAGE LOOSE FUEL RODS HYPOTHETICAL ACCIDENT CONDITIONS INPUT	341
6.11.7.	PACKAGE ARRAY LOOSE FUEL RODS NORMAL CONDITIONS OF TRANSPORT INPUT.....	344
6.11.8.	PACKAGE ARRAY LOOSE FUEL RODS HYPOTHETICAL ACCIDENT CONDITIONS INPUT.....	347
6.11.9.	DATA TABLES FOR FIGURES IN TN-B1 CSE	351
6.11.10.	SUMMARY OF EXPERIMENTS	369
6.12.	REFERENCES.....	387

7.	PACKAGE OPERATIONS	389
7.1.	PACKAGE LOADING	389
7.1.1.	PREPARATION FOR LOADING	389
7.1.2.	LOADING OF CONTENTS	389
7.1.3.	PREPARATION FOR TRANSPORT	393
7.2.	PACKAGE UNLOADING	393
7.2.1.	RECEIPT OF PACKAGE FROM CARRIER	393
7.2.2.	REMOVAL OF CONTENTS	394
7.3.	PREPARATION OF EMPTY PACKAGE FOR TRANSPORT	395
7.4.	OTHER OPERATIONS	395
7.5.	APPENDIX	396
8.	ACCEPTANCE TESTS AND MAINTENANCE PROGRAM	397
8.1.	ACCEPTANCE TESTS	397
8.1.1.	VISUAL INSPECTIONS AND MEASUREMENTS	397
8.1.2.	WELD EXAMINATIONS	397
8.1.3.	STRUCTURAL AND PRESSURE TESTS	397
8.1.4.	LEAKAGE TESTS	398
8.1.5.	COMPONENT AND MATERIAL TESTS	398
8.1.6.	SHIELDING TESTS	398
8.1.7.	THERMAL TESTS	398
8.1.8.	MISCELLANEOUS TESTS	398
8.2.	MAINTENANCE PROGRAM	398
8.2.1.	STRUCTURAL AND PRESSURE TESTS	398
8.2.2.	LEAKAGE TESTS	399
8.2.3.	COMPONENT AND MATERIAL TESTS	399
8.2.4.	THERMAL TESTS	399
8.2.5.	MISCELLANEOUS TESTS	399
8.3.	APPENDIX	400

LIST OF TABLES

Table 1-1	Maximum Weights and Outer Dimensions of the Packaging.....	24
Table 1-2	Quantity of Radioactive Materials (Type A and Type B).....	28
Table 1-3	Type B Quantity of Radioactive Material.....	29
Table 1-4	Isotopes and A2 Fractions.....	30
Table 1-5	Typical Dimensions of the Main Components of Fuel Assembly and Fuel Rod.....	32
Table 1-6	Example of Fuel Structural Materials.....	33
Table 1-7	Density of Structural Materials.....	33
Table 1-8	Outer Container Drawings.....	36
Table 1-9	Inner Container Drawings.....	37
Table 1-10	Contents Drawings.....	37
Table 2-1	TN-B1 Weight.....	62
Table 2-2	Representative Mechanical Properties of 300 Series Stainless Steel Components.....	65
Table 2-3	Mechanical Properties of Typical Components.....	66
Table 2-4	Properties of 300 Series Stainless Steel.....	69
Table 2-5	Material Properties.....	96
Table 2-6	Thermal Contraction at -40°C.....	99
Table 2-7	Thermal Expansion at 800°C.....	99
Table 2-8	Temperatures.....	107
Table 2-9	Summary of Tests for RAJ-II.....	115
Table 2-10	Test Unit Weights.....	119
Table 2-11	Testing Summary.....	122
Table 2-12	GNF-J CTU Test Series Summary.....	140
Table 2-13	GNF-J CTU Test Series Results.....	141
Table 3-1	Material Properties for Principal Structural/Thermal Components.....	154
Table 3-2	Material Properties for Air.....	155
Table 3-3	Convection Coefficients for Post-fire Analysis.....	165
Table 3-4	Calculated Temperatures for Different Positions on the Walls of the Inner Container Walls.....	166
Table 3-5	Maximum Pressure.....	167
Table 3-6	Material properties.....	195

Table 3-7	NCT Temperatures Through the Package Thickness	196
Table 6-1	TN-B1 Fuel Assembly Loading Criteria	203
Table 6-2	TN-B1 Fuel Rod Loading Criteria.....	205
Table 6-3	Criticality Evaluation Summary	207
Table 6-4	Nominal vs. Worst Case Fuel Parameters for the TN-B1 Criticality Analysis.....	208
Table 6-5	Uranium Isotopic Distribution	209
Table 6-6	TN-B1 Fuel Rod Transport Model Fuel Parameters	233
Table 6-7	Dimensional Tolerances	240
Table 6-8	Material Specifications for the TN-B1.....	241
Table 6-9	TN-B1 Normal Condition Model Fuel Parameters	243
Table 6-10	TN-B1 Normal Condition Model Polyethylene and Water Volume Fractions	243
Table 6-11	Single Package Normal and HAC Model Fuel Parameters	244
Table 6-12	Fuel Assembly Parameters for Polyethylene Mass Calculations.....	246
Table 6-13	Polyethylene Mass and Volume Fraction Calculations.....	246
Table 6-14	TN-B1 Array HAC Fuel Assembly Orientation.....	250
Table 6-15	TN-B1 Shipping Container 14x2x16 Array with Gadolinia- Urania Fuel Rods.....	252
Table 6-16	TN-B1 Sensitivity Analysis for Channeled Fuel Assemblies	256
Table 6-17	TN-B1 Array HAC Worst Case Parameter Fuel Designs.....	264
Table 6-18	TN-B1 Array HAC Part Length Fuel Rod Calculations	281
Table 6-19	TN-B1 Inner Container Thermal Insulator Region and Polyethylene Foam Material Study.....	293
Table 6-20	TN-B1 Inner Container Partially Filled with Moderator	294
Table 6-21	TN-B1 Array Spacing Sensitivity Study	296
Table 6-22	Fuel Rod Pitch Sensitivity Study Results	305
Table 6-23	Fuel Rod Maximum Quantity at Reduced Moderator Densities.....	306
Table 6-24	Results for 8x1x8 Array of Containers with Loose Fuel Rods.....	310
Table 6-25	Results for 4x2x6 Array of Containers with Loose Fuel Rods.....	310
Table 6-26	Data for Figure 6-25 TN-B1 Array HAC Polyethylene Sensitivity.....	351
Table 6-27	Data for Figure 6-26 TN-B1 Fuel Rod Pitch Sensitivity Study	354
Table 6-28	Data for Figure 6-27 TN-B1 Array HAC Pellet Diameter Sensitivity Study.....	355
Table 6-29	Data for Figure 6-28 TN-B1 Array HAC Fuel Rod Clad ID Sensitivity Study.....	356
Table 6-30	Data for Figure 6-29 TN-B1 Array HAC Fuel Rod Clad OD Sensitivity Study.....	357

Table 6-31	Data For Figure 6-37 Moderator Density Sensitivity Study for the TN-B1 HAC Worst Case Parameter Fuel Design	358
Table 6-32	Data for Figure 6-39 TN-B1 Single Package Normal Conditions of Transport Results	359
Table 6-33	Data for Figure 6-40 TN-B1 Single Package HAC Results.....	360
Table 6-34	Data for Figure 6-41 TN-B1 Package Array Under Normal Conditions of Transport Results	361
Table 6-35	Data for Figure 6-42 TN-B1 Package Array Hypothetical Accident Condition Results	362
Table 6-36	Data for Figure 6-45 TN-B1 Fuel Rod Transport in Stainless Steel Pipe	363
Table 6-37	Data for Figure 6-46 TN-B1 Fuel Rod Single Package Under Normal Conditions of Transport	365
Table 6-38	Data for Figure 6-47 TN-B1 Fuel Rod Transport Single Package HAC	366
Table 6-39	Data for Figure 6-48 TN-B1 Package Array Under Normal Conditions of Transport with Loose Fuel Rods	367
Table 6-40	Data for Figure 6-49 TN-B1 Fuel Rod Transport Under HAC	368
Table 6-41	Summary of Information for Experiment.....	370
Table 6-42	Parameters for Benchmark Cases for SCALE 4.4a 44 Group Cross-Section Set	371
Table 6-43	Parameters for Benchmark Cases for SCALE 4.4a 238 Group Cross-Section Set	372
Table 6-44	Urania Gadolinia Experiment Summary ^a	374
Table 6-45	Experimental Parameters for Calculating U-235 and H Atom Densities	375
Table 6-46	Urania Gadolinia Critical Experiment Trending Data	376
Table 6-47	Urania Gadolinia Benchmark k_{eff} Data	377
Table 6-48	Close Proximity Experiment Summary ^a	378
Table 6-49	Close Proximity Experiment Trending Data	379
Table 6-50	Close Proximity Experiment k_{eff} Data	381
Table 6-51	Tightly Packed Configuration Experiment Summary ^a	382
Table 6-52	Tightly Packed Configuration Experiment Trending Data.....	383
Table 6-53	Tightly Packed Configuration Experiment k_{eff} Data	384
Table 6-54	Reduced Density Moderation Experiments Summary and Trending Parameters ^a	385
Table 6-55	Reduced Density Moderation Experiments Trending Data and k_{eff} Data.....	386



LIST OF FIGURES

Figure 1-1 TN-B1 PACKAGE ASSEMBLY 17

Figure 1-2 Cross-Section of Inner Container..... 18

Figure 1-3 Inner Container..... 19

Figure 1-4 Inner and Outer Container 20

Figure 1-5 Shock Absorber Geometry..... 23

Figure 1-6 Example Fuel Rod (Primary Containment)..... 27

Figure 1-7 Protective Case 32

Figure 1-8 Assembly with Optional Packing Materials..... 34

Figure 2-1 Center of Gravity of Package Components..... 63

Figure 2-2 Inner Container Sling Locations..... 88

Figure 2-3 Sling Attachment Plate Detail 89

Figure 2-4 Lifting Configuration of Inner Container..... 89

Figure 2-5 Center of Gravity of Loaded Inner Container 90

Figure 2-6 Hooking Bar of Sling Fitting 91

Figure 2-7 Perforated Plate of Sling Fitting 92

Figure 2-8 Sling Fitting Weld Geometry for Attachment to Support Plate 92

Figure 2-9 Loads on Sling Fitting 93

Figure 2-10 Welds for Support Plate Attachment to Body 93

Figure 2-11 Tie-Down Configuration 94

Figure 2-12 Stacking Arrangement 108

Figure 2-13 Slap-down Orientation 116

Figure 2-14 Puncture Pin Orientation..... 116

Figure 2-15 End Drop Orientation..... 117

Figure 2-16 Inner Container Being Prepared to Receive Mockup Fuel and Added Weight..... 123

Figure 2-17 Partial Fuel Assemblies in CTU 1 124

Figure 2-18 Top End Fittings on Fuel in CTU 1 124

Figure 2-19 Contents of CTU 2..... 125

Figure 2-20 Outer Container without Inner Container..... 125

Figure 2-21 Inner Container Secured in Outer Container 126

Figure 2-22 CTU 2 Prior to Testing 126

Figure 2-23 Addition of Tare Weight to CTU 1 127



Figure 2-24 Addition of Tare Weight to CTU 2 127

Figure 2-25 CTU 1 Positioned for 15° 9-m (30-foot) Slap-down Drop 128

Figure 2-26 Alignment for Oblique Puncture 128

Figure 2-27 Position for Puncture Test..... 129

Figure 2-28 Position for End Drop..... 129

Figure 2-29 Primary Impact End Slap-down Damage 130

Figure 2-30 Secondary Impact End Damage 130

Figure 2-31 Puncture Damage..... 131

Figure 2-32 Close Up of Puncture Damage 131

Figure 2-33 End Impact 132

Figure 2-34 Damage from End Impact (Bottom and Side) 132

Figure 2-35 End Impact Damage (Top and Side)..... 133

Figure 2-36 Damage Inside Outer Container to CTU 1 133

Figure 2-37 Internal Damage to Outer Container CTU 1..... 134

Figure 2-38 Lid Crush on CTU 1 134

Figure 2-39 Damage to Fuel in CTU 1 135

Figure 2-40 Internal Damage to CTU 2..... 135

Figure 2-41 Fuel Damage CTU 2..... 136

Figure 2-42 Fuel Prior to Leak Testing CTU 2..... 136

Figure 2-43 CTU 1J 9 m CG-Over-Bottom Corner Free Drop: View of Impacted Corner 142

Figure 2-44 CTU 1J 9 m CG-Over-Bottom Corner Free Drop: View of Opposite Corner..... 142

Figure 2-45 CTU 1J 9 m CG-Over-Bottom Corner Free Drop: View of Bottom..... 143

Figure 2-46 CTU 1J 9 m CG-Over-Bottom Corner Free Drop: Close-up View of Top
Corner 143

Figure 2-47 CTU 1J 9-m Vertical End Drop: Close-up Side View of Bottom Damage 144

Figure 2-48 CTU 1J 9-m Vertical End Drop: Overall View of Damage 144

Figure 2-49 CTU 2J 9-m Horizontal Free Drop: Close-up Side View of Damage 145

Figure 2-50 CTU 2J 9-m Horizontal Free Drop: Overall Side View of Damage 145

Figure 3-1 Overall View of TN-B1 Package 151

Figure 3-2 Transverse Cross-Sectional View of the Inner Container..... 152

Figure 3-3 Calculated Temperature Evolution During Transient..... 168

Figure 3-4 Calculated Isotherms at the End of Fire Phase (1,800 s)..... 168

Figure 3-5 Calculated Isotherms at 100s After the End of Fire..... 169

Figure 3-6 Calculated Isotherms at 1,468 s After the End of Fire..... 169

Figure 3-7	Calculated Isotherms at 12 hr After the End of Fire	170
Figure 3-8	Vertical Face Model.....	191
Figure 3-9	Comparison Between Energy Equation Solution with a Sine Wave Equation	197
Figure 6-1	Polyethylene Insert (FANP Design)	213
Figure 6-2	Polyethylene Cluster Separator Assembly (GNF Design)	214
Figure 6-3	TN-B1 Outer Container Normal Conditions of Transport Model	215
Figure 6-4	TN-B1 Inner Container Normal Conditions of Transport Model	216
Figure 6-5	TN-B1 Container Cross-Section Normal Conditions of Transport Model.....	217
Figure 6-6	TN-B1 Outer Container Hypothetical Accident Condition Model	222
Figure 6-7	TN-B1 Inner Container Hypothetical Accident Condition Model	223
Figure 6-8	TN-B1 Cross-Section Hypothetical Accident Condition Model	224
Figure 6-9	TN-B1 Hypothetical Accident Condition Model with Fuel Assembly Orientation 1	225
Figure 6-10	TN-B1 Hypothetical Accident Condition Model with Fuel Assembly Orientation 2.....	226
Figure 6-11	TN-B1 Hypothetical Accident Condition Model with Fuel Assembly Orientation 3.....	227
Figure 6-12	TN-B1 Hypothetical Accident Condition Model with Fuel Assembly Orientation 4.....	228
Figure 6-13	TN-B1 Hypothetical Accident Condition Model with Fuel Assembly Orientation 5.....	229
Figure 6-14	TN-B1 Hypothetical Accident Condition Model with Fuel Assembly Orientation 6.....	230
Figure 6-15	TN-B1 Hypothetical Accident Condition Model with Fuel Assembly Orientation 7.....	231
Figure 6-16	TN-B1 Hypothetical Accident Condition Model with Channels	232
Figure 6-17	TN-B1 Fuel Rod Transport Single Package NCT Model	234
Figure 6-18	TN-B1 Fuel Rod Transport Single Package HAC Model.....	236
Figure 6-19	TN-B1 Fuel Rod Transport Package Array NCT Model.....	238
Figure 6-20	TN-B1 Fuel Rod Transport Package Array HAC Model	239
Figure 6-21	Visual Representation of the Clad/Polyethylene Smearred Mixture versus Discrete Modeling.....	245
Figure 6-22	Gadolinia-Urania Fuel Rod Placement Pattern for 10x10 Fuel Assemblies at 5.0 wt% 235U	253
Figure 6-23	Gadolinia-Urania Fuel Rod Placement Pattern for 9x9 Fuel Assemblies at 5.0 wt% 235U	254



Figure 6-24 Gadolinia-Urania Fuel Rod Placement Pattern for 8x8 Fuel Assemblies at 5.0 wt% 235U	255
Figure 6-25 TN-B1 Array HAC Polyethylene Sensitivity	258
Figure 6-26 TN-B1 Fuel Rod Pitch Sensitivity Study	259
Figure 6-27 TN-B1 Array HAC Pellet Diameter Sensitivity Study	260
Figure 6-28 TN-B1 Array HAC Fuel Rod Clad ID Sensitivity Study	261
Figure 6-29 TN-B1 Array HAC Fuel Rod Clad OD Sensitivity Study	262
Figure 6-30 Gadolinia-Urania Fuel Rod Placement Pattern for 10x10 Fuel Assemblies.....	265
Figure 6-31 Gadolinia-Urania Fuel Rod Placement Pattern for 9x9 Fuel Assemblies.....	272
Figure 6-32 Gadolinia-Urania Fuel Rod Placement Pattern for 8x8 Fuel Assemblies.....	277
Figure 6-33 FANP 10x10 Worst Case Fuel Parameters Model with Part Length Fuel Rods.....	287
Figure 6-34 GNF 10x10 Worst Case Fuel Parameters Model with Part Length Fuel Rods.....	288
Figure 6-35 FANP 9x9 Worst Case Fuel Parameters Model with Part Length Fuel Rods	289
Figure 6-36 GNF 9x9 Worst Case Fuel Parameters Model with Part Length Fuel Rods	290
Figure 6-37 Moderator Density Sensitivity Study for the TN-B1 HAC Worst Case Parameter Fuel Design.....	291
Figure 6-38 TN-B1 Inner Container Fuel Compartment Flooding Cases	295
Figure 6-39 TN-B1 Single Package Normal Conditions of Transport Results.....	298
Figure 6-40 TN-B1 Single Package HAC Results	299
Figure 6-41 TN-B1 Package Array Under Normal Conditions of Transport Results.....	300
Figure 6-42 TN-B1 Package Array Hypothetical Accident Condition Results	302
Figure 6-43 Fuel Rod Pitch Sensitivity Study	304
Figure 6-44 TN-B1 with Fuel Rods in 5-Inch Stainless Steel Pipes for Transport.....	307
Figure 6-45 TN-B1 Fuel Rod Transport in Stainless Steel Pipe	308
Figure 6-46 TN-B1 Fuel Rod Single Package Under Normal Conditions of Transport.....	312
Figure 6-47 TN-B1 Fuel Rod Transport Single Package HAC.....	313
Figure 6-48 TN-B1 Package Array Under Normal Conditions of Transport with Loose Fuel Rods.....	314
Figure 6-49 TN-B1 Fuel Rod Transport Under HAC.....	316
Figure 6-50 USL as a Function of Enrichment	321

Glossary of Terms and Acronyms

ASME – American Society of Mechanical Engineers

ASME B&PVC – ASME Boiler and Pressure Vessel Code

ASNT – American Society for Non-destructive Testing

CG – Center of Gravity

CTU – Certification Test Unit

BWR – Boiling Water Reactor

HAC – Hypothetical Accident Condition

IC – Inner Container

IC Inner Thermal Insulator (Aluminum Silicate) – The Alumina Silicate thermal insulation between the inner and outer walls of IC container to provide added margin to criteria set forth for HAC fire condition in 10 CFR 71.73(c)(4)

IC Lid – The lid of the inner container

IC Body – The body of the inner container consisting of the outer wall the thermal insulation, the inner wall, the polyethylene liner and the shock absorbing system along with the fuel securement system

JIS – Japanese Industrial Standards

JSNDI – Japanese Society for Non-destructive Inspection

LDPE – Low Density Polyethylene

NCT – Normal Conditions of Transport

NDIS – Non-destructive Inspection Society

OC – Outer Container

OC Body – The assembly consisting of the OC lower wall, and the internal shock absorbing material

OC Lid – The lid for the outer container.

Packaging – The assembly of components necessary to ensure compliance with packaging requirements as defined in 10 CFR 71.4. Within this SAR, the packaging is denoted as the TN-B1 packaging

Package – The packaging with its radioactive contents, as presented for transportation as defined in 10 CFR 71.4. Within this SAR, the package is denoted as the TN-B1 package.

Payload – Unirradiated fuel assemblies and fuel rods.

RAM – Radioactive Material

SAR – Safety Analysis Report (this document)

TI – Transport Index

USL – Upper Safety Limit

1. GENERAL INFORMATION

This chapter of the Safety Analysis Report (SAR) presents a general introduction and description of the TN-B1 package. The major components comprising the TN-B1 package are presented in Figure 1-1 through Figure 1-4. Detailed drawings presenting the TN-B1 packaging design are included in Appendix 1.4.1. Terminology and acronyms used throughout this document are presented in the Glossary of Terms and Acronyms on page 15. This package is intended to be used to transport Boiling Water Reactor (BWR) fuel assemblies containing both Type A and Type B fissile material.

1.1. Introduction

The model TN-B1 package is derived from the RAJ-II package (NRC CoC 9309) and has the same structural design. The only real difference between the TN-B1 and the RAJ-II will be the allowed contents.

The model TN-B1 package has been developed to transport unirradiated fuel for Boiling Water Reactors. The cladding of the fuel provides the primary containment for the radioactive material. The inner and outer containers provide both thermal protection as well as mechanical protection from drops or accident conditions.

The integrity of the fuel is maintained by the protective outer package, the insulated inner package and the fuel rod cladding through both Normal Conditions of Transport (NCT) and Hypothetical Accident Conditions (HAC) deformations. A variety of full-scale engineering development tests were included as part of the certification process. Ultimately, two full-scale Certification Test Units (CTUs) were subjected to a series of free drops and puncture drops.

The payload within each TN-B1 package consists of a maximum of two unirradiated Boiling Water Reactor (BWR) fuel assemblies or individual rods (BWR, Uranium Carbide, or generic Pressurized Water Reactor (PWR)) contained in a cylinder, protective case or bundled together and positioned in one or both sides of the inner container. See Table 6-1 TN-B1 Fuel Assembly Loading Criteria. See Table 6-2 TN-B1 Fuel Rod Loading Criteria. The containment is provided by the leak tested cladding making up the fuel rods.

The shielding and criticality assessments provided in Chapter 5.0 and Chapter 6.0. The Criticality Safety Index (CSI) for the TN-B1 package is defined in Chapter 6.0.

The TN-B1 package is designed for shipment by truck, ship, or rail as either a Type B(U) fissile material or Type A fissile material package per the definition in 10 CFR 71.4 and 49 CFR 173.403.

Dimensions of the packaging identified in the text, tables, figures, etc. of this SAR, are intended to be nominal. The drawings provided in Appendix 1.4.1 contain the dimensions and the tolerances.

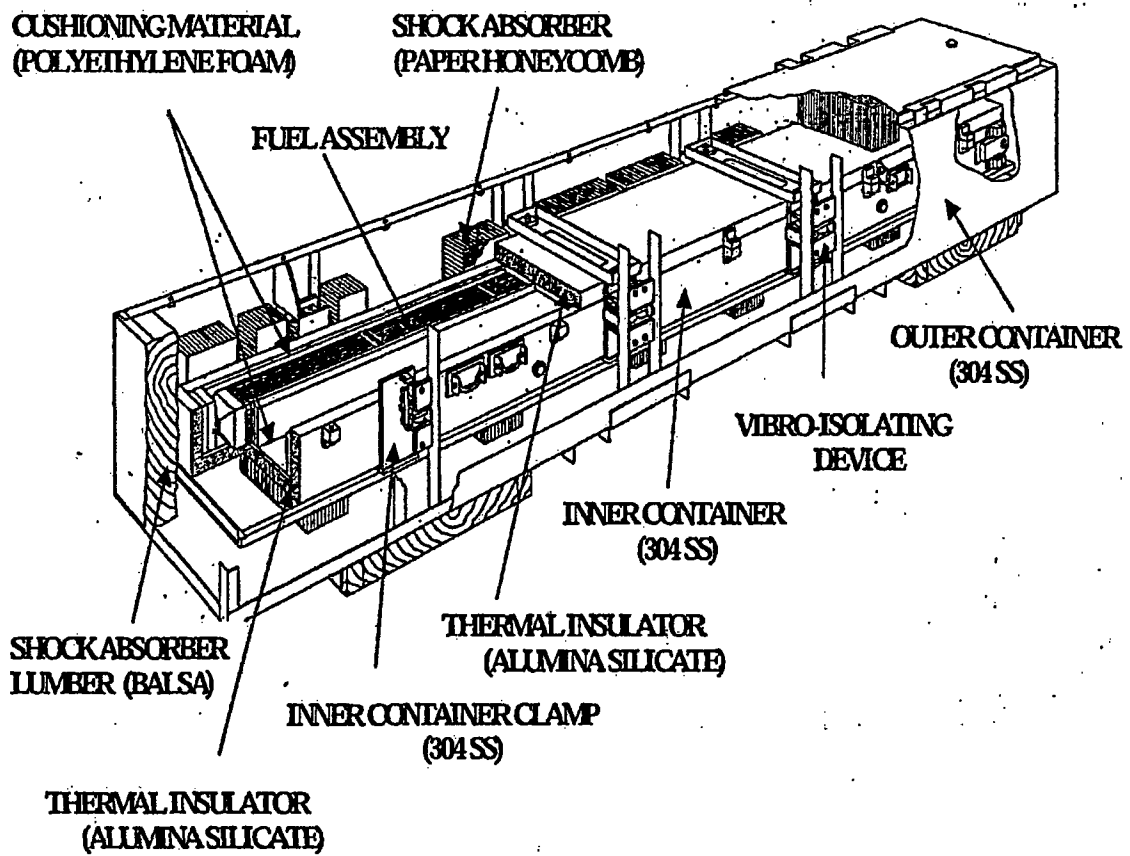


Figure 1-1 TN-B1 PACKAGE ASSEMBLY

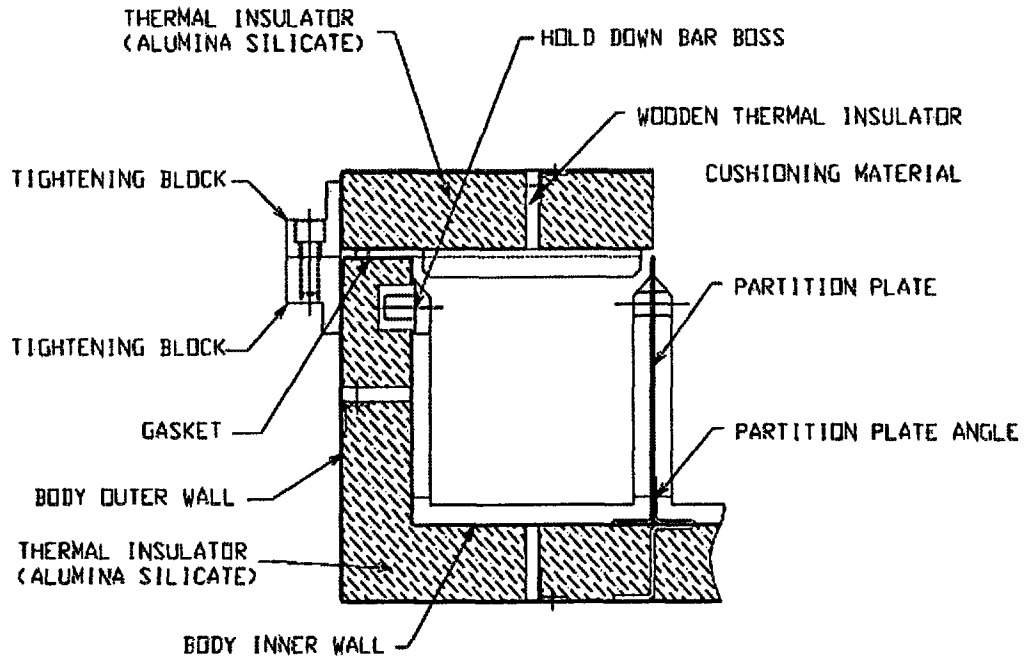


Figure 1-2 Cross-Section of Inner Container

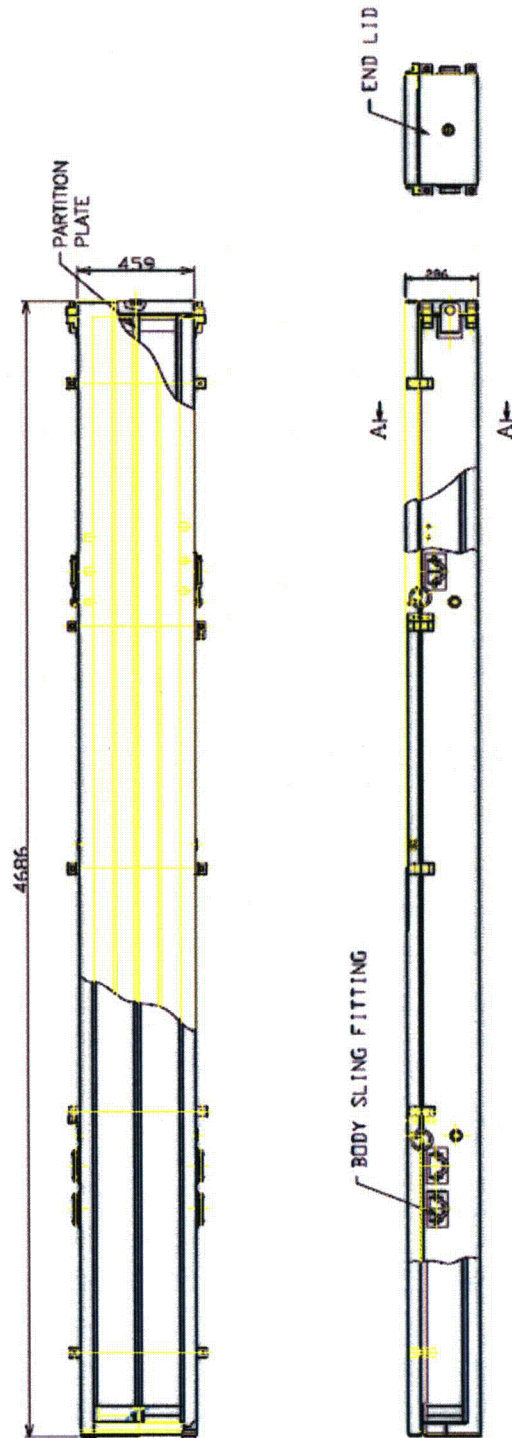


Figure 1-3 Inner Container

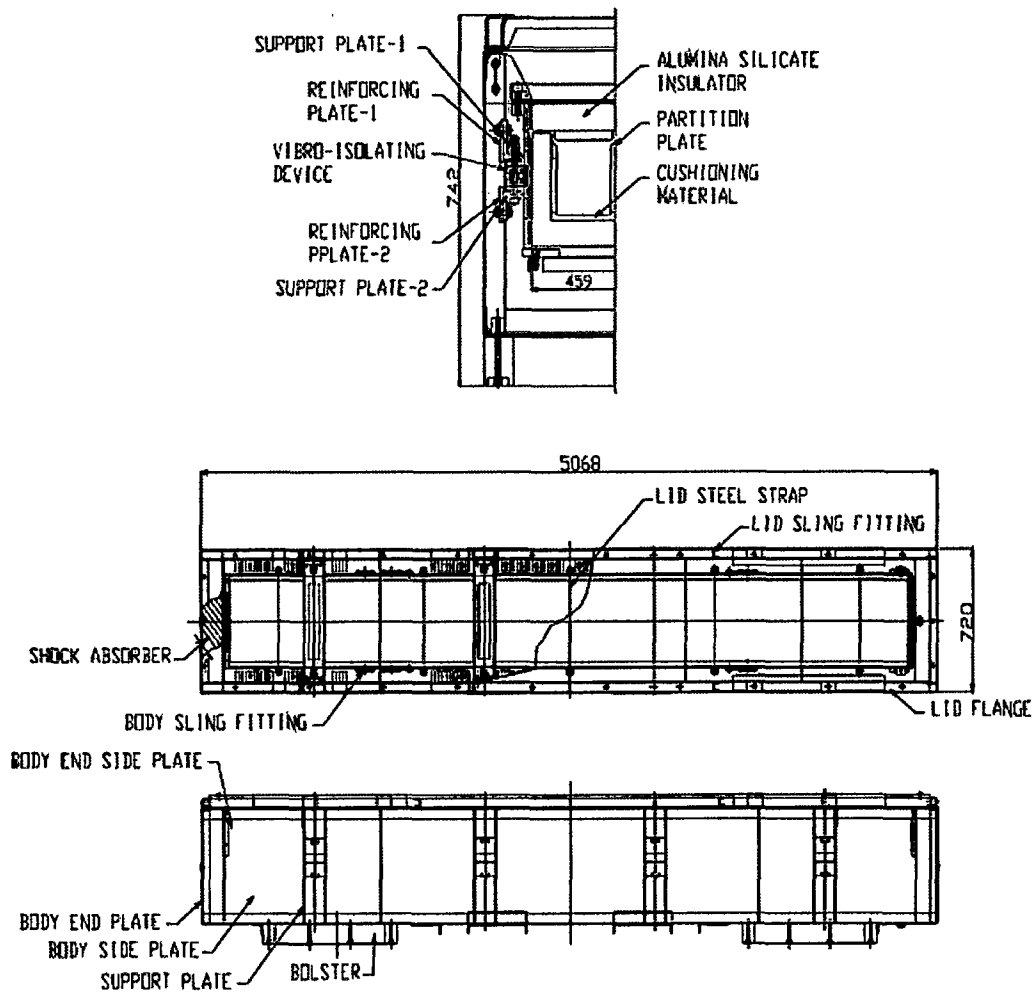


Figure 1-4 Inner and Outer Container

1.2. PACKAGE DESCRIPTION

This section presents a basic description of the model TN-B1 package. General arrangement drawings of the TN-B1 package are presented in Appendix 1.4.1. The Transport Index (TI) for this package is based on shielding and criticality assessments provided in Chapter 5.0 and Chapter 6.0.

1.2.1. *Packaging*

The packaging is comprised of one inner container and one outer container both made of stainless steel. The inner container is comprised of a double-wall stainless steel sheet structure with alumina silicate thermal insulator filling the gap between the two walls to reduce the flow of heat into the contents in the event of a fire. Foam polyethylene cushioning material is placed on the inside of the inner container for protection of the fuel assembly. The outer container is comprised of a stainless steel angular framework covered with stainless steel plates. Inner container clamps are installed inside the outer container with a vibro-isolating device between to alleviate vibration occurring during transportation. Additionally, wood and a honeycomb resin impregnated kraft paper (hereinafter called "paper honeycomb") are placed as shock absorbers to reduce shock due to a drop of the package. In addition to the packaging described above, the fuel rod clad and ceramic nature of the fuel pellets provide primary containment of the radioactive material.

The design details and overall arrangement of the TN-B1 packaging are shown in Appendix 1.4.1 TN-B1 General Arrangement Drawings.

1.2.1.1. Inner Container (IC)

The structure of the inner container is shown in Figure 1-2 and Figure 1-3. The inner container is comprised of three parts: an inner container body, an inner container end lid (removable), and an inner container top lid (removable). These components are fastened together by bolts made of stainless steel through tightening blocks. The inner container body is fitted with six sling fittings and the inner container lid is fitted with four sling fittings as shown in Figure 2-2 Inner Container Sling Locations. The inner container body has a double wall structure made of stainless steel. Its main components are an outer wall, inner wall and alumina silicate thermal insulator.

The outer wall is made of a 1.5 mm (0.0591 in) thick stainless steel sheet formed to a U-shape that constitutes the bottom and sides of the inner container body. A total of 14 stainless steel tightening blocks are attached on the sides of the outer wall, seven per side,

to fasten the inner container lid and the inner container end lid by bolts. Additionally, six stainless steel sling fittings are attached on the sides (three on each side) for handling.

The inner wall of the inner packaging is formed into U-shape with 1.0 mm (0.0391 in) thick stainless steel sheet. The inner packaging is partitioned down the center with 2.0 mm (0.0787 in) thick stainless steel sheet welded to the bottom of the packaging. Foam polyethylene is placed on the inner surface of the inner wall where the fuel assemblies are seated. The void space between the outer and inner steel sheeting is filled with an alumina silicate thermal insulation 48 mm (1.89 in) thick.

1.2.1.2. Outer Container (OC)

The structure of the outer container is shown in Figure 1-4. The outer container is comprised of three parts: a container body, a container lid and inner container hold clamps made of stainless steel and fastened together using stainless steel bolts.

Two tamper-indicating device attachment locations are provided, one on each end, of the outer container.

1.2.1.2.1. *Outer Container Body*

The outer container is made from a series of stainless steel angles (50mm x 50mm x 4mm)(1.97 inch x 1.97 inch x 0.157 inches) that make the framework. Welded to the framework are a bottom plate and side plates made of 2 mm (0.079 inch) thick stainless steel.

Sling holding angles for handling with a crane and protective plates for handling with a forklift are welded on the outside of the container body.

A total of eight sets of support plates are welded on the inside of the outer container body for installing the inner container hold clamps. Additionally, shock absorbers made of 146 mm (5.75 in) wood are attached to each end and paper honeycomb shock absorbers are attached to the bottom and sides for absorbing shock due to a drop. The geometry of the shock absorber is shown in Figure 1-5. The shock absorbers are 157 mm (6.18 in) thick and 108 mm (4.25 in) thick.

1.2.1.2.2. *Outer Container Lid*

The outer container lid is comprised of a lid flange and a lid plate made of stainless steel.

Stainless steel lid sling fittings are welded four places on the top surface of the outer container lid. A paper honeycomb shock absorber, 157 mm (6.18 in) thick by 160 mm (6.30 in) wide and 380 mm (14.96 in) long is attached to the bottom side of the lid similar to the attachment at the bottom of the container.

The outer container lid has holes for bolts in its flange so that it can be fastened to the outer container body by the stainless steel bolts.

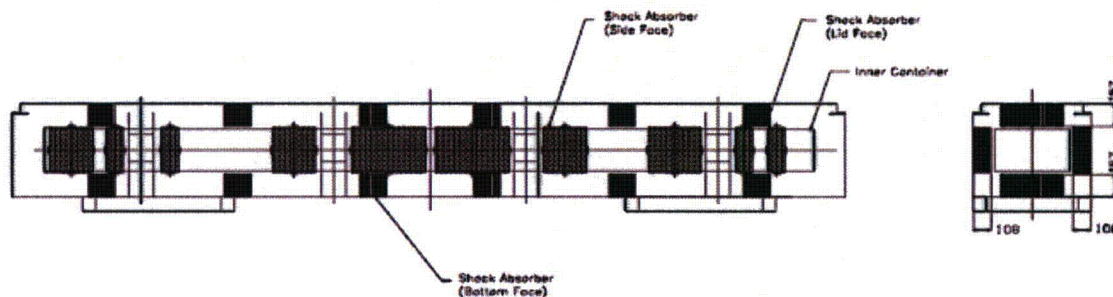


Figure 1-5 Shock Absorber Geometry

1.2.1.2.3. Inner Container Hold Clamp (Located on Outer Container)

The inner container hold clamp consists of an inner container receptacle and a vibro-isolating device.

The inner container receptacle consists of an inner container support plate, a support frame, a bracket and an inner container hold clamp fastener made of stainless steel. The receptacle guides the inner container to the correct position. The inner container receptacle is fitted with the vibro-isolating device through the gusset attached to the bracket.

The vibro-isolating material is attached on the upper and lower side of the gusset. Shock mount fastening bolts go through the center of each piece of vibro-isolating rubber. The bolts at both ends are tightened so that the vibro-isolating rubber pieces press the gusset.

There are four sets (eight pieces) of the vibro-isolating devices mounted on the outer container. Finally, a variety of stainless steel fasteners are used as specified in Appendix 1.4.1.

1.2.1.3. Gross Weight and Dimensions

The maximum gross shipping weight of a TN-B1 package is 1,614 kg (3,558 pounds) maximum. A summary of the major component weights and dimensions are given in Table 1 - 1. A summary of overall component weights is delineated in Table 2 - 1.

Table 1-1 Maximum Weights and Outer Dimensions of the Packaging

Item	Weight and outer dimensions
Maximum weight of inner	308 kg (679 lb)
Maximum weight of outer	622 kg (1,371 lb)
Maximum weight of packaging	930 kg (2,050 lb)
Dimensions of inner container	Length: 4,686 mm (184.49 in) Width: 459 mm (18.07 in) Height: 286 mm (11.26 in)
Dimensions of outer container	Length: 5,068 mm (199.53 in) Width: 720 mm (28.35 in) Height 742 mm (29.21 in) (including bolsters)

1.2.1.4. Materials and Component Dimensions

1.2.1.4.1. *Inner Container*

The materials and component dimensions of the inner container are shown in Appendix 1.4.1.

1.2.1.4.2. *Outer Container*

The materials and component dimensions of the outer container are shown in Appendix 1.4.1.

1.2.1.5. Criticality Control Features

The TN-B1 package does not require specific design features to provide neutron moderation and absorption for criticality control. The contents of the package rely on gadolinia loading for criticality control based on enrichment. Gadolinia loading requirements are provided in Table 6-1 TN-B1 Fuel Assembly Loading Criteria. There are no spacers required for criticality control. Fissile materials in the payload are limited to an amount that ensures safely sub-critical packages for both NCT and HAC. Further discussion of criticality control features is provided in Chapter 6.0.

1.2.1.6. Heat Transfer Features

The unirradiated fuel has negligible decay heat, therefore, the TN-B1 package is not designed for dissipating heat. The packaging is designed to protect the fuel and its containment by providing containment during the Hypothetical Accident Conditions (HAC). A more detailed discussion of the package thermal characteristics is provided in Chapter 3.0

1.2.1.7. Coolants

Due to the passive design of the TN-B1 package with regard to heat transfer, there are no coolants utilized within the TN-B1 package.

1.2.1.8. Protrusions

The only significant protrusions on the TN-B1 packaging exterior are those associated with the lifting features on the outer container exterior. These are the sling holding angles and the bolsters at the bottom of the packaging. The bolsters protrude the furthest at 80 mm (3.15 in).

The only significant protrusions on the inner container exterior are the lifting sling fittings and the tightening blocks that are used for securing the lid. There are lifting sling fittings on the body and the main lid. Each of the sling fittings fold down so they protrude only the thickness of the lifting rod or bail.

1.2.1.9. Lifting and Tie-down Devices

The lifting devices for the TN-B1 consist of the sling holding angles on the outer container which keep the slings from moving when used to sling the container during handling. The loaded container is designed to use four slings that form basket hitches under the

container. The empty container is handled with two slings. The package may also be handled by the use of a forklift. The sling hold angles are designed so that even if they failed it would not affect the performance of the package.

The inner container is handled by the use of a series of lifting sling fittings. They are attached in a manner that even if they fail it will not compromise the performance of the inner container. On both the inner and outer containers, the lid lifting devices are marked to ensure proper use. A detailed discussion of lifting and tie-down designs, with corresponding structural analyses, is provided in Section 2.4.1 and 2.4.2.

1.2.1.10. Shielding

Due to the nature of the unirradiated fuel payload, no biological shielding is necessary or provided by the TN-B1 packaging.

1.2.1.11. Packaging Markings

The packaging will be marked with its model number, serial number, gross weight and also with the package identification number assigned by the NRC.

1.2.2. **Containment System**

The containment system components are identified above in Section 1.2.1 and accompanying figures. The primary containment boundary of this package is the fuel rod cladding as shown in example Figure 1-6 Example Fuel Rod (Primary Containment). The fuel rod is completed by loading the uranium dioxide pellets into a zirconium alloy cladding tube. The tubes are pressurized with helium and zirconium end plugs are welded to the tube which effectively seals and contains the radioactive material. Welds of the fuel rods are verified for integrity by such means as X-ray inspection, ultrasonic testing, or process control. A representative nominal internal pressure of fuel rods at room temperature conditions is 1.1 MPa (160 psia) (absolute pressure). The TN-B1 package cannot be opened unintentionally. Both the OC and IC lids are attached to their respective bodies with socket-headed cap screws. There are twenty-four bolts holding the outer lid in place. There are no other openings in the outer container. The inner container has ten bolts holding the main lid in place and four bolts holding the end closure in place. Thus, the requirements of 10 CFR 71.43(c) are satisfied.

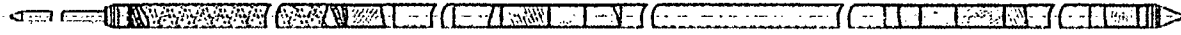


Figure 1-6 Example Fuel Rod (Primary Containment)

1.2.2.1. Pressure Relief System

There are no pressure relief systems included in the TN-B1 package design to relieve pressure from within either the inner or outer containers or the fuel rod. Fire-consumable fusible plugs are used on the exterior surface of both the outer and inner containers to prevent pressure build up from the insulating and shock absorbing material during a fire event. These fusible plugs may be made of plastic. Two plugs are installed in the outer container body and two in the outer container lid. Four are installed in the inner container body, one in the end lid and two in its main lid.

1.2.3. *Contents*

A maximum of two fuel assemblies are placed in each packaging, see Table 6-1. The packaging is designed and analyzed to ship fuel configured either in 8x8, 9x9 or 10x10 arrays or as loose rods contained in a cylinder, protective case or positioned in one or both sides of the inner container, see Table 6-2. Fuel assemblies may also be shipped in the BWR fuel channel. The nuclear fuel pellets located in rods and contained in the packaging are uranium oxides primarily as UO_2 and U_3O_8 . The fuel assembly average enrichment is less than or equal to 5.0% U-235 (the fuel rod maximum enrichment is less than or equal to 5.0% U-235). In addition to the shipment of fuel assemblies, Section 1.2.3.4.5, Section 1.2.3.4.6 and Section 1.2.3.4.7 describe contents configurations for shipping individual fuel rods not contained in a fuel assembly.

Where fuel rods are referenced as being loaded with uranium dioxide mixed with gadolinium oxide (hereinafter gadolinia) the pellets in the gadolinia fuel rods contain a minimum of 2.0% gadolinium.

1.2.3.1. Type A contents

Where the contents of the packaging is commercial grade uranium or other uranium materials where the A2 value is not exceeded, the packaging may be considered to contain Type A quantities.

1.2.3.2. Type B contents

Where the contents of the packaging is enriched reprocessed uranium or other origin uranium not exceeding the values in Table 1-3, the packaging is considered to contain Type B quantities.

1.2.3.3. Quantity of Radioactive Materials of Main Nuclides

Where the content of the packaging consists of Type B quantities of material, the main nuclides are treated as shown in Tables 1-2 through 1-4 to calculate total activity, activity fractions and A₂ for the mixture.

Table 1-2 Quantity of Radioactive Materials (Type A and Type B)

Fuel assembly	Type 8×8 fuel assembly	Type 9×9 fuel assembly	Type 10 x10 fuel assembly
Main nuclides	Low enriched uranium less than or equal to 5% U-235	Low enriched uranium less than or equal to 5% U-235	Low enriched uranium less than or equal to 5% U-235
State of uranium	Uranium oxide ceramic pellet (Solid)	Uranium oxide ceramic pellet (Solid)	Uranium oxide ceramic pellet (Solid)
Fuel assembly average enrichment (Fuel rod maximum enrichment)	5.0% maximum (5.0% maximum)	5.0% maximum (5.0% maximum)	5.0% maximum (5.0% maximum)
Number of fuel rods containing gadolinia	See Table 6-1	See Table 6-1	See Table 6-1
Weight of uranium dioxide pellets (per fuel assembly)	235 kg	240 kg	275 kg

Table 1-3 Type B Quantity of Radioactive Material

Isotope	Maximum content ¹	Maximum mass, g	Specific Activity ² , TBq/g	Total Activity, TBq	Total Activity, Ci
U-232	2.00E-09 g/gU	9.68E-04	0.83	8.03E-04	2.17E-02
U-234	2.00E-03 g/gU	9.68E+02	2.30E-04	2.23E-01	6.02E+00
U-235	5.00E-02 g/gU	2.42E+04	8.00E-08	1.94E-03	5.23E-02
U-236	2.50E-02 g/gU	1.21E+04	2.40E-06	2.90E-02	7.85E-01
U-238	9.23E-01 g/gU	4.47E+05	1.20E-08	5.36E-03	1.45E-01
Np-237	1.66E-06 g/gU	8.03E-01	2.61E-05	2.10E-05	5.67E-04
Pu-238	6.20E-11 g/gU	3.00E-05	6.33E-01	1.90E-05	5.13E-04
Pu-239	3.04E-09 g/gU	1.47E-03	2.3E-03	3.38E-06	9.15E-05
Pu-240	3.04E-09 g/gU	1.47E-03	8.40E-03	1.24E-05	3.34E-04
Gamma Emitters	5.18E+05 MeV-Bq/kgU	N/A	N/A	2.51E-02	6.78E-01
Total				2.85E-01	7.70E+00

1. Based on a maximum payload of 275 kg UO₂ per assembly, 242 kg U (550 kg UO₂, 484 kg U total)
2. 10CFR71, Appendix A
3. Assuming gamma energy of 0.01 MeV to maximize total content.

Table 1-4 Isotopes and A2 Fractions

Isotope	Maximum Radioactivity content (Ci)	10CFR71 A ₂ per isotope (Ci)	Activity Fraction	A ₂ Fraction
U-232	2.17E-02	0.0027	2.82E-03	1.04E-01
U-234	6.02E+00	0.1600	7.81E-01	4.88E+00
U-235	5.23E-02	Unlimited	NA	NA
U-236	7.85E-01	0.1600	1.02E-01	6.37E-01
U-238	1.45E-01	Unlimited	NA	NA
Np-237	5.67E-04	0.0540	7.36E-05	1.36E-03
Pu-238	5.13E-04	0.0270	6.67E-05	2.47E-03
Pu-239	9.15E-05	0.0270	1.19E-05	4.40E-04
Pu-240	3.34E-04	0.0270	4.34E-05	1.61E-03
Gamma Emitters	6.78E-01	0.5400	8.80E-02	1.63E-01
Total	7.70E+00		Sum of A₂ fractions	5.79E+00
Mixture A₂				0.17 Ci

1.2.3.4. Physical Configuration

1.2.3.4.1. *Fuel Assembly*

The configuration of typical fuel assemblies is shown in Figure 1-8 Fuel Assembly with Optional Packing Materials. The fuel assemblies may be of various model and type as long as they meet the requirements listed. The dimensions of the main components in the fuel assemblies are listed in Table 1 - 5. The maximum weight of contents including fuel and packing material is 684 kg (1,508 lb).

1.2.3.4.2. *Chemical Properties*

Example of structural materials of the fuel assembly is shown in Table 1 - 6. Zirconium alloy, stainless steel and Ni-Cr-Fe alloy are chemically stable materials, and they are excellent in heat resistance and corrosion resistance.

1.2.3.4.3. *Density of Materials*

The density for the fuel assembly materials is presented in Table 1 - 7.

1.2.3.4.4. *Packing Materials*

A number of packing materials may be used to guard the fuel assembly (e.g., cluster separators, and polyethylene bags). An example of the packing materials and their use is shown in Figure 1-8.

1.2.3.4.5. *Bundled Fuel Rods*

In addition to the fuel assembly configuration described above, fuel rods may be shipped bundled together in groups of rods up to 25 total rods. Fuel rods are fixed together using ring clamps. The criticality safety case for loose rods that shows that as many as 25 fuel rods per side can be arranged in any configuration within the volume of the inner container. Based on this criticality safety analysis the ring clamps are not relied on or needed for maintaining the configuration of the fuel rods.

1.2.3.4.6. *Fuel Rods In a 5-Inch Pipe*

Another physical configuration is the use of a 5-inch diameter schedule 40 stainless steel pipe. The physical configuration of the pipe is shown in drawing 0028B98. The number of fuel rods shipped in this configuration is limited by the quantities in Section 7.1.2. See Section 6.3.1.3.1 and 6.3.1.3.2 for other descriptions of the pipe.

1.2.3.4.7. *Fuel Rods in a Protective Case*

Figure 1-7 shows the configuration of the protective case. The protective case is a stainless steel box comprised of a body, lid, wood spacer absorber and end plate. In addition to the figure below, detailed drawings of the protective case are provided in Appendix 1.4.1. The protective case is surrounded by polyurethane foam cushioning material, which provides a snug fit within the inner container. Depending on the rod type, the protective case may be used to transport any number of authorized fuel rods up to a maximum of 30 rods. See Section 7.1.2.

Security-Related Information
Figure Withheld Under 10 CFR 2.390

Figure 1-7 Protective Case

Table 1-5 Typical Dimensions of the Main Components of Fuel Assembly and Fuel Rod

Item	Dimensions (mm)		
Type of fuel assembly	Boiling Water Reactor		
Fuel assembly full length	Up to 4,480		
Maximum cross-section of fuel assembly	134 x 134		
Fuel rod length	Up to 4,480 and includes partial rods		
Type	8x8	9x9	10x10
Maximum effective fuel length	3,810	3,810	3,850
Wall thickness of cladding tube	0 – 2.06	0 – 1.70	0 – 2.21
Fuel pellet diameter	9.0-10.7	9.2-9.6	8.28-9.2
Fuel Rod OD	10.72-12.50	9.60-11.2	10.0-11.21
Cladding ID	10.44-12.19	9.5-11.1	8.80-10.33

Table 1-6 Example of Fuel Structural Materials

Component parts	Structural materials
Pellets	Uranium dioxide sintered (in some cases uranium dioxide blended with gadolinia)
Cladding tube	Zirconium alloy, metallic zirconium
Internal spring	Stainless steel
Getter	Zirconium alloy and stainless steel
Upper and Lower end plug	Zirconium alloy
Water rod	Zirconium alloy
Upper and Lower tie plate	Stainless steel
Spacer	Zirconium alloy and Ni-Cr-Fe alloy (Inconel X-750)
Finger spring	Ni-Cr-Fe alloy
Expansion spring	Ni-Cr-Fe alloy
Nut	Stainless steel
Locking tab washer	Stainless steel

Table 1-7 Density of Structural Materials

Main structural materials	Density
Zirconium alloy metallic zirconium	Approximately 6.5 g/cm ³ (0.235lb/in ³)
Uranium dioxide pellet	Approximately 10.4 g/cm ³ (0.376 lb/in ³)
Stainless steel	Approximately 7.8 g/cm ³ (0.282 lb/in ³)
Ni-Cr-Fe alloy	Approximately 8.5 g/cm ³ (0.307 lb/in ³)

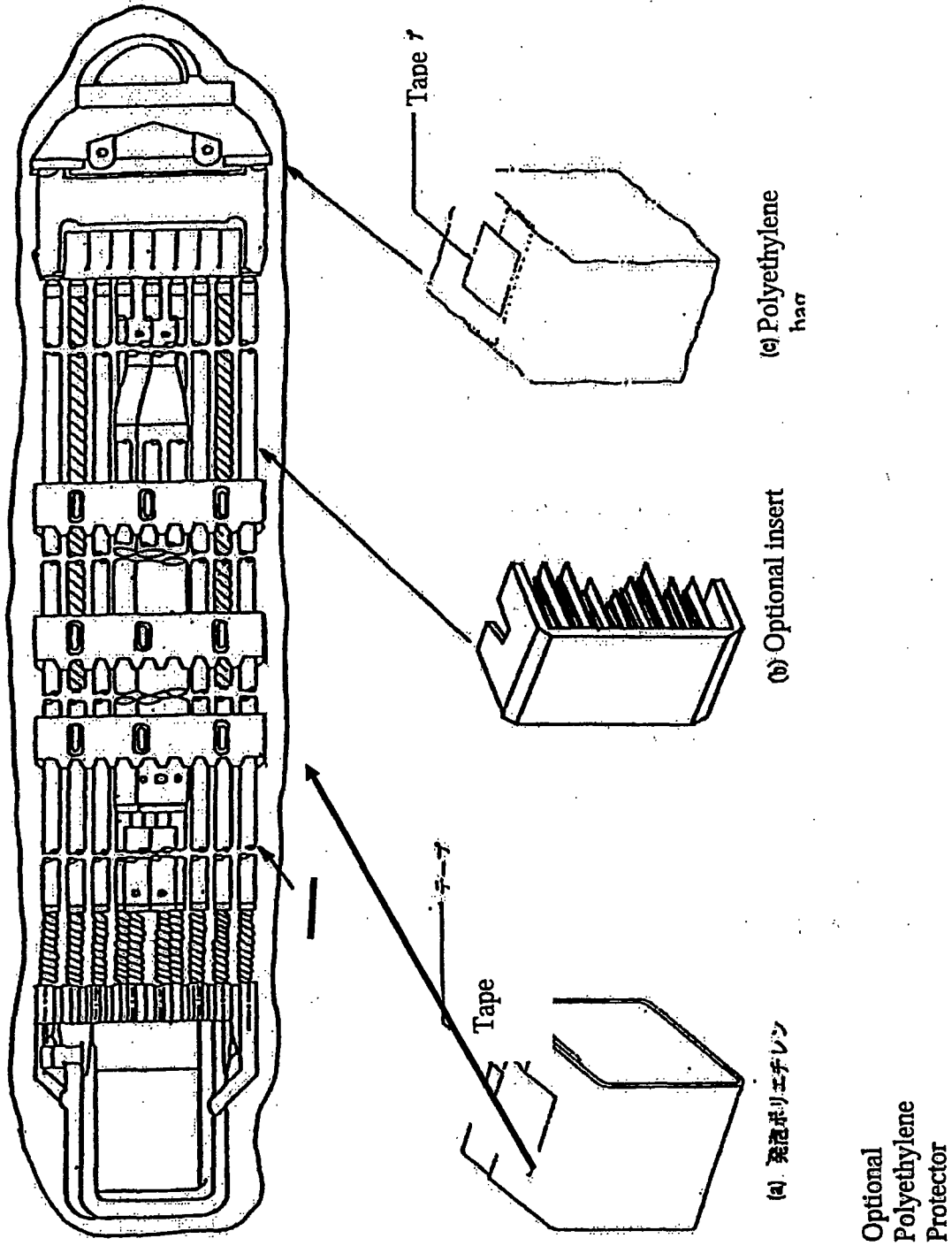


Figure 1-8 Assembly with Optional Packing Materials

1.2.4. Operational Features

The TN-B1 packaging is not considered operationally complex. Operational features are readily apparent from an inspection of the drawings provided in Appendix 1.4.1 and the previous discussions presented in Section 1.2.1. Operational procedures and instructions for loading, unloading, and preparing empty TN-B1 packages for transport are provided in Chapter 7.0

1.3. GENERAL REQUIREMENTS FOR ALL PACKAGES

1.3.1. Minimum Package Size

The TN-B1 package is a rectangular box that is 742 mm (29.21 in) high by 720 mm (28.35 in) wide by 5,068 mm (199.53 inches) long. Thus, the requirement of 10 CFR 71.43(a) is satisfied.

1.3.2. Tamper-Indicating Feature

Seal pins are provided at each end of the outer container body and lid for the use of tamper indicating seals. A tamper indicating seal is attached at each end of the loaded outer container by inserting the seal through the holes in the body and lid seal pins and securing the seal. The tamper indicating seal is not readily breakable and would provide evidence of tampering or opening by an unauthorized person. Thus, the requirement of 10 CFR 71.43(b) is satisfied.

1.4. APPENDIX

1.4.1. TN-B1 General Arrangement Drawings

This section presents the TN-B1 packaging general arrangement drawing consisting of 15 drawings entitled, *TN-B1 SAR Drawing*, see drawing list below. Within the packaging general arrangement drawing, dimensions important to the packaging safety are dimensioned and toleranced. Other dimensions are provided as a reference dimension, and are toleranced in accordance with the JIS (Japan Industrial Std.) B 0405. See 2.1.4.1 and 2.1.4.2.

1.4.1.1. Drawing List**Table 1-8 Outer Container Drawings**

Drawing number	Number of Sheets	Revision #	Name
105E3737	1	6	Outer/Inner Container Assembly Licensing Drawings
105E3738	2 (Sheets 1&2)	8	Outer Container Main Body Assembly Licensing Drawings
105E3738	1 (Sheet 3)	7	Outer Container Main Body Assembly Licensing Drawing
105E3739	1	4	Outer Container Fixture Assembly Licensing Drawings
105E3740	1	4	Outer Container Fixture Assembly Installation Licensing Drawings
105E3741	1	1	Outer Container Shock Absorber Assembly Licensing Drawings
105E3742	1	3	Outer Container Bolster Assembly Licensing Drawings
105E3743	1	5	Outer Container Lid Assembly Licensing Drawings
02-9162717	1	1	Outer Container Marking Licensing Drawings

Table 1-9 Inner Container Drawings

Drawing number	Number of Sheets	Revision #	Name
105E3745	4	8	Inner Container Main Body Assembly Licensing Drawings
105E3746	1	1	Inner Container Parts Assembly Licensing Drawings
105E3747	1	4	Inner Container Lid Assembly Licensing Drawings
105E3748	1	2	Inner Container End Lid Assembly Licensing Drawings
02-9162722	1	1	Inner Container Marking Licensing Drawings

Table 1-10 Contents Drawings

Drawing number	Number of Sheets	Revision #	Name
105E3773	1	1	Protective Case
0028B98	1	1	Shipping Container Loose Fuel Rods

N° FS1-0014159

Rev. 1.0

Handling: None

Page 38/400

AREVA TN-B1
Docket No. 71-9372
Safety Analysis Report



Security-Related Information

Figure Withheld Under 10 CFR 2.390

SAFETY-RELATED CLASSIFICATION CODE (S)	
CLASSIFICATION	SECRET
CONTROL	RESTRICTED
DATE OF REVIEW	01-14-03
DATE OF EXPIRY	01-14-03
DATE OF REVIEW	01-14-03
DATE OF EXPIRY	01-14-03
REVIEWED BY	RAJ-8 OUTER/INNER CONTAINER ASSEMBLY LOCKING DRAWING
APPROVED BY	105E3737
1. NAME DRAWING	105E3737
2. NAME DRAWING	105E3737
3. NAME DRAWING	105E3737

Security-Related Information
Figure Withheld Under 10 CFR 2.390

REV	DATE	DESCRIPTION	BY	CHKD
1	05/16/01	ISSUED FOR CONSTRUCTION
2	05/16/01
3	05/16/01
4	05/16/01
5	05/16/01
6	05/16/01
7	05/16/01
8	05/16/01
9	05/16/01
10	05/16/01
11	05/16/01
12	05/16/01
13	05/16/01
14	05/16/01

RAJ-4 OUTER CONTAINER
 MAIN BODY ASSEMBLY
 LOCKING DRAWING
 105E37.M
 05/16/01

Security-Related Information
Figure Withheld Under 10 CFR 2.390

Security-Related Information
Figure Withheld Under 10 CFR 2.390

N° FS1-0014159

Rev. 1.0

Handling: None

Page 42/400

AREVA TN-B1
Docket No. 71-9372
Safety Analysis Report

A
AREVA

Security-Related Information
Figure Withheld Under 10 CFR 2.390

SECURITY-RELATED INFORMATION	
CLASSIFICATION	CONFIDENTIAL
DATE OF CLASSIFICATION	10/23/99
CLASSIFIED BY	102E3739
REVIEWED BY	
REVIEW DATE	
REVISIONS	
1. PLAN NUMBER	102E3739
2. PLAN TITLE	102E3739
3. PLAN DATE	
4. PLAN REVISION	

AREVA - Fuel BU

Security-Related Information
Figure Withheld Under 10 CFR 2.390

SAFETY-RELATED CLASSIFICATION CODE (S)	
CLASSIFICATION	TOP SECRET
CONTROL	RESTRICTED TO OFFICIALS OF THE U.S. GOVERNMENT
EXEMPTION	EXEMPT FROM AUTOMATICALLY DECLASSIFYING
EXEMPTION CODE	25X(1)
EXEMPTION AUTHORITY	105E3740
EXEMPTION DATE	02/27/2011
EXEMPTION REVIEW DATE	02/27/2011
EXEMPTION REVIEW BY	02/27/2011

Security-Related Information
Figure Withheld Under 10 CFR 2.390

SAFETY-RELATED CLASSIFICATION CODE	
CLASSIFICATION	SECRET
DATE OF REVIEW	03/15/01
REVIEWED BY	105E3741
REASON FOR REVIEW	REVIEW OF OUTER CONTAINER SHOCK ASSEMBLY DRAWING
REVIEWED BY	105E3741
REASON FOR REVIEW	REVIEW OF OUTER CONTAINER SHOCK ASSEMBLY DRAWING
REVIEWED BY	105E3741
REASON FOR REVIEW	REVIEW OF OUTER CONTAINER SHOCK ASSEMBLY DRAWING

Security-Related Information
Figure Withheld Under 10 CFR 2.390

SAFETY-RELATED		CLASSIFICATION	
Item	Classification	Item	Classification
1	SECRET	2	SECRET
3	SECRET	4	SECRET
5	SECRET	6	SECRET
7	SECRET	8	SECRET
9	SECRET	10	SECRET
11	SECRET	12	SECRET
13	SECRET	14	SECRET
15	SECRET	16	SECRET
17	SECRET	18	SECRET
19	SECRET	20	SECRET
21	SECRET	22	SECRET
23	SECRET	24	SECRET
25	SECRET	26	SECRET
27	SECRET	28	SECRET
29	SECRET	30	SECRET
31	SECRET	32	SECRET
33	SECRET	34	SECRET
35	SECRET	36	SECRET
37	SECRET	38	SECRET
39	SECRET	40	SECRET
41	SECRET	42	SECRET
43	SECRET	44	SECRET
45	SECRET	46	SECRET
47	SECRET	48	SECRET
49	SECRET	50	SECRET
51	SECRET	52	SECRET
53	SECRET	54	SECRET
55	SECRET	56	SECRET
57	SECRET	58	SECRET
59	SECRET	60	SECRET
61	SECRET	62	SECRET
63	SECRET	64	SECRET
65	SECRET	66	SECRET
67	SECRET	68	SECRET
69	SECRET	70	SECRET
71	SECRET	72	SECRET
73	SECRET	74	SECRET
75	SECRET	76	SECRET
77	SECRET	78	SECRET
79	SECRET	80	SECRET
81	SECRET	82	SECRET
83	SECRET	84	SECRET
85	SECRET	86	SECRET
87	SECRET	88	SECRET
89	SECRET	90	SECRET
91	SECRET	92	SECRET
93	SECRET	94	SECRET
95	SECRET	96	SECRET
97	SECRET	98	SECRET
99	SECRET	100	SECRET

Nº FS1-0014159

Rev. 1.0

Handling: None

Page 46/400

AREVA TN-B1
Docket No. 71-9372
Safety Analysis Report

A
AREVA

Security-Related Information
Figure Withheld Under 10 CFR 2.390

ALL UNIT IN MILLIMETER	SECURITY-RELATED CLASSIFICATION CODE (C)	REVISION FOR CS
Rev. 01 01/04	SECRET	
Rev. 02 03/04	SECRET	
Rev. 03 07/04	SECRET	
Rev. 04 11/04	SECRET	
Rev. 05 01/05	SECRET	
Rev. 06 07/05	SECRET	
Rev. 07 07/05	SECRET	
Rev. 08 07/05	SECRET	
Rev. 09 07/05	SECRET	
Rev. 10 07/05	SECRET	
Rev. 11 07/05	SECRET	
Rev. 12 07/05	SECRET	
Rev. 13 07/05	SECRET	
Rev. 14 07/05	SECRET	
Rev. 15 07/05	SECRET	
Rev. 16 07/05	SECRET	
Rev. 17 07/05	SECRET	
Rev. 18 07/05	SECRET	
Rev. 19 07/05	SECRET	
Rev. 20 07/05	SECRET	
Rev. 21 07/05	SECRET	
Rev. 22 07/05	SECRET	
Rev. 23 07/05	SECRET	
Rev. 24 07/05	SECRET	
Rev. 25 07/05	SECRET	
Rev. 26 07/05	SECRET	
Rev. 27 07/05	SECRET	
Rev. 28 07/05	SECRET	
Rev. 29 07/05	SECRET	
Rev. 30 07/05	SECRET	
Rev. 31 07/05	SECRET	
Rev. 32 07/05	SECRET	
Rev. 33 07/05	SECRET	
Rev. 34 07/05	SECRET	
Rev. 35 07/05	SECRET	
Rev. 36 07/05	SECRET	
Rev. 37 07/05	SECRET	
Rev. 38 07/05	SECRET	
Rev. 39 07/05	SECRET	
Rev. 40 07/05	SECRET	
Rev. 41 07/05	SECRET	
Rev. 42 07/05	SECRET	
Rev. 43 07/05	SECRET	
Rev. 44 07/05	SECRET	
Rev. 45 07/05	SECRET	
Rev. 46 07/05	SECRET	
Rev. 47 07/05	SECRET	
Rev. 48 07/05	SECRET	
Rev. 49 07/05	SECRET	
Rev. 50 07/05	SECRET	
Rev. 51 07/05	SECRET	
Rev. 52 07/05	SECRET	
Rev. 53 07/05	SECRET	
Rev. 54 07/05	SECRET	
Rev. 55 07/05	SECRET	
Rev. 56 07/05	SECRET	
Rev. 57 07/05	SECRET	
Rev. 58 07/05	SECRET	
Rev. 59 07/05	SECRET	
Rev. 60 07/05	SECRET	
Rev. 61 07/05	SECRET	
Rev. 62 07/05	SECRET	
Rev. 63 07/05	SECRET	
Rev. 64 07/05	SECRET	
Rev. 65 07/05	SECRET	
Rev. 66 07/05	SECRET	
Rev. 67 07/05	SECRET	
Rev. 68 07/05	SECRET	
Rev. 69 07/05	SECRET	
Rev. 70 07/05	SECRET	
Rev. 71 07/05	SECRET	
Rev. 72 07/05	SECRET	
Rev. 73 07/05	SECRET	
Rev. 74 07/05	SECRET	
Rev. 75 07/05	SECRET	
Rev. 76 07/05	SECRET	
Rev. 77 07/05	SECRET	
Rev. 78 07/05	SECRET	
Rev. 79 07/05	SECRET	
Rev. 80 07/05	SECRET	
Rev. 81 07/05	SECRET	
Rev. 82 07/05	SECRET	
Rev. 83 07/05	SECRET	
Rev. 84 07/05	SECRET	
Rev. 85 07/05	SECRET	
Rev. 86 07/05	SECRET	
Rev. 87 07/05	SECRET	
Rev. 88 07/05	SECRET	
Rev. 89 07/05	SECRET	
Rev. 90 07/05	SECRET	
Rev. 91 07/05	SECRET	
Rev. 92 07/05	SECRET	
Rev. 93 07/05	SECRET	
Rev. 94 07/05	SECRET	
Rev. 95 07/05	SECRET	
Rev. 96 07/05	SECRET	
Rev. 97 07/05	SECRET	
Rev. 98 07/05	SECRET	
Rev. 99 07/05	SECRET	
Rev. 100 07/05	SECRET	

010E3743

AREVA - Fuel BU

N° FS1-0014159

Rev. 1.0

Handling: None

Page 47/400

AREVA TN-B1
Docket No. 71-9372
Safety Analysis Report

AREVA
A

Security-Related Information
Figure Withheld Under 10 CFR 2.390

AREVA - Fuel BU

Security-Related Information
Figure Withheld Under 10 CFR 2.390

REVISION	DATE	DESCRIPTION
01	10/12/01	ISSUE FOR REVIEW
02	10/12/01	ISSUE FOR REVIEW
03	10/12/01	ISSUE FOR REVIEW
04	10/12/01	ISSUE FOR REVIEW
05	10/12/01	ISSUE FOR REVIEW
06	10/12/01	ISSUE FOR REVIEW
07	10/12/01	ISSUE FOR REVIEW
08	10/12/01	ISSUE FOR REVIEW
09	10/12/01	ISSUE FOR REVIEW
10	10/12/01	ISSUE FOR REVIEW
11	10/12/01	ISSUE FOR REVIEW
12	10/12/01	ISSUE FOR REVIEW
13	10/12/01	ISSUE FOR REVIEW
14	10/12/01	ISSUE FOR REVIEW

Security-Related Information
Figure Withheld Under 10 CFR 2.390

ESSENTIAL TO SAFETY	
SAFETY-RELATED CLASSIFICATION CODE #	DESCRIPTION
1	SAFETY-RELATED CLASSIFICATION CODE #
2	DESCRIPTION
3	SAFETY-RELATED CLASSIFICATION CODE #
4	DESCRIPTION
5	SAFETY-RELATED CLASSIFICATION CODE #
6	DESCRIPTION
7	SAFETY-RELATED CLASSIFICATION CODE #
8	DESCRIPTION
9	SAFETY-RELATED CLASSIFICATION CODE #
10	DESCRIPTION
11	SAFETY-RELATED CLASSIFICATION CODE #
12	DESCRIPTION
13	SAFETY-RELATED CLASSIFICATION CODE #
14	DESCRIPTION

Security-Related Information
Figure Withheld Under 10 CFR 2.390

REVISIONS		DATE	BY	DESCRIPTION
1	10053748	05-15-04	10053748	10053748
2	10053748	05-15-04	10053748	10053748

REVISIONS		DATE	BY	DESCRIPTION
1	10053748	05-15-04	10053748	10053748
2	10053748	05-15-04	10053748	10053748

N° FS1-0014159

Rev. 1.0

Handling: None

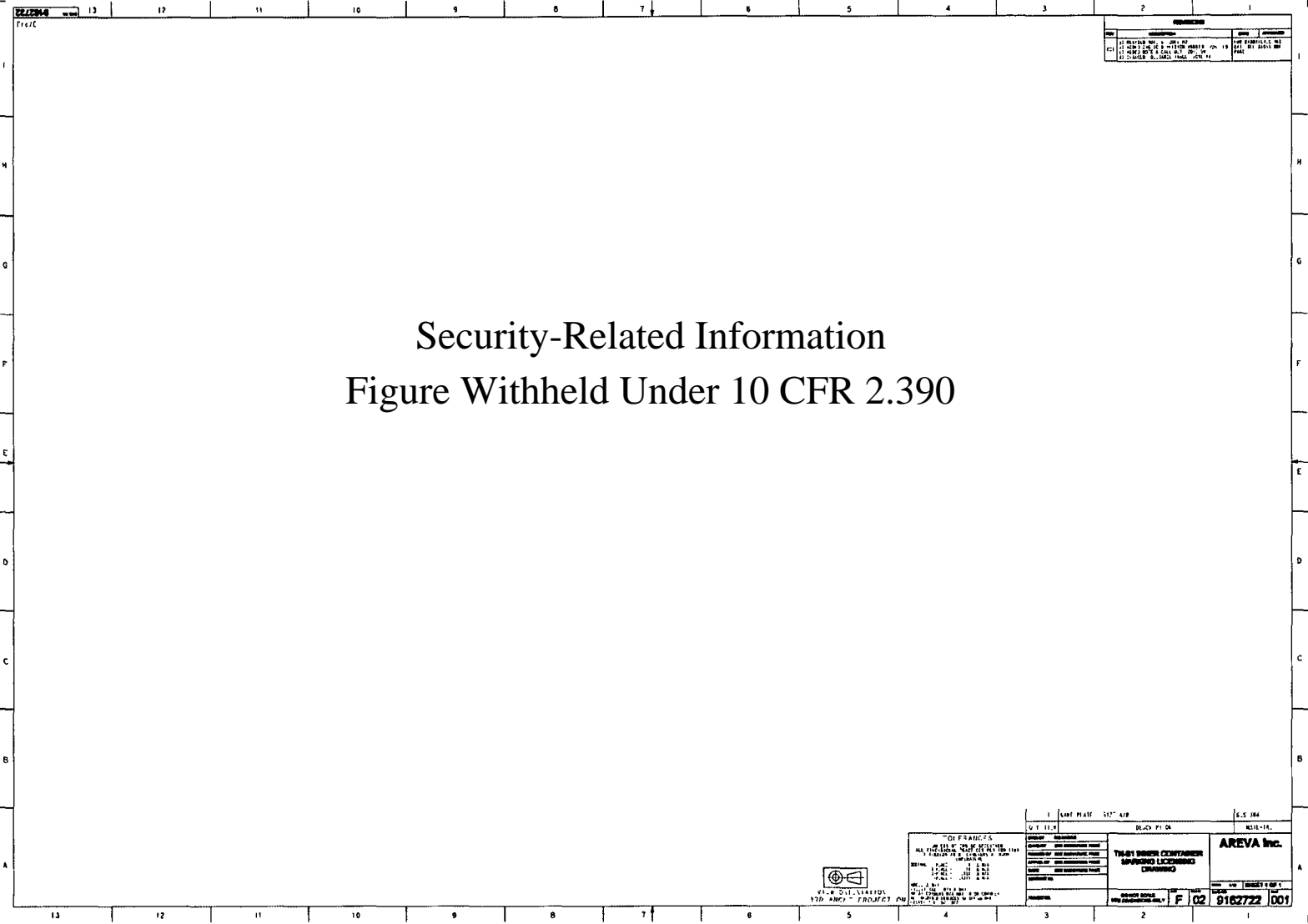
Page 52/400

AREVA TN-B1
Docket No. 71-9372
Safety Analysis Report

AREVA
A

Security-Related Information
Figure Withheld Under 10 CFR 2.390

AREVA - Fuel BU



N° FS1-0014159

Rev. 1.0

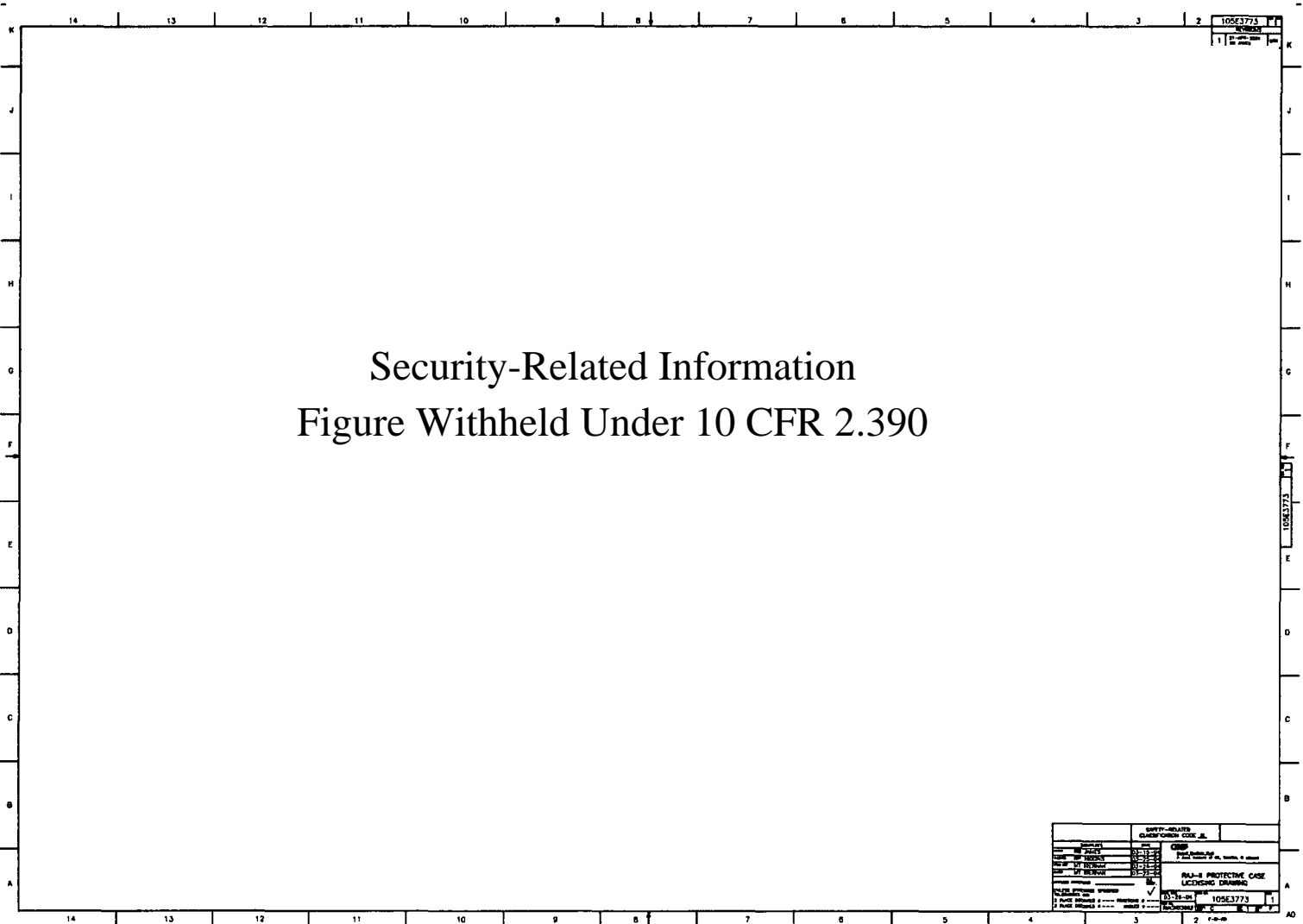
Handling: None

Page 53/400

AREVA TN-B1
Docket No. 71-9372
Safety Analysis Report




Security-Related Information
Figure Withheld Under 10 CFR 2.390



SAFETY-RELATED CLASSIFICATION CODE	
CLASSIFICATION	SECRET
GROUP	SECRET
GROUP 1	SECRET
GROUP 2	SECRET
GROUP 3	SECRET
GROUP 4	SECRET
GROUP 5	SECRET
GROUP 6	SECRET
GROUP 7	SECRET
GROUP 8	SECRET
GROUP 9	SECRET
GROUP 10	SECRET
GROUP 11	SECRET
GROUP 12	SECRET
GROUP 13	SECRET
GROUP 14	SECRET
GROUP 15	SECRET
GROUP 16	SECRET
GROUP 17	SECRET
GROUP 18	SECRET
GROUP 19	SECRET
GROUP 20	SECRET
GROUP 21	SECRET
GROUP 22	SECRET
GROUP 23	SECRET
GROUP 24	SECRET
GROUP 25	SECRET
GROUP 26	SECRET
GROUP 27	SECRET
GROUP 28	SECRET
GROUP 29	SECRET
GROUP 30	SECRET
GROUP 31	SECRET
GROUP 32	SECRET
GROUP 33	SECRET
GROUP 34	SECRET
GROUP 35	SECRET
GROUP 36	SECRET
GROUP 37	SECRET
GROUP 38	SECRET
GROUP 39	SECRET
GROUP 40	SECRET
GROUP 41	SECRET
GROUP 42	SECRET
GROUP 43	SECRET
GROUP 44	SECRET
GROUP 45	SECRET
GROUP 46	SECRET
GROUP 47	SECRET
GROUP 48	SECRET
GROUP 49	SECRET
GROUP 50	SECRET
GROUP 51	SECRET
GROUP 52	SECRET
GROUP 53	SECRET
GROUP 54	SECRET
GROUP 55	SECRET
GROUP 56	SECRET
GROUP 57	SECRET
GROUP 58	SECRET
GROUP 59	SECRET
GROUP 60	SECRET
GROUP 61	SECRET
GROUP 62	SECRET
GROUP 63	SECRET
GROUP 64	SECRET
GROUP 65	SECRET
GROUP 66	SECRET
GROUP 67	SECRET
GROUP 68	SECRET
GROUP 69	SECRET
GROUP 70	SECRET
GROUP 71	SECRET
GROUP 72	SECRET
GROUP 73	SECRET
GROUP 74	SECRET
GROUP 75	SECRET
GROUP 76	SECRET
GROUP 77	SECRET
GROUP 78	SECRET
GROUP 79	SECRET
GROUP 80	SECRET
GROUP 81	SECRET
GROUP 82	SECRET
GROUP 83	SECRET
GROUP 84	SECRET
GROUP 85	SECRET
GROUP 86	SECRET
GROUP 87	SECRET
GROUP 88	SECRET
GROUP 89	SECRET
GROUP 90	SECRET
GROUP 91	SECRET
GROUP 92	SECRET
GROUP 93	SECRET
GROUP 94	SECRET
GROUP 95	SECRET
GROUP 96	SECRET
GROUP 97	SECRET
GROUP 98	SECRET
GROUP 99	SECRET
GROUP 100	SECRET

Security-Related Information
Figure Withheld Under 10 CFR 2.390

1	DRP 0000-0018-1484	ADDED "ESHTL TO SAFETY"	DB	MITK	8/13/03
0	FIRST ISSUE	FMA-324	BA	<i>RES</i>	6-3-98
REV.	DESCRIPTION	BY	CR#	APPROVAL	DATE
REVISIONS					
SIGNATURES		DATE			
DESIGN	B. AYERS (IDD)	8/3/98	 NEP GENERAL ELECTRIC COMPANY <small>WOLFE BERRY PARKWAY WATSONVILLE, CA 95076, U.S.A.</small>		
ENGINEER					
DRAWN					
CHECKED					
SCALE 1/4		ALL SURF		SHIPPING CONTAINER LOOSE FUEL RODS FILED NRC LICENSING DRAWING	
UNLESS OTHERWISE SPECIFIED					
TOLERANCES ON:					
2 PLACE DECIMALS ±		FRACTIONS ±		ISSUE DATE: 6-3-98 DWG NO.: 0028B98 SHEET: 1	
3 PLACE DECIMALS ±		ANGLES ±		FILE NAME: 0028B98 SHEET NO.: 1 CON: F	

AREVA - Fuel BU

2. STRUCTURAL EVALUATION

This section presents evaluations demonstrating that the TN-B1 package meets applicable structural criteria. The TN-B1 packaging, consisting of unirradiated fuel assemblies that provide containment, an inner container, and an outer container with paper honeycomb spacers, is evaluated and shown to provide adequate protection for the payload. Normal Conditions of Transport (NCT) and Hypothetical Accident Condition (HAC) evaluations, using analytic and empirical techniques, are performed to address 10 CFR 71 performance requirements.

Numerous tests were successfully performed on the RAJ-II package during its initial qualification in Japan that provided a basis for selecting the certification tests. RAJ-II certification testing involved two full-scale Certification Test Units (CTU) at Oak Ridge, TN. The RAJ-II CTUs were subjected to a series of free drop and puncture drop tests. The RAJ-II CTUs protected the simulated fuel assemblies, allowing them to remain undamaged and leak tight throughout certification testing. Since the RAJ-II and TN-B1 structural designs are identical, the RAJ-II tests are completely applicable to the TN-B1 package. Details of the certification test program are provided in Appendix 2.12.1.

2.1. DESCRIPTION OF STRUCTURAL DESIGN

2.1.1. *Discussion*

A comprehensive discussion on the TN-B1 packaging design and configuration is provided in chapter 1.0. Drawings provided in Appendix 1.4.1 show the construction of the TN-B1 and how it protects the fuel assemblies. The containment is provided by the fuel cladding and welded end fittings of the fuel rods. The fuel is protected by an inner container that provides thermal insulations and soft foam that protects the fuel from vibration. The inner container is supported by vibration isolation system inside the outer container that has shock absorbing blocks of balsa and honeycomb made of resin impregnated kraft paper (hereinafter called "paper honeycomb"). Specific discussions relating to the aspects important to demonstrating the structural configuration and performance to design criteria for the TN-B1 packaging are provided in the following sections. Standard fabrication methods are used to fabricate the TN-B1 package.

Detailed drawings showing applicable dimensions and tolerances are provided in Appendix 1.4.1.

Weights for the various components and the assembled packaging are provided in Section 2.1.3.

2.1.1.1. Containment Structures

The primary containment for the radioactive material in the TN-B1 is the fuel rod cladding, which is manufactured to high standards for use in nuclear reactors. The fabrication standards for the fuel are in excess of what is needed to provide containment for shipping of the fuel. The fuel rod cladding is designed to provide containment throughout the life of the fuel, prior to loading, in transportation, and while used in the reactor where it operates at higher pressures and temperatures, and must contain fission products as well as the fuel itself.

The cladding tubes for the fuel are high quality seamless tubing. The clad fuel is verified leaktight before shipment.

2.1.1.2. Non-Containment Vessel Structures

The TN-B1 is made up of two non-containment structures, the inner container, and the outer container that are designed to protect the fuel assemblies and clad rods which serve as the containment. The inner container design provides some mechanical protection although its primary function is to provide thermal protection. The outer container consists of a metal wall with shock absorbing devices inside and vibration isolation mounts for the inner container. Section 1.2.1 provides a detailed description of the inner and outer container. Non-containment structures are fabricated in accordance with the drawings in Appendix 1.4.1.

Welds for the non-containment vessel walls are subjected to visual inspection as delineated on the drawings in Appendix 1.4.1.

2.1.2. ***Design Criteria***

Proof of performance for the TN-B1 package is achieved by a combination of analytic and empirical evaluations. The acceptance criteria for analytic assessments are in accordance with 10 CFR 71 and the applicable regulatory guides. The acceptance criterion for empirical assessments is a demonstration that both the inner and outer container are not damaged in such a way that their performance in protecting the fuel assemblies during the thermal event is not compromised and the fuel itself is not damaged throughout the NCT and HAC certification testing. Additionally, package deformations obtained from certification testing are considered in subsequent thermal, shielding, and criticality evaluations are validated.

2.1.2.1. Analytic Design Criteria (Allowable Stresses)

The allowable stress values used for analytic assessments of TN-B1 package structural performance come from the regulatory criteria such as yield strength or 1/3 of yield or from the ASME Code for the particular application. Material yield strengths, taken from the ASME Code, used in the analytic acceptance criteria, S_y , and ultimate strengths, S_u , are presented in Table 2 - 2 of Section 2.2.

2.1.2.2. Containment Structures

The fuel cladding provides the primary containment for the nuclear fuel.

2.1.2.3. Non-Containment Structures

For evaluation of lifting devices, the allowable stresses are limited to one-third of the material yield strength, consistent with the requirements of 10 CFR 71.45(a). For evaluation of tie-down devices, the allowable stresses are limited to the material yield strength, consistent with the requirements of 10 CFR 71.45(b).

2.1.2.4. Miscellaneous Structural Failure Modes

2.1.2.4.1. *Brittle Fracture*

By avoiding the use of ferritic steels in the TN-B1 packaging, brittle fracture concerns are precluded. Specifically, most primary structural components are fabricated of austenitic stainless steel. Since this material does not undergo a ductile-to-brittle transition in the temperature range of interest (above -40 °F), it is safe from brittle fracture.

The closure bolts used to secure the inner and outer container lids are stainless steel, socket head cap screws ensuring that brittle fracture is not of concern. Other fasteners used in the TN-B1 packaging assembly provide redundancy and are made from stainless steel, again eliminating brittle fracture concerns.

2.1.2.4.2. *Extreme Total Stress Intensity Range*

Since the response of the TN-B1 package to accident conditions is typically evaluated empirically rather than analytically, the extreme total stress intensity range has not been quantified. Two full-scale certification test units (see Appendix 2.12.1) successfully passed free-drop and puncture testing. The CTUs were also fabricated in accordance with the drawings in Appendix 1.4.1, thus incurring prototypic fabrication induced stresses. Exposure

to these conditions has demonstrated leak tight containment of the fuel, geometric configuration stability for criticality safety, and protection for the fuel. Thus the intent of the extreme total stress intensity range requirement has been met.

2.1.2.4.3. *Buckling Assessment*

Due to the small diameter of the containment boundary (the fuel rod cladding) and the fact that its radial deflection is limited by the internal fuel pellets, radial buckling is not a failure mode of concern for the containment boundary. Axial buckling deflection is also limited by the inner wall of the inner container and lid. The applied axial load to the fuel is also limited by the wood at the end of the packaging. The limited horizontal movement of the fuel during an end drop limits the ability of the fuel to buckle as demonstrated in tests performed on CTU 2 (see Appendix 2.12.1).

It is also noted that 30-foot drop tests performed on full-scale models with the package in various orientations produced no evidence of buckling of any of the fuel (see Appendix 2.12.1). Certification testing does not provide a specific determination of the design margin against buckling, but is considered as evidence that buckling will not occur. In addition buckling is a potential concern to ensure adequate geometric configuration control of the post accident package for criticality control. This involves not only the internal configuration of the package but the potential spacing between packages as well. Deformation of the TN-B1 is limited by its redundant structure. The wall of the package acts to stiffen the support plates that carry the load of the inner container via the vibration isolating mechanism. Part of the redundant system to minimize deformation of the fuel is the paper honeycomb that absorbs shocks that would impart side loading to the fuel. The inner container, consisting of an inner wall separated from an outer wall by thermal insulation, is lined with cushioning material that supports the fuel. Regardless of the specific failure mechanism of the support plates, the total deformation is limited by the shock absorbers (paper honeycomb). These blocks immediately share the load. Hence, even if the support plates would buckle allowing the outer wall to plastically deform, the amount of deformation is limited by the shock absorbing material. This has been demonstrated by test to allow only 118 mm (4.7 inches) of deformation of the shock absorbing blocks. The criticality evaluation takes into consideration this deformation. The redundant support system combined with the vibro-isolation and shock absorption system prevents the deformation of the inner container and the fuel.

The axial deformation resulting from an end drop is controlled in a similar manner. The end of the outer container has a wood shock absorber built in that carries the load from the inner container to the outer wall after the vibro-isolation device deflects. This reduces the load carried by the outer wall and support plates. It prevents large loads and deformations

that could contribute to buckling of the fuel. The inner container constrains the fuel from large deformations or buckling.

Therefore, the support system prevents buckling of the packaging or fuel that would affect the criticality control or containment.

2.1.3. Weights and Centers of Gravity

The maximum gross weight of a TN-B1 package, including a maximum payload weight of 684 kg (1,508 pounds) is 1,614 kg (3,558 pounds). The maximum vertical Center of Gravity (CG) is located 421 mm (16.57 inches) above the bottom surface of the package for a fully loaded package. A maximum horizontal shift of the horizontal CG is 92 mm (3.62 inches). This is allowed for in the lifting and tie-down calculations presented in Section 2.5.1. Figure 2-1 shows the locations of the center of gravity for the major components and the location of the center of gravity for the assembled. A detailed breakdown of the TN-B1 package component weights is summarized in Table 2 - 1.

2.1.3.1. Effect of CG Offset

The shift of the CG of the package 92 mm (3.6 inches) has very little effect on the performance of the package due to the length of the package, 5,068 mm (199.53 in). This results in a small shift of the weight and forces from one end of the package to the other. The actual total shift is:

$$3.6\% = 1 - \frac{(2)((5068/2) - 92)}{5068}$$

The offset of the CG is taken into account in the lifting and tie down calculations. The effect of this relatively small offset can be neglected.

2.1.4. Identification of Codes and Standards for Package Design

The radioactive isotopic content of the fuel is primarily U-235 with small amounts of other isotopes that make it Type B. Using the isotopic content limits shown in Section 1.2.3 the package would be considered a Category II. As such the applicable codes that would apply are the ASME Boiler and Pressure Vessel Code Section III, Subsection ND for the containment boundary which is the fuel cladding and Section III, Subsection NG for the criticality control Structure and the Section VIII for the non containment components.

The fuel cladding, due to its service in the reactor and need for high integrity, is designed to and fabricated to standards that exceed those required by ASME Section III Subsection ND. The structure used to maintain criticality control is demonstrated by test. The packaging capabilities are verified by test and the codes used in fabrication are called out on the drawings in Appendix 1.4.1. The sheet metal construction of the packaging requires different joint designs and manufacturing techniques that would normally be covered by the above referenced codes.

2.1.4.1. JIS/ASTM Comparison of Materials

The Certification Test Units (CTUs) were manufactured in Japan using material meeting JIS specifications. The fuel cladding and ceramic pellets were manufactured in the US to US specifications. The future manufacturing of TN-B1 packages may be performed using American standards (ASTM or ASME) that are appropriate substitutes for the Japanese standards (JIS) material comprising the CTUs. In order to assure that the packaging manufactured in the future meets the performance requirements demonstrated for the RAJ-II CTUs a detailed review of the differences between the American and Japanese standards was performed. The scope of the study included the: stainless steel products, wood products, rubber, paper honeycomb, and polyethylene foam. The study concluded that American standards material is available and compatible to the JIS standards. Future manufacturing of these packages for domestic use may be to American or Japanese specifications meeting the tolerances specified in the general arrangement drawings.

2.1.4.2. JIS/ASME Weld Comparison

Based upon an evaluation, it is concluded that the following standards are equivalent for the purposes of fabrication of the TN-B1 container in the United States:

Japanese Specification	American Specification
JIS Z 3821 Standard qualification procedure for welding technique of stainless steel	ASME Section IX
JIS Z 3140 Method of inspection for spot weld	ASME Section IX
JIS Z 3145 Method of bend test for stud weld	ASME Section IX

2.1.4.3. JIS/JSNDI/ASNT Non-destructive Examination Personnel Qualification and Certification Comparison

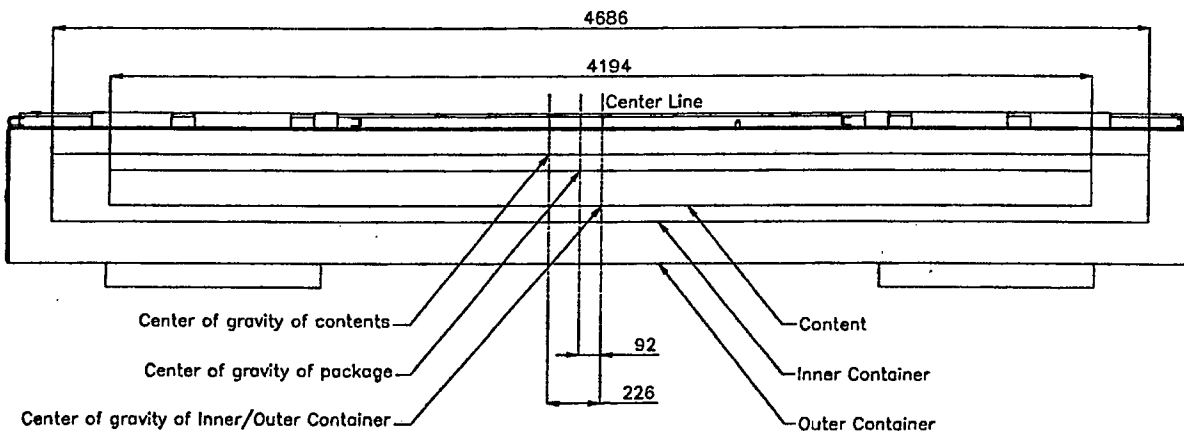
The following standards are considered equivalent for Non-destructive Examination Personnel Qualification and Certification. Personnel with these qualifications and certifications are authorized to perform examinations of the fabrication inspection requirements for the TN-B1 container in the United States. Although these documents cover other disciplines, this comparison only applies to Liquid Penetrant Examination.

Japanese Specification	American Specification
JIS Z 2305 Qualification and Certification for NDT Personnel	SNT-TC-1A* Recommended Practice
Certification NDIS 0601	SNT-TC-1A Recommended Practice
Certification NDIS J001	SNT-TC-1A Recommended Practice

*Society of Non-destructive Testing – Technical Council

Table 2-1 TN-B1 Weight

Contents	Number of assemblies per package	Maximum 2 Assemblies
	Number of fuel rods per package	See section 1.2.3
	Total weight	684 kg (1,508 lb)
Inner container	Body	200 kg (441 lb) (including bolts)
	Lid	101 kg (223 lb)
	End lids	7 kg (15.4 lb)
	Total weight	308 kg (679 lb)
Outer container	Body	485 kg (1,069 lb) (including bolts)
	Lid	137 kg (302 lb)
	Total weight	622 kg (1,371 lb)
Total weight of package		1,614 kg (3,558 lb)



(unit: mm)

Figure 2-1 Center of Gravity of Package Components

2.2. MATERIALS

2.2.1. *Material Properties and Specifications*

The major structural components, i.e., the Outer Container (OC) and Inner Container (IC) walls, supports, and attachment blocks are fabricated from austenitic stainless steel. Other materials performing a structural function are lumber (bolster), balsa (shock absorber), paper honeycomb (shock absorber), alumina silicate (thermal insulator), polyethylene foam (cushioning material), and zirconium alloy (fuel rod cladding). The drawings presented in Appendix 1.4.1 delineate the specific material(s) used for each TN-B1 packaging.

The remainder of this section presents and discusses pertinent mechanical properties for the materials that perform a structural function. Both the materials that are used in the analytics and those whose function in the package is demonstrated by test such as the shock absorbing material are presented. In general the analytics covering the lifting and tie down capabilities of the package and some normal condition events are limited to the stainless steel structure of the packaging.

Table 2 - 2 presents the bounding mechanical properties for the series 300 stainless steel used in the TN-B1 packaging. Each of the representative mechanical properties is those of Type 304 stainless steel and is taken from Section II, Parts A and D, of the ASME Boiler and Pressure Vessel Code. These properties are applicable to both packages that may have been made in Japan to Japanese specifications, Japanese Industrial Standards (JIS) or using ASME specification material. The density of stainless steel is taken as 0.29 lb/in³ (8.03E3 kg/m³), and Poisson's Ratio is 0.3.

Table 2 - 3 presents the mechanical properties of the main non-stainless steel components of the package necessary for the structural analysis.

**Table 2-2 Representative Mechanical Properties of 300 Series
Stainless Steel Components**

①	②	③	④	⑤	
Minimum Elongation (%)	Temperature °C (°F)	Yield Strength, S_y MPa ($\times 10^3$ psi)	Ultimate Strength, S_u MPa ($\times 10^3$ psi)	Elastic Modulus, E GPa ($\times 10^6$ psi)	Thermal Expansion Coefficient, α $\times 10^{-6}$ mm/mm/°C ($\times 10^{-6}$ in/in/°F)
35	-29 (-20)	206.8 (30.0)	517.1 (75.0)	----	----
40	21 (70)	206.8 (30.0)	517.1 (75.0)	195.1 (28.3)	----
30	38 (100)	206.8 (30.0)	517.1 (75.0)	----	15.39 (8.55)
25	93 (200)	172.4 (25.0)	489.5 (71.0)	190.3 (27.6)	15.82 (8.79)
30	149 (300)	155.1 (22.5)	455.1 (66.0)	186.2 (27.0)	16.2 (9.00)
40	204 (400)	142.7 (20.7)	444.0 (64.4)	182.7 (26.5)	16.54 (9.19)
40 ^⑥	23°C ^⑥	205 MPa Min ^⑥	520 MPa Min ^⑥	----	----
40 ^⑦	21°C ^⑦	205 MPa Min ^⑦	515 MPa Min ^⑦	----	----

- Notes:**
- ① ASME Code, Section II, Part A
 - ② ASME Code, Section II, Part D, Table Y-1
 - ③ ASME Code, Section II, Part D, Table U
 - ④ ASME Code, Section II, Part D, Table TM-1, Material Group G
 - ⑤ ASME Code, Section II, Part D, Table TE-1, 18Cr-8Ni, Coefficient B
 - ⑥ JIS Handbook Ferrous Materials and Metallurgy I, Sections G4303, G4304, G4305 Material Specifications
 - ⑦ ASTM A240, A666 & A276 Material Specifications

Table 2-3 Mechanical Properties of Typical Components

Materials (Usage)	Yield stress or yield strength	Tensile strength	Compressive strength	Bending strength	Static initial peak stress	Modulus of longitudinal elasticity	Density (g/cm ³)
Lumber (bolster)	56.3 MPa Nominal	-	50.5 MPa Nominal	72.0 MPa Nominal	-	7.85 GPa Nominal	0.53 Nominal
Balsa (shock absorber)	-	-	16 MPa Nominal	-	-	-	0.18 Nominal
Paper honeycomb (shock absorber)	-	-	-	-	2.35 MPa Nominal	-	0.06 Nominal
Alumina Silicate (thermal insulator)	-	-	294 kPa Nominal	314 kPa Nominal	-	-	0.25 Nominal
Foam polyethylene (cushioning mat'l)	-	-	Approx. 0.2MPa @ 50% strain	-	0.69 MPa Nominal	-	0.068 Nominal
Zirconium alloy (fuel rods) ASTM B811	241 MPa (35,000psi)	413 MPa (60,000psi)	-	-	-	97.1 GPa Nominal	6.5 Nominal
300 Series Stainless Socket Headed Cap screw	241 MPa (35,000psi) (Min)	379 MPa (75,000psi) (Min)	-	-	-	-	-

2.2.2. Chemical, Galvanic, or Other Reactions

The major materials of construction of the TN-B1 packaging (i.e., austenitic stainless steel, polyurethane foam, alumina thermal insulator, resin impregnated paper honeycomb, lumber (hemlock and balsa), and natural rubber) will not have significant chemical, galvanic or other reactions in air, inert gas or water environments, thereby satisfying the requirements of 10 CFR 71.43(d). These materials have been previously used, without incident, in radioactive material (RAM) packages for transport of similar payload materials. A successful RAM packaging history combined with successful use of these fabrication materials in similar industrial environments ensures that the integrity of the TN-B1 package will not be compromised by any chemical, galvanic, or other reactions.

The TN-B1 packaging is primarily constructed of series 300 stainless steel. This material is highly corrosion resistant to most environments. The metallic structure of the TN-B1 packaging is composed entirely of this material and compatible 300 series weld material. Since both the base and weld materials are 300 series materials, they have nearly identical electrochemical potential thereby minimizing any galvanic corrosion that could occur.

The stainless steel within the IC cavity between the inner and outer walls is filled with a ceramic alumina silicate thermal insulator. This material is non-reactive with either the wood or the stainless steel, both dry or in water. The alumina silicate is very low in free chlorides to minimize the potential for stress corrosion of the IC structure.

The polyethylene foam that is used in the IC for cushioning material has been used previously and is compatible with stainless steel. The polyethylene foam is very low in free halogens and chlorides.

Resin impregnated paper honeycomb is used in the TN-B1 packaging as cushioning material. The impregnated paper is resistant to water and break down. It is low in leachable halides.

The natural rubber that is used as a gasket for the lids and in the vibro-isolating system, contains no corrosives that would react adversely affect the TN-B1 packaging. This material is organic in nature and non-corrosive to the stainless steel boundaries of the TN-B1 packaging.

2.2.2.1. Content Interaction with Packaging Materials of Construction

The materials of construction of the TN-B1 packaging are checked for compatibility with the materials that make up the contents or fuel rods that are to be shipped in the TN-B1. The primary materials of construction of the fuel assembly that could come in contact with the packaging are the stainless steel and the zirconium alloy material that is used for the cladding of the fuel rods. Zirconium alloy (including metal zirconium), stainless steel, and

Ni-Cr- Fe alloy, which form a passivated oxide film on the surface under normal atmosphere with slight moisture, are essentially stable. The contact of the above three kinds of metals with polyethylene is chemically stable. These materials are compatible with the stainless steel, polyethylene, and natural rubber that could come in contact with the contents.

2.2.3. *Effects of Radiation on Materials*

Since this is an unirradiated fuel package, the radiation to the packaging material is insignificant. Also, the primary materials of construction and containment, austenitic stainless steel and the zirconium alloy cladding of the fuel are highly resistant to radiation.

2.3. FABRICATION AND EXAMINATION

2.3.1. *Fabrication*

The TN-B1 is fabricated using standard fabrication techniques. This includes cutting, bending and welding the stainless steel sheet metal. As shown on the drawing the welding is done to AWS D1.6 Welding of Stainless Steel. The process may also be controlled by ASME Section IX or other international codes. The containment, the cladding of the fuel rods is fabricated to standards that exceed the required Section VIII of the ASME Boiler and Pressure vessel code due to the service requirements of the fuel in reactors.

2.3.2. *Examination*

The primary means of examination to determine compliance of the TN-B1 to the design requirements is visual examination of each component and the assembled units. This includes dimensional verification as well as material and weld examination. The materials will also be certified to the material specifications. Shock absorbing material such as the paper honeycomb will also have verified material properties.

2.4. LIFTING AND TIE-DOWN STANDARDS FOR ALL PACKAGES

For analysis of the lifting and tie-down components of the TN-B1 packaging, material properties from Section 2.2 are taken at a bounding temperature of 75°C (167 °F) per Section 2.6.1.1. This is the maximum temperature that the container reaches when in the sun. The primary structural material is 300 series stainless steel that is used in the Outer Container (OC).

A loaded TN-B1 package can be lifted using either a forklift or by slings. The gross weight of the package is a maximum of 1,614 kg (3,558 lb). Locating/protection plates for the forklift and locating angles for the sling locate the lift points for the package. In both cases

the package is lifted from beneath. The failure of these locating/protective features would not cause the package to drop nor compromise its ability to perform its required functions.

The inner container may be lifted empty or filled with the contents using the sling fittings that are attached at the positions shown in Figure 2-2. The details of the sling fittings are as shown in Figure 2-3. Since the center of gravity depends on existence of the contents, the sling fittings for the filled container and the empty container are marked respectively as "Use When Loaded" and "Use When Empty" to avoid improper operations. Also, the sling fittings on the lid of inner container to lift the lid only are marked as "Use for Lifting Lid" similar to the outer container.

The sling devices are mechanically designed to be able to handle the package and the inner container filled with the fuel assemblies in safety; they can lift three times the gross weight of the package, or three times the gross weight of the filled inner container respectively, so that they can with stand rapid lifting.

Properties of 300 series stainless steel are summarized below.

Table 2-4 Properties of 300 Series Stainless Steel

Material Property	Value	Reference
At 75°C (167 °F)		
Elastic Modulus, E	191.7 GPa (27.8 × 10 ⁶ psi)	Table 2 - 2
Yield Strength, σ_y	184.7 MPa (26,788 psi)	
Shear Stress, equal to (0.6) σ_y	110.8 MPa (16,073 psi)	

2.4.1. *Lifting Devices*

This section demonstrates that the attachments designed to lift the TN-B1 package are designed with a minimum safety factor of three against yielding, per the requirements of 10 CFR71.45 (a).

The lifting devices on the outer container lid are restricted to only lifting the outer container lid, and the lifting devices in the inner lid are restricted to only lifting the inner container lid. Although these lifting devices are designed with a minimum safety factor of three against yielding, detailed analyses are not specifically included herein since these lifting devices are not intended for lifting a TN-B1 package.

The outer container can be handled by either forklift or slings in a basket hitch around the package, requiring no structural component whose failure could affect the performance of the package.

2.4.1.1. Lifting of Inner Container

The inner container is lifted when loaded with fuel from the outer container with sling fittings attached to the body of the inner container. Three pairs (six in total) of the sling fittings are attached to the inner container as shown in Figure 2-2. The center of gravity depends upon whether the container is filled or not. Since the six sling fittings are the same, the stress in the sling fittings are evaluated for the case of at the maximum weight condition that occurs when the inner container is filled with fuel assemblies.

The stress on the sling fitting when lifting the inner container filled with contents is evaluated by determining the maximum load acting on any given fitting.

The maximum load, P_v , (see Figure 2-9) acting on one of the sling fitting vertically when lifting is given by the following equation:

$$P_v = \frac{(W_2 + W_3)}{n} \cdot g$$

Where:

P_v : maximum load acting to sling fitting in vertical direction	N
W_2 : mass of inner container	308 kg (679 lb)
W_3 : mass of contents	684 kg (1,508 lb)
n: number of sling fittings	4
g: acceleration of gravity	9.81 m/s ²

Accordingly, the maximum load acting on the sling fitting vertically is calculated as:

$$P_v = \frac{684 + 308}{4} \times 9.81 = 2.433 \times 10^3 \text{ N (546.9 lbf)}$$

The load, P, acting to the sling fitting when the sling is at a minimum angle of 60° is calculated as:

$$P = \frac{P_v}{\sin \theta} = \frac{2.433 \times 10^3}{\sin 60^\circ} = 2.809 \times 10^3 \text{ N (631 lbf)}$$

Also, the maximum load, PH, acting on the sling fitting horizontally is calculated as:

$$P_H = \frac{P_v}{\tan \theta} = \frac{2.433 \times 10^3}{\tan 60^\circ} = 1.405 \times 10^3 \text{ N (316 lbf)}$$

Each sling fitting is made up of a hooking bar which is a 12mm diameter bent rod and a perforated plate that is made up of two pieces of angle that are welded together. The perforated plate of the sling fitting is welded to a support of that is welded to the body of the inner container.

The shearing stress in the hooking bar (see Figure 2-6) is given by the following equation:

$$\tau_N = \frac{P \times \phi}{A}$$

Where

τ_N : shearing stress on hooking bar of sling fitting	MPa
P: maximum load	$2.809 \times 10^3 \text{ N (631 lbf)}$
A: cross-section of hooking bar of sling fitting in ²)	$\pi/4 \times 12^2 = 113 \text{ mm}^2 \text{ (0.175)}$
ϕ : load factor	3

Accordingly, the shearing stress on the hooking bar of the sling fitting at its center is calculated as:

$$\tau_N = \frac{2.809 \times 10^3 \times 3}{113} = 74.58 \text{ MPa (10,820 psi)}$$

The yield stress for stainless steel is 184.7 MPa (26,790 psi) and the shear allowable is $0.6 \times 184.7 = 110.8$ MPa (16,070 psi) at the maximum normal temperature, hence the margin (MS) is

$$MS = \frac{110.8}{74.58} - 1 = 0.48$$

Therefore, the sling fitting can withstand three times the load without yielding in shear.

The strength of the perforated plate of a sling fitting is evaluated for failure by shearing. The shear stress on a perforated plate (see Figure 2-7) of the sling fitting by the total load is given by the following equation:

$$\tau_N = \frac{Px\emptyset}{A}$$

Where:

τ_N : shearing stress on the perforated plate of a sling fitting	MPa
P: maximum load	2.809×10^3 N (631 lbf)
A: cross-section of the upper part of the perforated plate:	$2 \times \frac{50-14}{2} \times 6 = 216 \text{ mm}^2 (0.33 \text{ in}^2)$
\emptyset : load factor	3

Accordingly, the shearing stress, τ_N , on the perforated plate of sling fitting is calculated as:

$$\tau_N = \frac{2.809 \times 10^3 \times 3}{216} = 39.01 \text{ MPa (5,658 psi)}$$

The allowable shearing stress for stainless steel is 110.8 MPa (16,073 psi). Then the margin of Safety (MS) is:

$$MS = \frac{110.8}{39.01} - 1 = 1.84$$

Therefore, the shear strength of the plate meets the requirement of not yielding under three times the load.

Next, the strength of welds of the sling fittings is evaluated for the torsional loads applied. Torsional loads are applied to the welds of sling fitting per Figure 2-8.

The moment of inertia of area, I_P , to the welds of sling fittings is given by the following equation:

$$I_P = I_X + I_Y$$

$$I_X = I_{X2} - I_{X1}$$

$$I_Y = \sum I_{Yi}$$

Where

I_P : moment of inertia of area to welds	mm^4
I_X : moment of inertia of area to welds for X-axis	mm^4
I_Y : moment of inertia of area to welds for Y-axis	mm^4
I_{X1} : moment of inertia of area to inside of weld for X-axis	mm^4
I_{X2} : moment of inertia of area to outside of weld for X-axis	mm^4
I_{Y1} : moment of inertia of area to each weld for Y-axis	mm^4

The moment of inertia of area, I , to a cross-sectional area of width, b , and height, h , is given by:

$$I = \frac{1}{12}bh^3$$

Conservatively only the outside welds not including any corner wrap around that attach the sling fitting to the support plate are considered. Thus, the moment of inertia of area, I_X and I_Y to the welds for X-axis and Y-axis are calculated as:

$$I_x = \left(\frac{1}{12} \times 88 \times 54^3\right) - \left(\frac{1}{12} \times 88 \times 50^3\right) = 2.38 \times 10^5 \text{ mm}^4 (0.57 \text{ in}^4)$$

$$I_y = 2I_{Y1} = 2 \times \frac{1}{12} \times 2 \times 88^3 = 2.27 \times 10^5 \text{ mm}^4 (0.55 \text{ in}^4)$$

Accordingly, the moment of inertia of area, I_P , to the welds is calculated as

$$I_p = (2.38 \times 10^5) + (2.27 \times 10^5) = 4.65 \times 10^5 \text{ mm}^4 (1.12 \text{ in}^4)$$

The shearing stress, S_d , on the weld due to the load acting on the sling fitting is given by the following equation:

$$s_d = \frac{P \cdot \phi}{A}$$

Where:

S_d shearing stress on welds due to the load to sling fitting	MPa
P: maximum load acting to one of sling fitting	2.809×10^3 N (631 lbf)
A: overall cross-section of welds	$2 \times 88 = 176$ mm ² (0.273 in ²)
ϕ : load factor	3

Accordingly, the shearing stress on welds due to the load acting to the sling fitting is calculated as:

$$S = \frac{2.809 \times 10^3 \times 3}{176} = 47.9 \text{ MPa (6,950 psi)}$$

The maximum bending moment acting to the sling fitting is given by the following equation from Figure 2-9.

$$M_{\max} = P \cdot l$$

Where:

M_{\max} : maximum bending moment acting to sling fitting	N · mm
P: maximum load acting to one of sling fitting	2.809×10^3 N (631 lbf)
l: distance from fulcrum to load point	17 mm (0.67 in)

Therefore, the maximum bending moment acting to the sling fitting is calculated as:

$$\begin{aligned} M_{\max} &= 2.809 \times 10^3 \times 17 \\ &= 4.8 \times 10^4 \text{ N} \cdot \text{mm (424.8 in} \cdot \text{lbf)} \end{aligned}$$

The stress due to this bending moment is given by the following equation:

$$S_m = \frac{M_{max} \cdot r \cdot \phi}{I_p}$$

Where:

S_m : Stress acting to a point at r from center of gravity due to bending moment MPa

r : distance from center of gravity to end of welds $\sqrt{44^2 + 25^2} = 50.6 \text{ mm (1.99 in)}$

M_{max} : maximum bending moment acting to sling fitting $4.8 \times 10^4 \text{ N}\cdot\text{mm (424.8 in}\cdot\text{lbf)}$

I_p : moment of inertia of area to welds $4.65 \times 10^5 \text{ mm}^4 (1.12 \text{ in}^4)$

ϕ : load factor 3

From this equation, the maximum bending moment, S_m , acting to the sling fitting is calculated as:

$$S_m = \frac{4.8 \times 10^4 \times 50.6 \times 3}{4.65 \times 10^5} 15.6 \text{ MPa (2,260 psi)}$$

In addition, the composite shearing stress, S , on the welds is given by the following equation:

$$S = \sqrt{S_d^2 + S_m^2 + 2S_d S_m \cos \theta}$$

Where

$$\cos \theta = 25/50.6$$

From this equation, the composite shearing stress, S , is calculated as

$$S = \sqrt{47.9^2 + 15.5^2 + 2 \times 47.9 \times 25/50.6}$$

$$= 57.2 \text{ MPa (8,300 psi)}$$

Meanwhile, the allowable shearing stress for 300 series stainless steel is 110.8 MPa (16,073 psi).

Then the margin (MS) is:

$$MS = \frac{110.8}{57.2} - 1 = 0.94$$

The welds are capable of carrying 3 times the expected load without yielding.

Likewise the welds of the support plates for sling fittings are evaluated in the same manner. Since the welds of the support plates (see Figure 2-10) receive the same load as mentioned above in the case of the welds of the sling fittings, it is evaluated by same analytic method as mentioned above. The symbols used here shall have same meaning.

The moment of inertia of area, I_P , to the welds of support plate is given by the following equation:

$$I_P = I_X + I_Y$$

Where:

$$I_X = I_{X2} - I_{X1}$$

$$I_Y = I_{Y2} - I_{Y1}$$

The moment of inertia of areas I_X and I_Y to the welds for X-axis and Y-axis are calculated as:

$$I_X = \frac{1}{12} \times 153 \times 83^3 - \frac{1}{12} \times 150 \times 80^3$$

$$= 8.903 \times 10^5 \text{ mm}^4 (2.14 \text{ in}^4)$$

$$I_Y = \frac{1}{12} \times 83 \times 153^3 - \frac{1}{12} \times 80 \times 150^3$$

$$= 2.273 \times 10^6 \text{ mm}^4 (5.46 \text{ in}^4)$$

Accordingly, the moments of inertia of areas to the welds for the support plates are calculated as:

$$I_P = 8.903 \times 10^5 + 2.273 \times 10^6$$

$$= 3.163 \times 10^6 \text{ mm}^4 (7.60 \text{ in}^4)$$

The overall cross-section, A, of welds of the support plate is:

$$A = (153 \times 83) - (150 \times 80)$$

$$= 699 \text{ mm}^2 (1.08 \text{ in}^2)$$

The shearing stress, S_d , on the welds of the support plate for the sling fitting is calculated by a similar equation as the welds of the sling fitting.

$$S_d = \frac{2.809 \times 10^5 \times 3}{699} = 12.1 \text{ MPa (1,760 psi)}$$

In addition, the stress, S_m , on the welds of the support plate due to the bending moment is calculated as:

Where:

$$r = \sqrt{75^2 + 40^2} = 85 \text{ mm (3.35 in)}$$

$$S_m = \frac{5.9 \times 10^4 \times 85 \times 3}{3.163 \times 10^6} = 4.76 \text{ MPa (690 psi)}$$

Accordingly, the composite shearing stress S on the welds of support plate is calculated as:

$$S = \sqrt{S_d^2 + S_m^2 + 2S_d S_m \cos \theta}$$

Where:

$$\cos \theta = 40/85$$

$$S = \sqrt{12.1^2 + 4.76^2 + (2 \times 12.1 \times 4.76 \times (40/85))}$$

$$= 14.9 \text{ MPa (2,160 psi)}$$

Meanwhile, the allowable shearing stress for 300 series stainless steel is 110.8 MPa (16,073 psi). Then the margin of safety (MS) is:

$$MS = \frac{110.8}{14.9} - 1 = 6.4$$

Therefore, the support plate welds are capable of carrying three times the normal load and not yielding.

As indicated by the margins of safety calculated for each component, the hook bar has the lowest margin; therefore in case of an overload the hook bar will fail prior to any other component. This ensures that, at failure, the rest of the packaging is capable of performing its function of protecting the fuel.

2.4.1.2. Package Lifting Using the Outer Container Lid Lifting Lugs

The outer container lid is lifted by four (4) $\varnothing 8$ -mm ($\varnothing 0.315$ in.) Type 304 stainless steel bars that are welded to the $50 \times 50 \times 4$ stainless steel lid flange angle. Under a potential excessive loading condition, such as lifting the entire loaded package, these four lifting lugs are required to fail prior to damaging the outer container lid structure.

The outer container lid is also equipped with the four (4) $\varnothing 6$ -mm ($\varnothing 0.236$ in.) Type 304 stainless steel bar handles, which may be used to manually lift the lid. These bars are welded to the vertical leg of the lid flange angle with single-sided flare-bevel welds for an approximate length of 13 mm, as shown in View G-G on General Arrangement Drawing 105E3743. Since the handles have smaller cross-section ($\varnothing 6$ -mm vs. $\varnothing 8$ -mm), and have smaller and shorter attachment welds, the analysis of the lid lifting bars bounds the handles.

The four lifting bars will be used for this analysis with an assumed lifting angle of 45 degrees. From Table 2-1, the TN-B1 package weighs 1,614 kg [15,827 N] (3,558 lb). For the assumed lifting arrangement, the maximum load on the bar is:

$$F = 1/4 \left[\frac{15,827}{\sin 45^\circ} \right] = 5,596 \text{ N (1,258 lbs)}$$

Assuming that the lift point is centered above the midpoint of the package (located 1,025 mm longitudinally and 318 mm laterally from lifting bar), the resultant forces on the lifting bar will be:

$$F_{\text{horizontal}} = F_{\text{vertical}} = F \cos 45^\circ = 3,957 \text{ N (890 lbs)}$$

$$F_{//} = F_{\text{horizontal}} \sin \left(\tan^{-1} \left(\frac{1,025}{318} \right) \right) = 3,779 \text{ N (850 lbs)}$$

$$F_{\perp} = F_{\text{horizontal}} \cos \left(\tan^{-1} \left(\frac{1,025}{318} \right) \right) = 1,173 \text{ N (264 lbs)}$$

where: $F_{\text{horizontal}}$ = Force in horizontal plane
 F_{\parallel} = Force parallel to longitudinal axis of package
 F_{\perp} = Force perpendicular to longitudinal axis of package

These reaction loads will develop both bending and shear stresses in the bar, shear stresses in the attachment welds, and tensile stresses in the flange angle. Each of these stress components will be analyzed separately.

Bending of Bar

The maximum reaction load on the lifting bar will be bending stresses in the bar. Treating the bar as a fixed-fixed beam, the maximum bending stress, σ_b , will be:

$$\sigma_b = \frac{M_{\max}}{Z_{\text{Bar}}}$$

where: $M_{\max} = 1/8[(F_{\text{vertical}})^2 + (F_{\parallel})^2]^{1/2}(l) = 1/8(5,472)(76) = 51,984 \text{ N}\cdot\text{mm} (460 \text{ lb}\cdot\text{in})$
 $Z_{\text{bar}} = \pi(d^3)/32 = \pi(8^3)/32 = 50.3 \text{ mm}^3 (0.003 \text{ in}^3)$
 $l = 2(46-8) = 76 \text{ mm} (2.99 \text{ in})$ [assumed equal to bent free length of bar]

Substituting these values results in a maximum bending stress of 1,033 MPa (149,824 psi). The allowable bending stress for the Type 304 material is equal to $S_y = 184.7 \text{ MPa} (26,788 \text{ psi})$. Therefore, the margin of safety against yielding in bending is:

$$MS = \frac{184.7}{1,033} - 1.0 = -0.8$$

Shear of Bar

The maximum reaction load on the lifting bar will result in shear stresses in the bar. For the shearing the bar, the maximum shear stress will be:

$$\tau_{\text{bar}} = \frac{[(F_{\text{vertical}})^2 + (F_{\parallel})^2]^{1/2}}{\text{Area}} = \frac{5,472}{(\pi/4)(8)^2} = 108.9 \text{ MPa} (15,795 \text{ psi})$$

The allowable shear stress for the Type 304 material is equal to $0.6S_y = 0.6(184.7) = 110.8 \text{ MPa} (16,070 \text{ psi})$. Therefore, the margin of safety against yielding in shear is:

$$MS = \frac{110.8}{108.9} - 1.0 = 0.02$$

Tension in Bar

Since the bending stress is well beyond the yield strength, the bar will bend until the reaction load will be reacted as pure tension in the bar. For this condition, the tensile stress, σ_{t-bar} , in the bar will be:

$$\sigma_{t-bar} = \frac{F}{2(Area)} = \frac{5,596}{2 \left[\left(\frac{\pi}{4} \right) (8^2) \right]} = 55.7 MPa (8,079 psi)$$

The allowable tensile stress for the Type 304 material is equal to the minimum yield strength, 184.7 MPa (26,788 psi). The margin of safety for this condition is then:

$$MS = \frac{184.7}{55.7} - 1.0 = 2.3$$

Attachment Welds

As shown in View F-F on General Arrangement Drawing 105E3743, the lifting bars are welded to the lid flange angle with double-sided flare-bevel welds for an approximate length of 28 mm (1.10 in.) on each leg of the bar. The ends of the bar are welded with a seal fillet weld, which has minimal strength and hence, will be ignored. Since the bar is relatively small, the flare-bevel weld will be treated as an equivalent fillet weld with a 4-mm leg. For this assumption, the maximum primary shear stress, τ_{weld} , in the weld will be:

$$\tau_{weld} = \frac{[(F_{vertical})^2 + (F_{//})^2]^{1/2}}{\text{Shear area of welds}} = \frac{5,472}{4(4\cos 45^\circ)(28)} = 17.3 MPa (2,509 psi)$$

Due to the off-set, there will also be a secondary (torsion) shear stress, τ'_{weld} , component:

$$\tau'_{weld} = \frac{Mr}{J}$$

where: M = applied moment to weld group
 = $[(F_{vertical})^2 + (F_{//})^2]^{1/2}$ (distance from centroid + bend radius + $\frac{1}{2}$ bar diameter)
 = $5,472(14 + 8 + 4) = 142,272$ N-mm (1,259 lb_f - in)
 r_{max} = distance from centroid of weld group to farthest point in weld
 = $[(1/2(46-8))^2 + (14)^2]^{1/2} = 23.6$ mm (0.929 in)

J = second polar moment of inertia of weld group, mm^4

Since the four flare-bevel welds are the same size and location, the second polar moment of inertia for the weld group is determined treating the welds as a line*. For this case, the second polar moment of inertia is:

$$J = 0.707(h) \frac{d(3b^2 + d^2)}{6}$$

where:

h = leg length of weld = 4 mm

d = length of weld = 28 mm

b = distance between weld groups = $(462 + 462)/2 = 65.1$ mm

Substituting these values results in a secondary polar moment of inertia of $178,138 \text{ mm}^4$ (0.428 in^4). The secondary shear stress then becomes:

$$\tau'_{weld} = \frac{(142,272)(23.6)}{178,138} = 18.8 \text{ MPa (2,727 psi)}$$

The total shear stress in the weld is then the square root of the sum of the squares of the primary shear and secondary shear:

$$\tau_{total} = [(\tau_{weld})^2 + (\tau'_{weld})^2]^{1/2} = 25.5 \text{ MPa (3,698 psi)}$$

The allowable shear stress for the Type 304 material is equal to $110.8 \text{ MPa (16,070 psi)}$. Therefore, the margin of safety against yielding in shear for the welds is:

$$MS = \frac{110.8}{25.5} - 1.0 = 3.3$$

Shear Tearout of Base Metal

Shear tearout of the 4-mm thick base metal is evaluated by conservatively considering only the area of a section equal to the weld length of the two welds. The 2-mm thick sheet that is attached to the vertical leg of the flange angle is ignored for this calculation. The total tensile area, A_t , will be:

* Shigley, Joseph E., and Mischke, Charles R., *Mechanical Engineering Design, Fifth Edition*, McGraw-Hill, Inc., 1989.

$$A_{\text{shear}} = 2[4(28)] = 224 \text{ mm}^2 (0.347 \text{ in}^2)$$

For this case, the shear stress of the base metal, $\tau_{\text{base metal}}$, is:

$$\tau_{\text{base metal}} = \frac{F}{A_{\text{Shear}}} = \frac{5,596}{224} = 25.0 \text{ MPa (3,624 psi)}$$

The allowable shear stress for the Type 304 material is equal to 110.8 MPa (16,070 psi). The margin of safety for this condition is then:

$$MS = \frac{110.8}{25.0} - 1.0 = 3.4$$

Summary

As demonstrated by these calculations, the minimum margin of safety for the outer container lid lifting lugs is -0.8, which results in failure of the bar in bending for lifting the complete loaded package. The largest positive margin of safety (+3.4) occurs in the base metal of the lid flange angle, which demonstrates that the outer container lid structure would not fail in an excessive load condition. All other margins of safety in the load path are positive, but are lower than the base metal. Therefore, potentially lifting the complete package by these lid lifting lugs will fail the lifting bar and have no detrimental effect on the effectiveness of the TN-B1 package.

2.4.2. Tie-Down Devices

There are no tie-down features that are a structural part of the TN-B1 package. The packages are transported either in container vans or on flatbed trucks. When transported in container vans, blocking and bracing is provided that distributes any loads into the packages. This bracing and blocking is customized to address individual shipping configurations and the specific container van being used. When transported on a flatbed trailer, straps going over the package are used to secure it to the trailer. Therefore, the requirements of 10 CFR 71.45(b) are satisfied since no structural part of the package is used as a tie-down device.

An evaluation is performed on the ability of the package to withstand loadings of 2 g vertical and 5 g laterally when restrained by strapping. The worst case loading situation for the packages is when they are stacked in groups of 9 on a flatbed trailer and secured with a minimum of 3 straps. Although the packages may be shipped in other configurations such as 2x3 the greatest strap loading that would be applied to the package when secured in a

3x3 configuration. Between each adjacent column of packages 2 × 4 wood shoring may be placed where the straps will be applied. The evaluation below is conservatively performed without the 2 × 4 shoring in place.

As a bounding evaluation, it is assumed that the outside corners of the top outside packages carry all the vertical loads that would result from the vertical acceleration and the vertical load required to resist the over-turning moment from the horizontal acceleration. The corners of all top packages would actually carry the vertical load. See Figure 2-11.

For modeling purposes, the matrix of nine packages is treated as a rigid body. By summing moments, the vertical force required to prevent the over-turning of the stack by the horizontal loads is determined. This load is conservatively applied to one edge of one container

The key dimensions and weights for each package are:

Width	w = 720 mm (28.3in)
Total Height	h = 742 mm (29.2in)
CG height	cgy = 421 mm (16.6 in)
Mass of each package	m = 1,614 kg (3,558 lb) Gravitational
acceleration	g = 9.81 m/sec ²
Vertical acceleration factor	g _v = 2
Horizontal acceleration factor	g _h = 5

The vertical center of gravity of the 9-package matrix is:

$$CG_y = 3mg(2h + cgy)/9mg + 3mg(h + cgy)/9mg + 3mg(cgy)/9mg = 1.163 \times 10^3 \text{ mm (45.8 in)}$$

Summing the forces in the vertical direction due to the 2 g loading, the strap load applied at the two locations can be determined for this load condition.

$$R_{st} = 9 g_v m g/2 = 1.425 \times 10^5 \text{ N (3.202} \times 10^4 \text{ lb}_f)$$

Summing moments about one of the bottom corners of the stack will determine the strap force required to resist overturning due to the horizontal loading.

$$R_s = \frac{(CG_y)9mg}{(3w)} = 3.835 \times 10^5 \text{ N (8.621} \times 10 \text{ lb}_f)$$

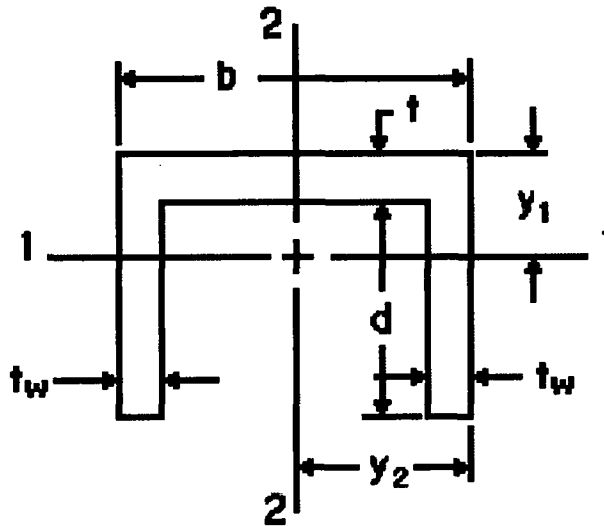
Total vertical strap load is:

$$R_t = R_{st} + R_s = 5.260 \times 10^5 \text{ N } (1.182 \times 10^5 \text{ lbf})$$

Checking the support plate carrying capability:

There are eight (8) 5mm × 55mm support plates in groups of two (2) that carry the vibro-isolation frame inside the outer container. These are skipped welded to the wall, plus have two thick (10 and 15 mm) by 80 mm and 70 mm wide plates welded between them. These plates are in addition to the body straps and the body struts (angles) in corners that provide vertical stiffening to the side panels. On top of the side panel, there are two angles that make up the flange in both the body and the lid that provide load distribution capability to the side wall and the internal structure. In addition these angles are stiffen at the ends by the bolster support angle that further distributes the end strap loads to the end structure of the package reducing load in the sides of the package.

Since the eight support plates are assembled together in groups of two with the reinforcement plates connecting the plates along with the welding to the wall, each two-plate section is considered as a column that is capable of carrying the tie-down loads. Addressing the support plates as a channel section, which is 140 mm wide and 57 mm deep, its properties can be determined.



Channel section

Length of web

$$b = 140 \text{ mm } (5.5 \text{ in})$$

Length of flange

$$d = 55 \text{ mm } (2.2 \text{ in})$$

Web thickness

$$t = 2 \text{ mm } (0.08 \text{ in})$$

Flange thickness

$$t_w = 5 \text{ mm } (0.2 \text{ in})$$

Area

$$A = t_b + 2t_w d = 830.3 \text{ mm}^2 (1.287 \text{ in}^2)$$

Since there are four of these assemblies to a side the total area is:

$$A_{\text{spt}} = 4A = 3,321 \text{ mm}^2 (5.148 \text{ in}^2)$$

The compressive stress is

$$\sigma_c = R_t/A_{\text{spt}} = 158.4 \text{ MPa (23.0 ksi)}$$

This is less than the yield stress of the Type 304 stainless steel $S_y = 206.8 \text{ MPa (30.0 ksi)}$.

The resistance of the plate to buckling is also evaluated. The equation to obtain the moments of inertia of area of the support plate which are subject to buckling is:

$$y_1 = (bt^2 + 2t_w d(2t + d))/2(tb + 2t_w d) = 19.9 \text{ mm (0.783 in)}$$

$$y_2 = b/2 = 70 \text{ mm (2.756 in)}$$

Moments of Inertia

$$I_1 = b(d+t)^3/3 + d^3(b-2t_w)/3 - A(d+t-y_1)^2 = 2.894 \times 10^5 \text{ mm}^4 (0.695 \text{ in}^4)$$

$$I_2 = (d+t)b^3/12 - d(b-2t_w)^3/12 = 2.110 \times 10^7 \text{ mm}^4 (7.122 \text{ in}^4)$$

The radius of gyration can then be calculated for each axis:

$$r_1 = \sqrt{\frac{I_1}{A}} = 18.7 \text{ mm (0.736 in)} \quad r_2 = \sqrt{\frac{I_2}{A}} = 59.7 \text{ mm (2.35 in)}$$

The minimum radius of gyration indicates the weakest orientation for buckling:

$$k = r_1 = 18.7 \text{ mm (0.736 in)}$$

$$l: \text{Length of support plate} = 160 \text{ mm (6.3 in)}$$

Also, the slenderness ratio, $\frac{l}{k}$ is:

$$\frac{L}{k} = \frac{160}{18.7} = 8.6$$

As the ends are fixed, the coefficient "n" becomes 4, so the limit value of the slenderness ratio becomes:

$$85\sqrt{n} = 85\sqrt{4} = 170$$

Because the slenderness ratio of this material is less than the limit value slenderness ratio, Euler's equation is not applicable, and the secant formula for buckling is used. The equation to obtain the support plate's buckling strength is:

$$\frac{P}{A} = \frac{S_y}{1 + \frac{ec}{k^2} \sec \left[\frac{Cl}{2k} \sqrt{\frac{P}{AE}} \right]}$$

Where:

- P: Buckling strength (load) of support column N
- A: Area of column = 830.3 mm² (1.287 in²)
- S_y: Minimum yield strength of Type 304 stainless steel = 206.8 MPa (30.0 ksi)
- C: Coefficient to the long support fixed at both ends = 1.2
- E: Elastic modulus of Type 304 stainless steel = 1.95 × 10⁵ MPa (Table 2-2 at 40°C)
- e: Eccentricity small since the strap load is centered = 5 mm (0.2 in)
- ℓ: Unsupported length of the support column = 160 mm (6.3 in)
- c: Shortest distance to an outside side edge from the centroid = 19.9 mm (0.783 in)

Substituting these values in the above equation and solving for P iteratively results in a buckling strength of the support plate column of:

$$P = 1.332 \times 10^5 \text{ N (29,945 lb}_f\text{)}$$

There are four support columns to a side, which results in the sidewall frame having a minimum capacity of:

$$P_t = 4P = 5.328 \times 10^5 \text{ N (119,780 lb}_f\text{)}$$

Since this load capacity is greater than the applied load ($R_t = 5.259 \times 10^5 \text{ N (1.182} \times 10^5 \text{ lb}_f\text{)}$), the supports will not buckle when the worst case tie-down loads are applied to a package. This capacity approaches the force required to yield the columns in compression (i.e., $A_{spt}S_y = 6.868 \times 10^5 \text{ N (1.544} \times 10^5 \text{ lb}_f\text{)}$).

By considering the stiffening of the support plates with the reinforcement plates used to carry the inner support frame, it has been demonstrated that the support plates have

sufficient capacity to react the tie-down load if the package experiences a 5 g lateral and a 2 g vertical loading simultaneously. This evaluation does not take into consideration the large carrying capability of the ends of the package where there are corner angles, end plates, and wood overlay plates that further strengthen the package's buckling capability. The use of three or more straps ensures that the load is distributed along the package so that the load can be reacted by the support plates and other internal structure. The stiffness of the OC lid, when the bolster support angles are considered with the reinforced edge of the OC body, ensures that the load is distributed to the internal structure of the package.



Security-Related Information
Figure Withheld Under 10 CFR 2.390

Figure 2-2 Inner Container Sling Locations



Security-Related Information
Figure Withheld Under 10 CFR 2.390

Figure 2-4 Lifting Configuration of Inner Container



Security-Related Information
Figure Withheld Under 10 CFR 2.390

Figure 2-5 Center of Gravity of Loaded Inner Container



Security-Related Information
Figure Withheld Under 10 CFR 2.390

Figure 2-6 Hooking Bar of Sling Fitting



Security-Related Information
Figure Withheld Under 10 CFR 2.390

Figure 2-8 Sling Fitting Weld Geometry for Attachment to Support Plate



Security-Related Information
Figure Withheld Under 10 CFR 2.390

Figure 2-10 Welds for Support Plate Attachment to Body



Figure 2-11 Tie-Down Configuration

2.5. GENERAL CONSIDERATIONS

2.5.1. *Evaluation by Test*

The primary means of demonstrating that the package meets the regulatory accident conditions was by test. The package was tested full-scale by dropping two units from 9 meters in different orientations. The weight of the units was maximized to provide bounding conditions.

Within both units, the fuel was mocked up by a metal boxed section that provided the representative weight in one fuel assembly shipping location. The steel section was segmented to prevent the mockup from adding unrealistic stiffness to the package. In the other fuel assembly shipping position a mock up fuel assembly was used. This had the same cross-sectional properties of the actual fuel. The rods were filled with lead to represent the actual fuel. Weights were added along side of the assembly to provide the correct mass for fuel that may be shipped with channels as well as allowing for the different density between the lead and the uranium oxide pellets.

Details of the prototypes used in the drop testing can be found in Section 2.7 and Appendix 2.12.

The damage caused by the test was evaluated in each of the affected sections, Section 3.0, Section 4.0, and Section 6.0. Both the inner and outer lids stayed in place, although damaged. The inner container holding frame deformed but restrained the inner container. Due to the end drop there was some plastic deformation of the fuel but well within the limits of the criticality evaluation. After the testing the fuel passed a helium leak test demonstrating containment.

2.5.2. *Evaluation by Analysis*

The normal conditions of transport were evaluated by analysis and by comparison to the accident testing. The primary analysis was done for the compression loading. The material properties are taken from Table 2-4, which is based on published ASME properties. A static analysis was performed in Section 2.6.9 Compression.

Since the normal condition pressure and temperatures are well below the design conditions for the fuel cladding no separate analysis was performed.

2.6. NORMAL CONDITIONS OF TRANSPORT

The TN-B1 package, when subjected to the Normal Conditions of Transport (NCT) specified in 10 CFR 71.71, is shown to meet the performance requirements specified in Subpart E of 10 CFR 71. As discussed in the introduction to this chapter, with the exception of the NCT free drop, the primary proof of NCT performance is via analytic methods. Regulatory Guide 7.6 criteria are demonstrated as acceptable for NCT analytic evaluations presented in this section. Specific discussions regarding brittle fracture and fatigue are presented in Sections 2.1.2.4 and 2.6.5 and are shown not to be limiting cases for the TN-B1 package design. The ability of the welded containment fuel rod cladding to remain leak-tight is documented in Section 4.0.

Properties of Type 304 stainless steel as representative of those properties for 300 series stainless steel are summarized below.

Table 2-5 Material Properties

Material Property	Material Property Value (psi)			Reference
	-40 °C (-40 °F)	21°C (70 °F)	75°C (167°F)	
	Type 304 Stainless Steel			
Elastic Modulus, E	198.6GPa (28.8×10 ⁶ psi)	195.1GPa (28.3×10 ⁶ psi)	191.7GPa (27.8×10 ⁶ psi)	Table 2-2
Design Stress Intensity, S _m	137.9MPa (20,000 psi)	137.9MPa (20,000 psi)	137.9MPa (20,000 psi)	
Yield Strength, S _m	206.8MPa (30,000psi)	206.8MPa (30,000psi)	184.7MPa (26,788psi)	
Tensile Strength	517.1MPa (75,000psi)	517.1MPa (75,000psi)	498.6MPa (72,300)	

The TN-B1 package's ability to survive HAC, 30-foot free drop, 40-inch puncture drop, and 30-minute thermal event also demonstrated the packages ability to also survive the NCT. Evaluations are performed, when appropriate, to supplement or expand on the available test results. This combination of analytic and test structural evaluations provides an initial configuration for NCT thermal, shielding and criticality performance. In accordance with 10 CFR 71.43(f), the evaluations performed herein successfully demonstrate that under NCT

tests the TN-B1 package experiences “no substantial reduction in the effectiveness of the packaging”. Summaries of the more significant aspects of the full-scale free drop testing are included in Section 2.6.7, with details presented in Appendix 2.12.1.

2.6.1. Heat

The NCT thermal analyses presented in Section 3.0, consist of exposing the TN-B1 package to direct sunlight and 100 °F still air per the requirements of 10 CFR 71.71(b). Since there is negligible decay heat in the unirradiated fuel, the entire heating came from the solar insolation. The maximum temperature of 77°C (171°F) was located on the lid of the outer container.

2.6.1.1. Summary of Pressures and Temperatures

The fuel assembly exhibits negligible decay heat. The TN-B1 package and internal components, when loaded with the required 10 CFR 71.71(c) (1) insulation conditions, develop a maximum temperature of 77 °C (171 °F). The resulting pressure at the maximum temperature is 1.33 MPa (192.9 psia).

2.6.1.2. Differential Thermal Expansion

With NCT temperatures throughout the packaging being relatively uniform (i.e. no significant temperature gradients), the concern with differential expansions is limited to regions of the TN-B1 packaging that employ adjacent materials with sufficiently different coefficients of thermal expansion. The IC is a double-walled, composite construction of alumina silicate thermal insulator between inner and outer walls of stainless steel. The alumina silicate thermal insulator is loosely packed between the two walls and does not stress the walls. Differential thermal expansion stresses are negligible in the OC for three reasons: 1) the temperature distribution throughout the entire OC is relatively uniform, 2) the OC is fabricated from only one type of structural material, and 3) the OC is not radially or axially constrained within a tight-fitting structure due to the relatively low temperature differentials and lack of internal restraint within the TN-B1 package.

The cladding of the fuel which serves as containment is not stressed due to differential thermal expansion since a gap remains between the fuel pellet and the cladding at both the cold temperature -40°C and the highest temperature the fuel could see due to the HAC which is 800°C. This is demonstrated as follows:

The nominal fuel pellet and cladding dimensions and the resulting radial gap (0.00335 inches) is shown below based on a temperature of 20°C:

As-Built Dimensions (inches)		
Nominal Clad OD	D_{co}	0.3957
Nominal Clad ID	D_{ci}	0.348
Nominal Pellet OD	D_{fo}	0.3413
Nominal Radial Pellet/Clad	g_n	0.00335

The strain due to thermal expansion or contraction in the Zr cladding is equal to*

$$\left(\frac{\Delta D}{D}\right)_{clad} = 7.4 \times 10^6 (\Delta T)$$

Where ΔT is positive for an increase in temperature and negative for a decrease in temperature.

The strain due to thermal expansion or contraction in the fuel pellet is equal to†:

$$\left(\frac{\Delta D}{D}\right)_{clad} = -3.28 \times 10^{-3} + 1.179 \times 10^{-5} T - 2.429 \times 10^{-9} T^2 + 1.219 \times 10^{-12} T^3$$

Where T is the absolute final temperature in degrees Kelvin (K).

The following table summarizes the thermal strain and the thermal growth in the cladding and pellets with a temperature change from 20°C to -40°C ($\Delta T = -60$ C, $T = 233$ K). All dimensions are expressed in inches.

* Framatome ANP MOX Material Properties Manual 51-5010288-03

† Framatome ANP MOX Material Properties Manual 51-5010288-02

Table 2-6 Thermal Contraction at -40°C

	Strain at -40°C $\left(\frac{\Delta D}{D}\right)$	Thermal Expansion at -40°C $\left(\frac{\Delta D}{D}\right)D$	Dimension at -40°C $D + \left(\frac{\Delta D}{D}\right)D$
Pellet OD	-6.49×10^{-4}	-2.22×10^{-4}	0.3411
Cladding ID	-4.44×10^{-4}	-1.55×10^{-4}	0.3478

This results in a radial gap at -40°C of:

$$g_{-40} = \frac{0.3478 - 0.3411}{2} = 0.0034 \text{ in}$$

The following table summarizes the thermal strain and the thermal growth in the cladding and pellets with a temperature change from 20°C to 800°C ($\Delta T = 780^\circ\text{C}$, $T = 1,073\text{K}$). All dimensions are expressed in inches.

Table 2-7 Thermal Expansion at 800°C

	Strain at 800°C $\left(\frac{\Delta D}{D}\right)$	Thermal Expansion at 800°C $\left(\frac{\Delta D}{D}\right)D$	Dimension at 800°C $D + \left(\frac{\Delta D}{D}\right)D$
Pellet OD	8.08×10^{-3}	2.76×10^{-3}	0.3441
Cladding ID	5.77×10^{-3}	2.01×10^{-3}	0.3500

This results in a radial gap at 800°C of:

$$g_{800} = \frac{0.3500 - 0.3411}{2} = 0.0030 \text{ in}$$

2.6.1.3. Stress Calculations

Since the temperatures and pressures generated under normal conditions of transport are well below the design conditions for the boiling water reactor fuel no specific calculations were performed for the fuel containment.

2.6.1.4. Comparison with Allowable Stresses

The normal conditions of transport conditions are well below the operating conditions of the fuel no comparison to allowable stresses was performed.

2.6.2. *Cold*

The NCT cold condition consists of exposing the TN-B1 packaging to a steady-state ambient temperature of -40 °F. Insulation and payload internal decay heat are assumed to be zero. These conditions will result in a uniform temperature throughout the package of -40 °F. With no internal heat load (i.e., no contents to produce heat), the net pressure differential will only be reduced from the initial conditions at loading.

For the containment, the principal structural concern due to the NCT cold condition is the effect of the differential expansion of the fuel to the zirconium alloy tube. During the cool-down from 20 °C to -40 °C, the tube could shrink onto the fuel because of difference in the thermal expansion coefficient. However, the clearance between the fuel and the cladding is such that even if the fuel did not shrink, there would still be clearance. Differential thermal expansion stresses are negligible in the package for three reasons: 1) the temperature distribution throughout the entire package is relatively uniform, 2) the package is fabricated from only one type of structural material, and 3) the package is not radially or axially constrained.

Brittle fracture at -40 °F is addressed in Section 2.1.2.4.1.

2.6.3. *Reduced External Pressure*

The effect of a reduced external pressure of 25 kPa (3.5 psia) per 10 CFR 71.71(c)(3) is negligible for the TN-B1 packaging. The TN-B1 package contains no pressure-tight seal and therefore cannot develop differential pressure. Therefore, the reduced external pressure requirement of 3.5 psia delineated in 10 CFR 71.71(c)(3) will have no effect on the package. Compared with the 1.115 MPa (161.7 psia) internal pressure in the fuel rods, a reduced external pressure of 3.5 psia will have a negligible effect on the fuel rods.

2.6.4. Increased External Pressure

The TN-B1 package contains no pressure-tight seal and, therefore, cannot develop differential pressure. Therefore, the increased external pressure requirement of 140 kPa (20 psia) delineated in 10 CFR 71.71(c)(4) will have no effect on the package. The pressure-tight cladding of the fuel rods is designed for much higher pressures in its normal service in a reactor and is not affected by the slight increase in external pressure.

The containment is provided by the cladding tubes of the fuel. These tubes, designed for the conditions in an operating reactor, have the capability of withstanding the increased external pressure. The failure mode of radial buckling is not a plausible failure mode since the fuel pellets would prevent any significant deformation due to external pressure.

2.6.5. Vibration

The TN-B1 packaging contains an internal shock mount system and, therefore, cannot develop significant vibratory stresses for the package's internal structures. Therefore, vibration normally incident to transportation, as delineated in 10 CFR 71.71(c)(5), will have a negligible effect on the package. Due to concerns of possibly damaging the fuel so it cannot be installed in a reactor after transport, extreme care is taken in packaging the fuel using cushioning material and vibration isolation systems. These systems also ensure that the fuel containment boundary also remains uncompromised. The welded structure of the light weight TN-B1 package is unaffected by vibration. However, after each use the packaging is visually examined for any potential damage.

2.6.6. Water Spray

The materials of construction of the TN-B1 package are such that the water spray test identified in 10 CFR 71.71(c)(6) will have a negligible effect on the package.

2.6.7. Free Drop

Since the maximum gross weight of the TN-B1 package is 1,614 kg (3,558 lb), a 1.2 m or four-foot free drop is required per 10 CFR 71.71(c)(7). The Hypothetical Accident Condition (HAC), 9 m (30 foot) free drop test required in 10 CFR 71.73(c)(1) is substantially more damaging than the 1.2 m (4 foot) NCT free drop test. Section 2.7.1 demonstrates the TN-B1 package's survivability and bounds the free drop requirements of 10 CFR 71.71(c)(7). Due to the relatively fragile nature of the fuel assembly payload in maintaining its configuration for operational use, any event that would come close to approximating the NCT free drop would cause the package to be removed from service and re-examined prior to continued use.

As part of the effort to obtain package certification in Japan by GNF-J, certification testing of the package, which included both an end drop and a lid-down horizontal drop, was performed. In each case a 0.3-meter (1-foot) and a 1.2 meter (4-foot) drop was performed prior to the 9-meter (30-foot) drop. In both cases the test package was slightly damaged but the damage had no significant effect on the performance of the package in relation to either the containment or the ability of the package to meet the requirements of 10 CFR 71. The GNF-J certification testing is discussed in Appendix 2.12.2.

Therefore, the requirements of 10 CFR 71.71(c)(7) are met.

2.6.8. Corner Drop

This test does not apply, since the package weight is in excess of 100 kg (220 pounds), and the structural materials used in the TN-B1 are not primarily wood or fiberboard, as delineated in 10 CFR 71.71(c)(8).

2.6.9. Compression

Since the package weighs less than 5,000 kg (11,000 pounds), as delineated in 10 CFR 71.71(c)(9), the package must be able to support five times its weight without damage.

The load to be given as the test condition is the load (W_1) times five of the weight of this package or the load (W_2) which is obtained through multiplying the package's vertical projected area by 13 kPa, whichever is heavier. In the case of this package, the equations to obtain each load are:

$$W_1 = 5 \times m \times g$$

$$W_2 = 13 \text{ kPa} \times L \times B$$

Where:

m: Mass of package	1,614 kg (3,558 lb)
g: Gravitational acceleration	9.81 m/s ²
L: Length of package	5,068 mm (199.53 in)
B: Width of package	720 mm (28.35 in)

From this

$$W_1 = 5 \times 1,614 \times 9.81 = 79.16 \text{ kN (17,800 lbf)}$$

$$W_2 = 13 \times 10^{-3} \times 5,068 \times 720 = 47.4 \text{ kN (10,660 lbf)}$$

Therefore, as $W_1 > W_2$, the stacking load is assumed as $W = 79.16 \text{ kN (17,800 lbf)}$.

The stacking of these packages is as shown in Figure 2-12, so the outer container only sustains the stacking load. In this case, it is assumed that loads are carried by a total of eight support plates positioned in the center of the bolster out of sixteen support plates of the outer container body positioned at the lowest layer. This assumption makes the load sustaining area smaller, so the evaluation is conservative. The compressive load given to the support plate is the above-mentioned stacking load plus the weight of the outer container's lid.

The equation to obtain the support plate's compressive load is:

$$W_c = W_1 + W_3$$

W_c : Compressive load N

W_1 : Stacking load 79.16 kN (17,800 lbf)

W_3 : Load by the outer container's lid 1.34 kN (301 lbf)

m_F : Mass of outer container lid 137 kg (302 lb)

g : Gravitational acceleration 9.81m/s²

From this, the 80.5 kN (18,100 lbf)

When the fuel assemblies are packed, the gravity center of the outer container is shifted longitudinally, so the load acting on the support plate, which is closer to the gravity center, becomes larger.

Therefore, the equation to obtain the vertical maximum load given to one support plate, which is closer to the gravity center, is:

$$P = \frac{W}{4} \frac{\ell_2}{\ell_0}$$

Where:

P : Maximum load acting on one support plate
which is nearer to the gravity center N

W : Compressive load given to the support plate 80.5 kN (18,100 lbf)

ℓ_0 : Longitudinal support plate space 3,510 mm (138.2 in)

l_2 : Distance from the package's gravity center position to the support

$$\frac{3,510}{2} + 92 = 1,847 \text{ mm (73.76 in)}$$

From this, the maximum load P acted to one support plate, which is nearer to the gravity center, is:

$$P = \frac{80.5 \times 10^3 \times 1,847}{4 \times 3,510} = 10.6 \times 10^3 \text{ N (2,380 lbf)}$$

The resistance of the plate to buckling is also evaluated. The equation to obtain the moment of inertia of area of the support plate which is subject to buckling is:

$$I_z = \frac{1}{12} hb^3$$

Where:

I_z : Moment of inertia of area of support plate mm⁴

b: Thickness of support plate 5 mm (0.2 in)

h: Width of support plate 55 mm (2.2 in)

From this, the moment of inertia of area, I_z , of the support plate is:

$$I_z = \frac{1}{12} \times 55 \times 5^3 = 572.9 \text{ mm}^4 (1.376 \times 10^{-3} \text{ in}^4)$$

Also, the equation to obtain the radius of gyration of the area of the support plate is:

$$k = \sqrt{\frac{I_z}{A}}$$

Where:

k: Radius of gyration of area of support plate mm

I_z : Moment of inertia of area of support plate 572.9 mm⁴ (1.376x10⁻³ in⁴)

A: Cross-sectional area of support plate $5 \times 55 = 275 \text{ mm}^2 (0.426 \text{ in}^2)$

ℓ: Length of support plate 559 mm (22.4 in)

From this, the radius of gyration of area k of the support plate is:

$$k = \sqrt{\frac{572.9}{275}} = 1.44 \text{ mm (0.0568 in)}$$

Also, the slenderness ratio $\frac{\ell}{k}$ is:

$$\frac{\ell}{k} = \frac{559}{1.44} = 388$$

As the ends are fixed, the coefficient n becomes 4, so the limit value of the slenderness ratio becomes as below.

$$85\sqrt{n} = 85\sqrt{4} = 170$$

Because the slenderness ratio of this material, 388, exceeds the limit value of slenderness, Euler's equation is used. The equation to obtain the support plate's buckling strength is:

$$P_k = \frac{n\pi^2 E I_z}{\ell^2}$$

Where:

P_k : Buckling strength (load) of support plate	N
n: Coefficient to the long support fixed at both ends	4
E: Longitudinal elasticity modulus of Gr304 stainless steel	$1.94 \times 10^5 \text{ MPa (at } 40^\circ\text{C)}$
I_z : Moment of inertia of area of support plate	$572.9 \text{ mm}^4 (1.376 \times 10^{-3} \text{ in}^4)$
ℓ: Length of the support plate	559 mm (22.4 in)

From this, the buckling strength P_k of the support plate is:

$$P_k = \frac{4 \times 3.14^2 \times 1.94 \times 10^5 \times 572.9}{559^2} = 14 \times 10^3 \text{ N (3,050 lb)}$$

Therefore, $P_k > P$, so the body support plate will not buckle.

2.6.10. Penetration

The one-meter (40-inch) drop of a 6 kg (13-pound), hemispherical-headed, 3.2 cm (1.3-inch) diameter, steel cylinder, as delineated in 10 CFR 71.71(c)(10), is of negligible consequence to the TN-B1 package. This is due to the fact that the TN-B1 package is designed to minimize the consequences associated with the much more limiting case of a 40-inch drop of the entire package onto a puncture bar as discussed in Section 2.7.3. The drop of the 6 kg bar will not damage the outer container.

Table 2-8 Temperatures

Location	Maximum temperature
Environment (Open air)	38°C
Package's external surface	77°C
Inner container	<77°C

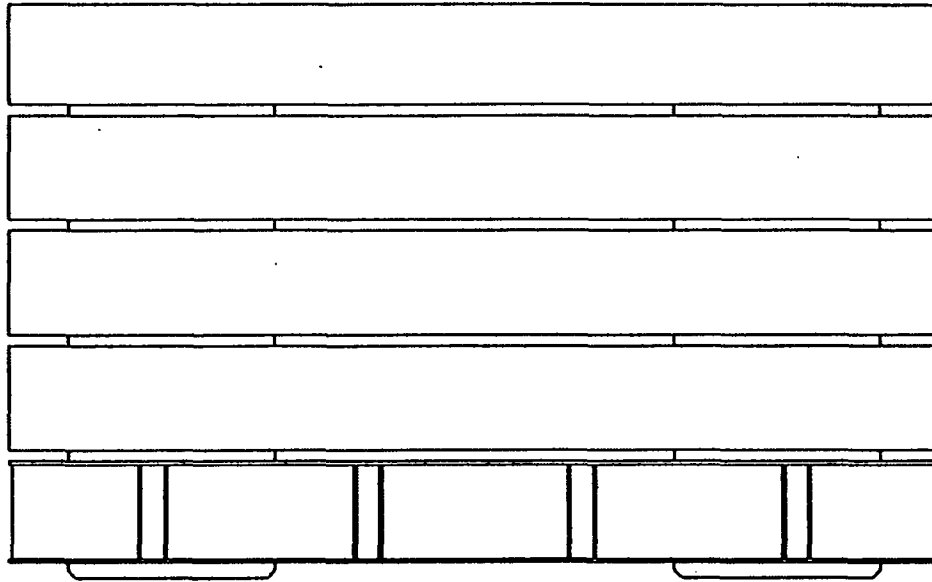


Figure 2-12 Stacking Arrangement

2.7. HYPOTHETICAL ACCIDENT CONDITIONS

The TN-B1 package, when subjected to the sequence of Hypothetical Accident Condition (HAC) tests specified in 10 CFR 71.73 is shown to meet the performance requirements specified in Subpart E of 10 CFR 71. The primary proof of performance for the HAC tests is via the use of full-scale testing. A certification test unit (CTU) was free dropped, and puncture tested to confirm that both the inner and outer containers protected the fuel and allowed containment to be maintained after a worst-case HAC sequence. Another CTU was free dropped from 9 meters on its end with the fuel maintaining containment after the drop. Observations from CTU testing confirm the conservative nature of the deformed geometry assumptions used in the criticality assessment provided in Chapter 6.0. Immersion is addressed by comparison to the design basis for the fuel.

Test results are summarized in Section 2.7.8, with details provided in Appendix 2.12.1.

2.7.1. *Free Drop*

Subpart F of 10 CFR 71 requires performing a free drop test in accordance with the requirements of 10 CFR 71.73(c)(1). The free drop test involves performing a 30-foot, HAC free drop onto a flat, essentially unyielding, horizontal surface, with the package striking the surface in a position (orientation) for which maximum damage is expected. The ability of the TN-B1 package to adequately withstand this specified free drop condition is demonstrated via testing of four full-scale, certification test units (CTUs).

To properly select a worst-case package orientation for the 30-foot free drop event, items that could potentially compromise containment integrity, shielding integrity, and/or criticality safety of the TN-B1 package must be clearly identified. For the TN-B1 packaging design, there are two primary considerations 1) protect the fuel so that containment is maintained and 2) ensure sufficient structure is around the package to maintain the geometry used in the criticality safety evaluation. Shielding integrity is not a controlling case for the reasons described in Section 5.0. Criticality safety is conservatively evaluated based on measured physical damage to the outer container from certification testing, as described in Section 6.0.

Since the containment is welded closed, the leak-tight capability of the containment may be compromised by two methods: 1) as a result of excessive deformation leading to rupture of the containment boundary, and/or 2) as a result of thermal degradation of the containment material itself in a subsequent fire event and rupture of the weld or the cladding tube by over-pressurization. Importantly, these methods require significant impact damage to the

surrounding outer and inner container so that the fuel is either loaded externally or the fuel is directly exposed to the fire.

Additional items for consideration include the possibility of separating the OC lid from the OC body and buckling or deforming of the Outer Container (OC) and/or Inner Container (IC) from an end drop or horizontal drop.

For the above reasons, testing must include impact orientations that affect the lid and stability of the walls of the containers. In general, the energy absorbing capabilities of the TN-B1 are governed by the deformation of the stainless steel and impregnated paper honeycomb that is not significantly affected by temperature.

Appendices 2.12.1 and 2.12.2 provide a comprehensive report of the certification test process and results. Discussions specific to CTU test orientations for free drop and puncture, including initial test conditions, are also provided.

The TN-B1 package has undergone extensive testing during its development. Testing has included 1.2-meter (4-foot) drops on the end in the vertical orientation and the lid in the horizontal orientation. The package has been also dropped from 9 meters in the same orientation demonstrating that the damage from the 1.2-meter (4-foot) drops has little consequence on the performance of the package in 9-meter (30-foot) drop. Based on these preliminary tests it was determined that the worst case orientation for the 9-meter (30-foot) drop test would be slap-down on the lid. The lid down drop demonstrated that the vibration isolation frame bolts would fail allowing the inner container to come in contact with the paper honeycomb in the lid and partially crush the honeycomb. It was expected that the slap-down orientation would maximize the crush of this material minimizing the separation distance between the fuel assemblies in the post accident condition.

A single "worst-case" 9-meter (30-foot) free drop is required by 10 CFR 71.73(c)(1). Based on the above discussion and experience with other long slender packages similar to the TN-B1, a 15 degree slap-down on the lid was chosen for the 9-meter (30-foot) drop. Following that drop, a 25 degree oblique puncture drop on the damaged lid was performed. See Figure 2-13, Figure 2-14 and Appendix 2.12.1.

Other free drop orientations that were tested include vertical end and bottom corner. These tests demonstrated that the TN-B1 package contains the fuel assemblies without breaching the fuel cladding (containment boundary).

2.7.1.1. End Drop

9-meter (30-foot) end free drops were performed on GNF-J CTU 1J and GNF-A CTU 2. The orientation was selected with the lower end of the fuel down to maximize the damage since the expansion springs in the fuel rods are located in the upper end. This orientation

maximized the damage to the energy absorbing wood in the end of the TN-B1 and maximized the axial loading on the fuel assembly. Both tests resulted in deformations of the fuel but were within the limits evaluated in the criticality evaluation in Section 6.0. Following the GNF-A tests, the fuel rods were demonstrated to maintain containment after the free and puncture drops, thus maintaining its containment boundary integrity. Although this orientation caused the most severe damage to the fuel, the damage was well within the structural limits for the fuel and package.

2.7.1.2. Side Drop

No side drop testing was performed in this certification sequence. A side drop test was done in previous testing of the package. That testing resulted in the inner container holding frame top bolts failing and allowing the inner container to come in contact with the outer lid. The inner package showed little damage and the fuel was not deformed. It was judged that the slapdown and the horizontal drop tests bounded the side drop orientation.

2.7.1.3. Corner Drop

A 9-meter (30-foot) free drop on the OC body bottom corner was performed on GNF-J CTU 1J. The impact point previously sustained damage due to 0.3-meter (1-foot) and 1.2-meter (4-foot) free drops. The resultant cumulative deformation was approximately 163 mm (6 inches). There was no loss of contents or significant structural damage to the OC as a result of this free drop. The maximum recorded impact acceleration was 203g. Refer to Appendix 2.12.2 for complete details of the corner free drop.

2.7.1.4. Oblique Drops

An orientation of 15 degrees from horizontal was tested with GNF-A CTU 1. The IC holding frame was plastically deformed and only a portion of the bolts failed. Neither the fuel nor the IC were not significantly damaged. The damage sustained was bounded by the assumptions utilized in the criticality and thermal evaluations. The fuel was leak tested after the test and was demonstrated to have maintained containment boundary. Refer to Appendix 2.12.1 for complete details of the 15-degree oblique free drop.

2.7.1.5. Horizontal Drop

A 9-meter (30-foot) horizontal free drop on the OC lid was performed on GNF-J CTU 2J. The impact results in a maximum deformation of 19 mm (0.8 inch), which occurred in the OC lid. The side wall of the OC body bulged approximately 19 mm (0.8 inches). Some localized weld failure of OC lid flange/OC lid interface occurred where the bolster angles attach to the lid. None of the OC lid bolts failed as a result of the impact. There was no loss

of contents as a result of the free drop. The maximum recorded impact acceleration was 146g. Refer to Appendix 2.12.2 for complete details of the horizontal free drop.

2.7.1.6. Summary of Results

Successful HAC free drop testing of the test units indicates that the various TN-B1 packaging design features are adequately designed to withstand the HAC 30-foot free drop event. The most important result of the testing program was the demonstrated ability of the fuel to remain undamaged and hence maintain its containment capability as defined by ANSI N14.5.

The TN-B1 also maintained its basic geometry required for nuclear criticality safety. Observed permanent deformations of the TN-B1 packaging were less than those assumed for the criticality evaluation.

The GNF-A mock-up fuel assembly rods were leakage rate tested after the conclusion of the testing and were demonstrated to be leaktight, as defined in ANSI N14.5.

A comprehensive summary of free drop test results are provided in Appendices 2.12.1 and 2.12.2.

2.7.2. *Crush*

Subpart F of 10 CFR 71 requires performing a dynamic crush test in accordance with the requirements of 10 CFR 71.73(c)(2). Since the TN-B1 package weight exceeds 500 kg (1,100 pounds), the dynamic crush test is not required.

2.7.3. *Puncture*

Subpart F of 10 CFR 71 requires performing a puncture test in accordance with the requirements of 10 CFR 71.73(c)(3). The puncture test involves a 1-meter (40-inch) free drop of a package onto the upper end of a solid, vertical, cylindrical, mild steel bar mounted on an essentially unyielding, horizontal surface. The bar must be 150 mm (6 inches) in diameter, with the top surface horizontal and its edge rounded to a radius of not more than 6 millimeter (0.25 inch). The package is to be oriented in a position for which maximum damage will occur. The length of the bar used was approximately 1.5 meters (60 inches). The ability of the TN-B1 package to adequately withstand this specified puncture drop condition is demonstrated via testing of the full-scale RAJ-II CTUs.

To properly select a worst-case package orientation for the puncture drop event, items that could potentially compromise containment integrity and/or criticality safety of the TN-B1 package must be clearly identified. For the TN-B1 package design, the foremost item to be addressed is the ability of the containment to remain leak-tight. Shielding integrity is not a

controlling case for the reasons described in Chapter 5.0. Criticality safety is conservatively evaluated based on measured physical damage to the outer container walls as described in Section 6.0.

Previous testing has shown that the 1-meter drop onto the puncture bar did not penetrate the outer wall or damage the fuel. Based on this previous testing and other experience, an oblique and horizontal puncture drop orientations centered over the fuel were chosen as the most damaging.

Appendices 2.12.1 and 2.12.2 provide a comprehensive report of the certification test process and results. Discussions specific to the configuration and orientation of the test unit are provided.

The "worst-case" puncture drop as required by 10 CFR 71.73(c)(3) was performed on the package with the lid down and 25 degrees from horizontal. The angle was chosen based on experience with other packages and the TN-B1. The puncture bar was aimed at the CG of package to maximize the energy imparted to the package.

The puncture pin did not penetrate the outer container. It deformed the lid inward and it contacted the inner container lid and deformed it a small amount. The outer lid total deformation was less than 12 cm (4.7 inches) and the inner container lid deformed less than 5 cm (2.0 inches).

2.7.4. Thermal

Thermal testing of the GNF-J CTU 2J was performed following the free drop and puncture drop tests (refer to Appendix 2.12.2). Although there was no failure of the containment boundary due to the thermal testing, the thermal evaluation of the TN-B1 package for the HAC heat condition as presented in Section 3.0, demonstrates the regulatory compliance to 10 CFR 71.73(c)(4). Because the TN-B1 package does not contain pressure-tight seals, the HAC pressure for the OC and the IC is zero. The fuel assembly exhibits negligible decay heat.

2.7.4.1. Summary of Pressures and Temperatures

The maximum predicted HAC temperature for the fuel assembly is 921 K (1,198 °F) during the fire event. The fuel rods are designed to withstand a minimum temperature of 1,073 K (1,475°F) without bursting. This has been demonstrated by heating representative fuel rods to this temperature for over 30 minutes. This heating resulted in rupture pressures in the excess of 3.6MPa (520 psi). The pressure due to the accident conditions does not exceed 3.5 MPa (508 psig). Summary of pressures and related stresses are provided in Section 3.0.

2.7.4.2. Differential Thermal Expansion

The fuel cladding is not restricted by the packaging and hence can not develop any significant differential thermal expansion stresses. The packaging itself is made of the same metal (austenitic stainless steel) eliminating any significant stresses due to differential thermal expansion.

2.7.4.3. Stress Calculations

Stress calculations for the controlling hoop stress for the fuel cladding that provides containment is provided in Section 3.0.

2.7.4.4. Comparison with Allowable Stresses

The allowable stress used in the analysis in Section 3.0 is based on empirical data from burst tests performed on fuel rods when heated to 800 °C and above. The allowed fuel cladding configurations for the TN-B1 have a positive margin of safety based on stresses required to fail the fuel in the test.

2.7.5. ***Immersion – Fissile Material***

Subpart F of 10 CFR 71 requires performing an immersion test for fissile material packages in accordance with the requirements of 10 CFR 71.73(c)(5). The criticality evaluation presented in Chapter 6.0 assumes optimum hydrogenous moderation of the contents, thereby conservatively addressing the effects and consequences of water in-leakage.

2.7.6. ***Immersion – All Packages***

Subpart F of 10 CFR 71 requires performing an immersion test for packages in accordance with the requirements of 10 CFR 71.73(c)(6). Since the TN-B1 package is not sealed against pressure, there will not be any differential pressure with the water immersion loads defined in 10 CFR 71.73(c)(6). The water immersion will have a negligible effect on the container and the payload, consisting of the fuel assemblies that provide the containment. The fuel rods are designed to withstand differential pressures greater than 1,000 psi. Submergence is a normal design condition for the fuel assemblies and the evaluations are performed on that condition.

2.7.7. ***Deep Water Immersion Test (for Type B Packages Containing More than 10⁵ A₂)***

Not applicable. The TN-B1 does not contain more than 10⁵ A₂.

2.7.8. Summary of Damage

As discussed in the previous sections, the cumulative damaging effects of the free drops and a puncture drop were satisfactorily withstood by the RAJ-II packaging during certification testing. Subsequent helium leak testing confirmed that containment integrity was maintained throughout the test series. The package was also successfully evaluated for maintaining containment during and after the fire event. The deformation of the package in the worst case HAC did not exceed that which is evaluated for in Chapter 6.0. Therefore, the requirements of 10 CFR 71.73 have been satisfied.

Table 2-9 Summary of Tests for RAJ-II

Test No.	Test Description	Test Unit Angular Orientation		CTU Temperature	Remarks
		Axial ¹	Rotational		
1	9 - meter (30-foot) slap down	15°	Lid down	Ambient	Top of package impacted first. Lid crushed over 11 cm (4.3 in).
2	Puncture	25°	Lid down	Ambient	Puncture pin crushed the outer lid down to the inner container lid. It did not rupture the outer lid or significantly deform the inner container lid or fuel.
3	9 - meter (30-foot) end drop	90°	Bottom down	Ambient	Crushed end wood impact absorber. Deformed the fuel assembly but did little damage to the rods

Notes:

¹ Axial angle, θ , is relative to horizontal (i.e., side drop orientation)

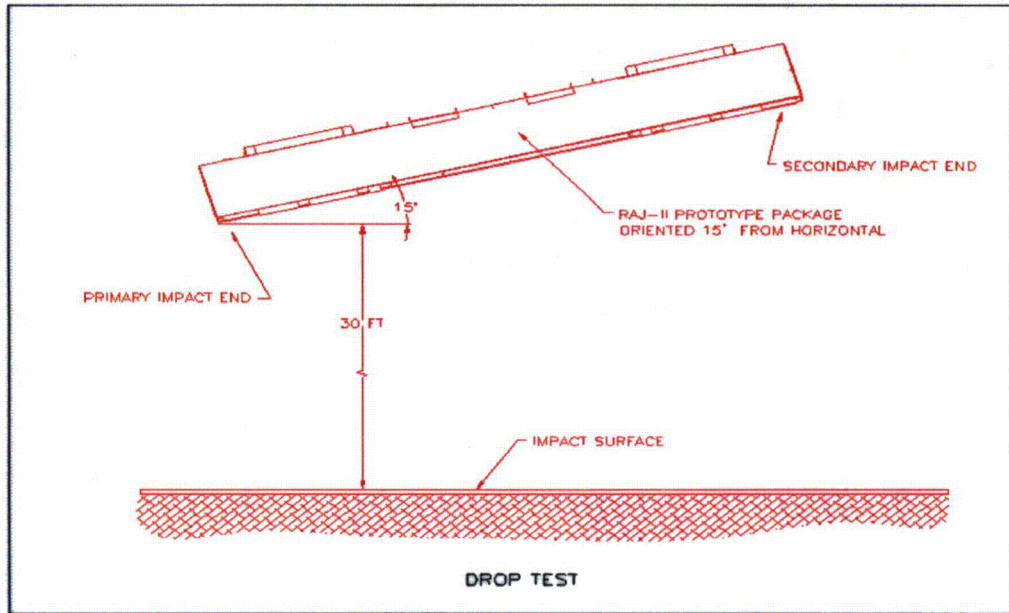


Figure 2-13 Slap-down Orientation

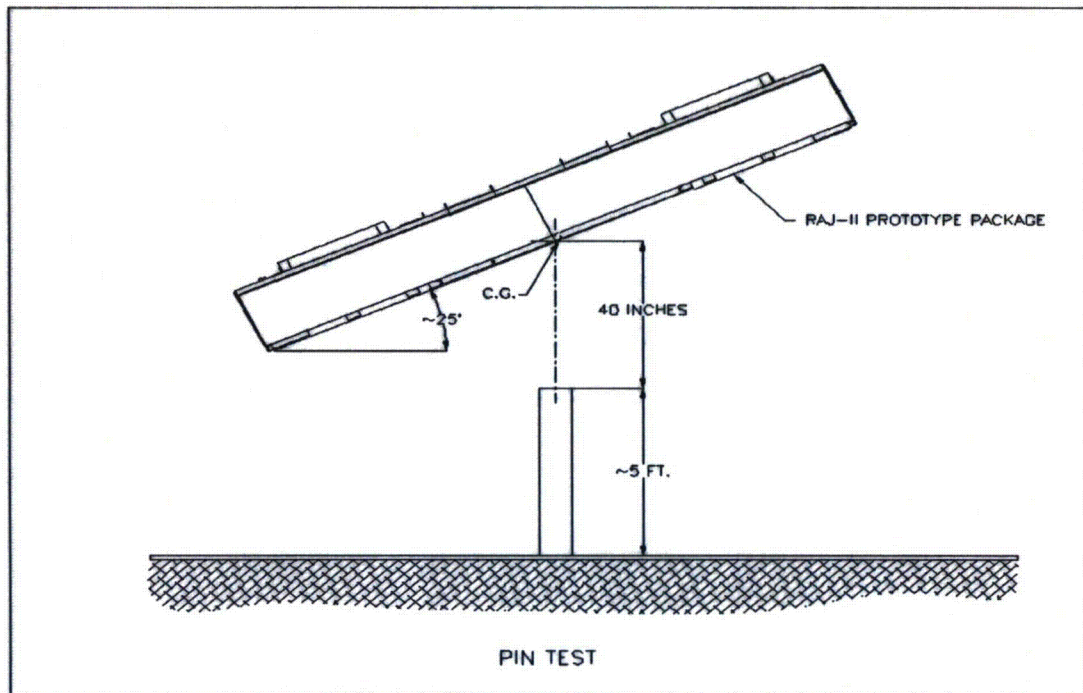


Figure 2-14 Puncture Pin Orientation

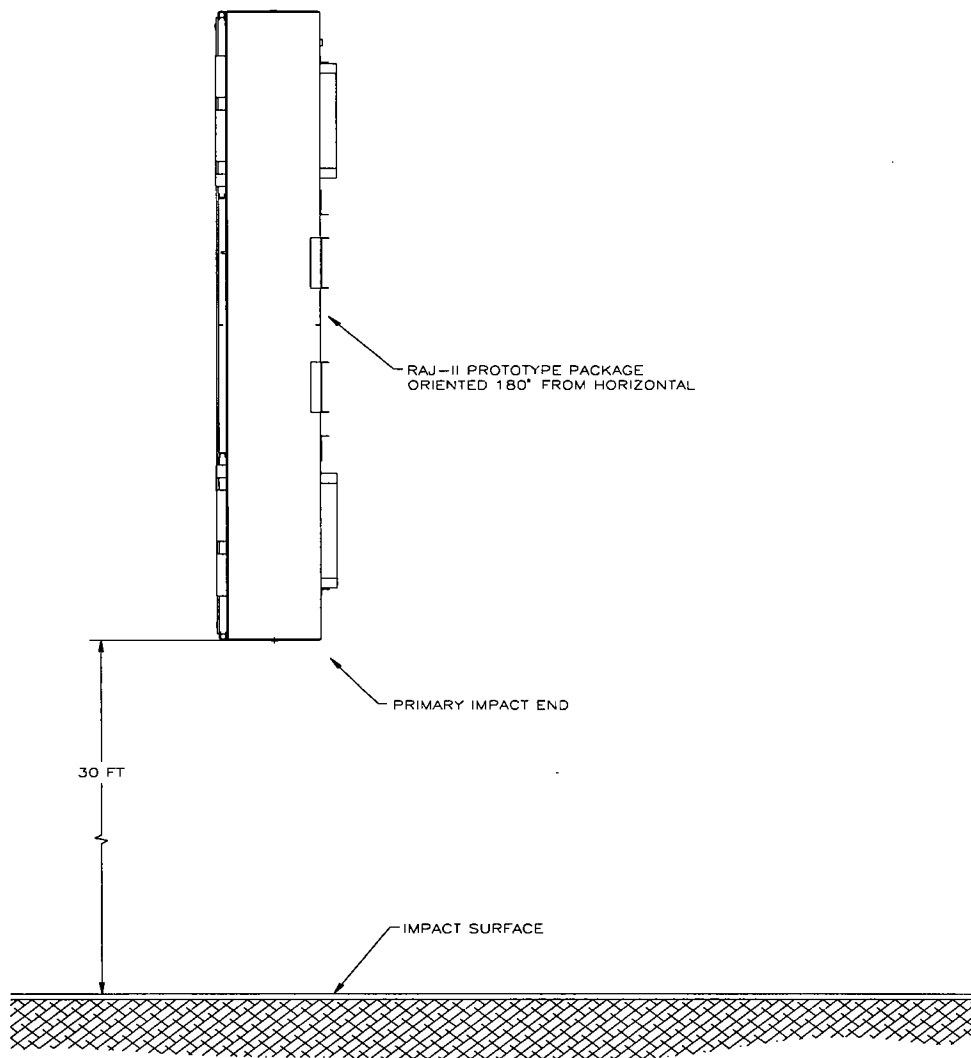


Figure 2-15 End Drop Orientation

2.8. ACCIDENT CONDITIONS FOR AIR TRANSPORT OF PLUTONIUM

Not Applicable. This package will not be used for the air transport of plutonium.

2.9. ACCIDENT CONDITIONS FOR FISSILE MATERIAL PACKAGES FOR AIR TRANSPORT

Not applicable. This package will not be used for the air transport of fissile material.

2.10. SPECIAL FORM

This section does not apply for the TN-B1 package, since special form is not claimed.

2.11. FUEL RODS

In each event evaluated above either by analysis or by test, the unirradiated fuel rods were protected by the TN-B1 package so that they sustained no significant damage. Fuel rod cladding is considered to provide containment of radioactive material under both normal and accident test conditions. Discussion of this cladding and its ability to maintain sufficient mechanical integrity to provide such containment is described in Section 1.2.3 and Chapter 4.0.

2.12. APPENDIX**2.12.1. *Certification Test*****2.12.1.1. Certification Test Unit**

The TN-B1 test packages were fabricated identically to the configuration depicted in the Packaging General Arrangement Drawing found in Appendix 1.4.1. The certification test unit is identical to the production TN-B1 packages except for some minor differences.

1. For ease in documentation/evaluation, tape and marker were used for reference markings during testing.
2. Minor amounts of the internal foam cushioning material were cut out to accommodate added weight in the fuel cavity.
3. Weight was added to the exterior of the package to allow the test units to be at the maximum allowed package weight.

The fuel assemblies were represented by a mock up fuel assembly (an ATRIUM-10 design). Lead rods inside the cladding replaced the fuel pellets. The fuel rods were seal welded using the same techniques used on the production fuel rods. A composite fuel assembly was used to represent the second fuel assembly. Steel tubes represented the ends with added steel for correct weight. The center section was made up of a mock up fuel assembly similar to the full size mock up fuel assembly. The mock up of the fuel approximated the stiffness of the fuel and added no extra strength to the center section of the package that would potentially be damaged by the puncture test. See Figure 2-16 through Figure 2-22 for container and mock up fuel preparation. Weight was added to the fuel assembly cavity by placing lead sheeting on the side of the fuel where normally there is foam. The lead weighing 143 pounds represented the weight of the water channels that could be shipped with some fuel assemblies. The lead plate was cut into strips that were not over half the height of the fuel assemblies to ensure that there was no support or protection added to the fuel during any of the tests. The total weight of the CTUs is provided in Table 2 - 10. The added weight in the contents represents the maximum payload weight including the fuel, fuel assembly fittings and packing material that could be required in the future.

For CTU 1 that was dropped lid down for a 30-foot slap down event and a 1-meter oblique puncture event, the weight was added between the bolster boards at each end. The added weight representing the difference between the actual tare weights of the package and the maximum allowed tare weight consisted of two ½ inch carbon steel plates. For CTU 1, these were held in place by the bolster and brackets attached to the bolster with lag bolts. See Figure 2-23. These plates were taken off CTU 1 and placed on the opposite end of CTU 2 for the end drop. See Figure 2-24.

Table 2-10 Test Unit Weights

Property	CTU 1		CTU 2	
	kg	lb	kg	lb
As fabricated weight	849 kg	1,872 lb	848 kg	1,869 lb
Max. fabricated weight	930 kg	2,050 lb	930 kg	2,050 lb
Added weight	81.7 kg	180 lb	81.7 kg	180 lb
Content weight	684 kg	1,508 lb	685 kg	1,510 lb
Measured drop weight	1,614 kg	3,558 lb	1,611 kg	3,552 lb
Approximate weight of attaching frame	2.3 kg	5.1 lb	11.3 kg	24.9 lb
Approximate drop weight	1,616 kg	3,562 lb	1,622 kg	3,576 lb

2.12.1.2. Test Orientations

Three certification tests were performed. Two tests were performed on CTU 1, a 9-meter (30-foot) slap-down on the lid and a 1-meter (40-inch) oblique puncture test on the lid. A 9-meter (30-foot) end drop was performed on CTU 2.

The 9-meter (30-foot) drop on the lid was designed to provide maximum acceleration to the end of the fuel as well as maximize the crush of the package for criticality evaluation purposes. The top down orientation was chosen since the lid contains the least material. The lid down orientation was also chosen since on previous tests horizontal lid down tests had maximized the crush and had resulted in the failure of the retaining bolts on the frame holding the inner container. As discussed in Section 2.7.1.1, the drop orientation was at 15 degrees with the horizontal. See Figure 2-25.

The 1-meter (40-inch) puncture test was performed on CTU 1 with the lid down after the 9-meter (30-foot) slap-down test. The package was oriented at a 25-degree angle to maximize the possibility of the corner of the puncture bar penetrating the outer container and maximizing the damage to the inner container and fuel. The puncture bar was aligned over the center of gravity of the package. See Figure 2-26 and Figure 2-27.

CTU 2 was dropped 9-meters (30-feet) with its bottom end down. The purpose of this orientation was to maximize the damage to the fuel. The bottom end was chosen since it is the most rigid end of the fuel assembly. The expansion springs inside the cladding tubes are on the upper end. See Figure 2-28

2.12.1.3. Test Performance

Testing was performed at the National Transportation Research Center in Oak Ridge, Tennessee. The CTUs were shipped to the facility fully assembled. Only the additional tare weight as described in Section 2.12.1.1 was added at the test facility. Tests were performed on the packages prior to them being transported to the Framatome-ANP facility at Lynchburg, Virginia. At Lynchburg the packages were disassembled and examined and the fuel rods were helium leak tested.

The slapdown test at 15 degrees to horizontal demonstrated the ability of the outer package to protect the fuel and the inner container. The energy absorbing capabilities of the package allowed the package to deform and limited the secondary impact to less than the primary impact. See Figure 2-29 and Figure 2-30. This test resulted in deformation inside the package. See Figure 2-36 and Figure 2-37. The crush of the paper honeycomb was limited by the stiffening plates in the lid. See Figure 2-38. The inner container lid was deformed as well. Neither the lid bolts on either container nor the bolts on the inner

container clamping device failed. The frame did bend over 3 cm. The fuel rods, although slightly deformed due to the test and the added weight in the fuel cavity, were not damaged. See Figure 2-39. The added weight placed between the bolster timbers caused a slight deformation of the bottom wall of the outer package in the local area of the weights.

The puncture test was performed with the lid down at a 25 degree angle from horizontal. See Figure 2-25. The puncture pin was bolted with three bolts to the drop pad. The puncture pin struck the lid over the CG of the package after the package had undergone the slapdown test. See Figure 2-26. The pin did not penetrate the outer lid. The outer lid was deformed inward until it came in contact with the inner container. This was confirmed by a slight mark on the inner container lid. The pin appears to have bounced since there are two indentations very close together which could have been caused by the outer lid bottoming out against the inner container lid. See Figure 2-31 and Figure 2-32. No significant internal package or fuel damage appeared to be attributable to the pin puncture test.

The 9-meter (30-foot) end drop test was performed on CTU 2 with the bottom end down. There was little exterior damage to the outer container. See Figure 2-33, Figure 2-34, and Figure 2-35. Extensive damage occurred to the inside of the inner container as the fuel assemblies and the added weight impacted the interior of the inner container. The rigid end fitting of the assembly crushed the wood located at the end of the package. Although some welds broke, the bottom end of the package remained in place. The fuel rods partially came out of the end fitting. The fuel assemblies bent to the side. See Figure 2-40, Figure 2-41, and, Figure 2-42.

The mock up fuel assemblies from both CTU 1 and CTU 2 were helium leak tested. The Assembly from CTU 1 was found to meet the leak tight requirements of having a leak rate less than 1×10^{-7} atm-cc/s. The assembly from CTU 2 was found to have a He leak rate of 5.5×10^{-6} atm-cc/s. This is within the allowable leakage for the fuel as shown in Section 4.0.

2.12.1.4. Test Summaries

Two 9-meter (30-foot) drops and one oblique puncture pin test were performed on two certification test units. The packages retained the fuel assemblies and protected the fuel. Mockup fuel assemblies from both certification units were leak tested after the drop tests and were determined to have maintained containment. The tests are summarized below.

Table 2-11 Testing Summary

Test	CTU	Orientation with horizontal	Exterior damage	Interior damage	Fuel
9-meter (30-foot) lid down	1	15°	Minor deformation on both ends.	No bolts broken on the frame or the lids. Significant deformation to inner container and internal clamp frame. Reduction of spacing between outside of package and fuel to about 4 inches.	Minimal damage to the fuel assemblies. Some twist to the assembly. No real damage to the fuel rods. The fuel was demonstrated to have a leak rate of less than 1×10^{-7} atm-cc/s after the testing.
1-meter (40 in) lid down over cg	1	25°	Did not penetrate outer wall	Outer wall contacted inner container. Section 2.12 Figure 2-39 through 2-42 show some damage to the inner container, however, this damage is conservatively modeled in the HAC criticality analyses in Section 6.0 and is not sufficient to allow fuel to leak from the container.	The fuel appeared not to be affected by this test. Passed helium leak test.
9-meter (30-foot) lower end	2	90°	Localized damage on impact end.	Major crushing of the wood at the end of the inner package and breaking of the inner wall of the inner container on the impacted end. The outer wall was damaged but did not fail completely.	Fuel was bent and separated from end fittings. Fuel spacers were damaged. Fuel rods had no significant damage. Fuel bending was influenced by the movement of the weight added to the fuel cavity. Post drop leak test giving a He leak rate of 5.5×10^{-6} atm-cc/s demonstrated that containment had been maintained.



Figure 2-16 Inner Container Being Prepared to Receive Mockup Fuel and Added Weight

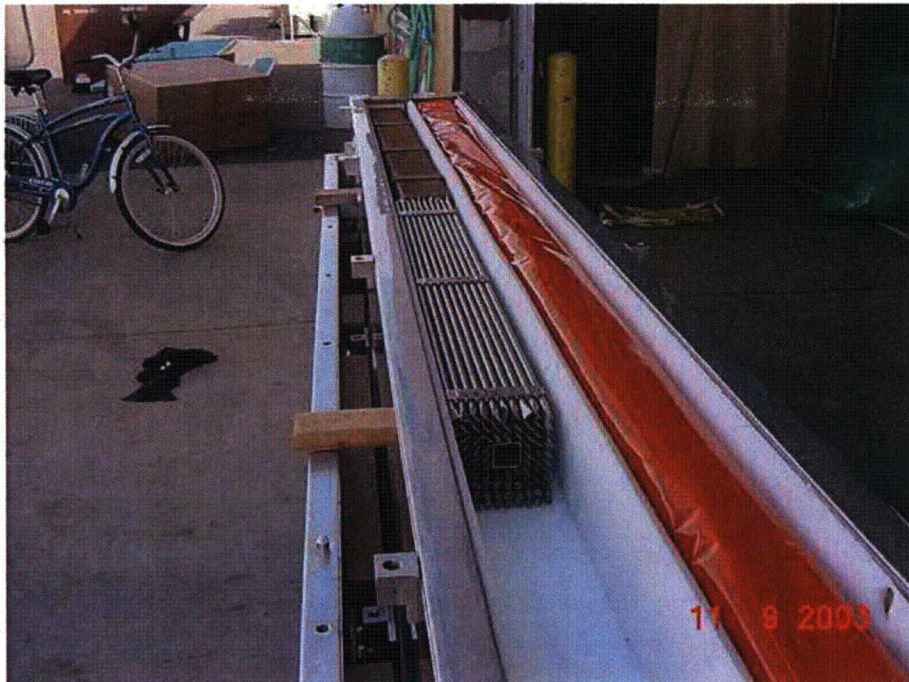


Figure 2-17 Partial Fuel Assemblies in CTU 1

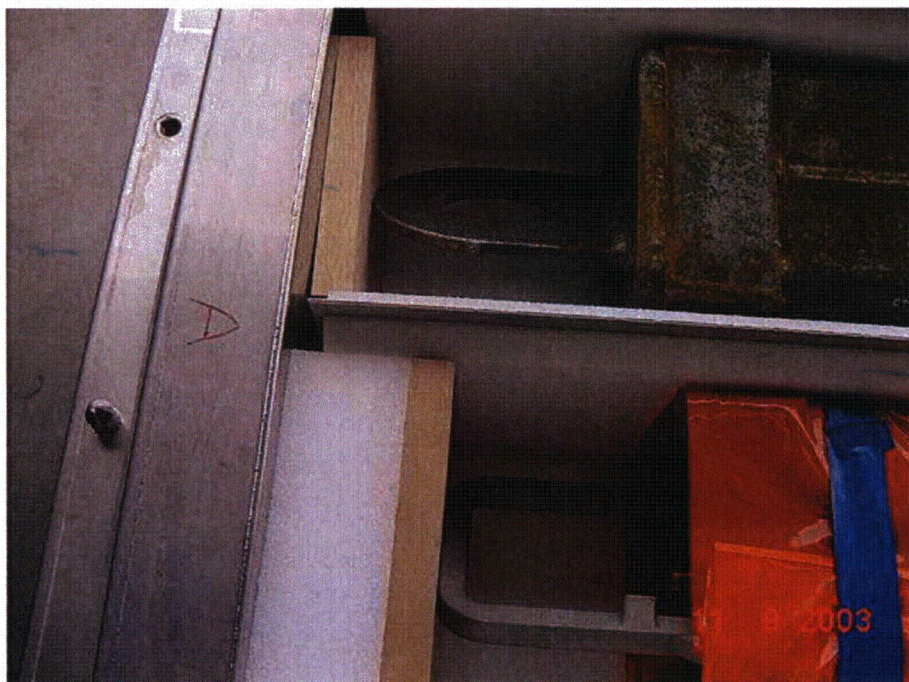


Figure 2-18 Top End Fittings on Fuel in CTU 1

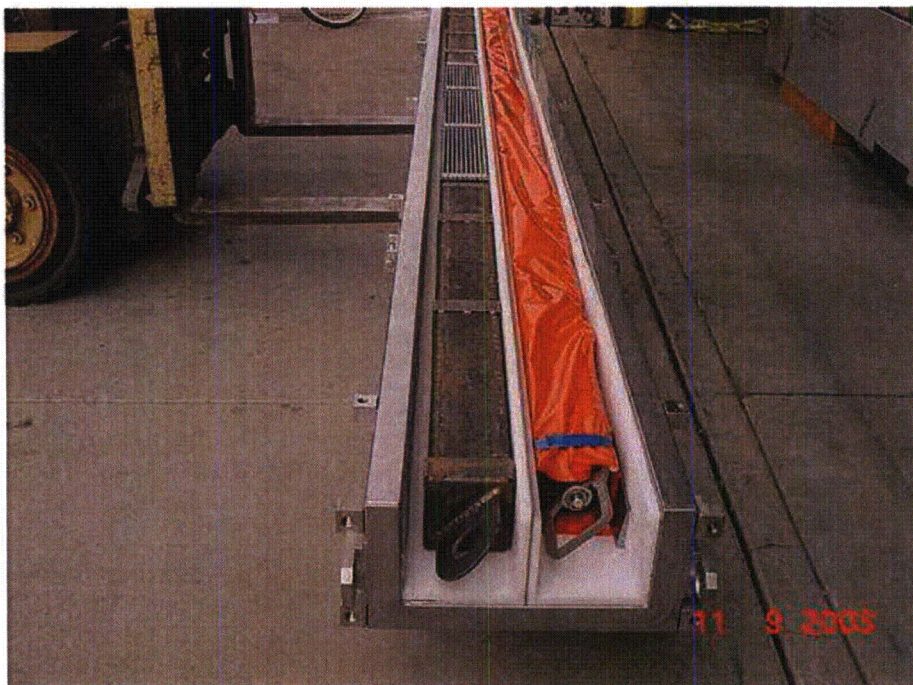


Figure 2-19 Contents of CTU 2



Figure 2-20 Outer Container without Inner Container

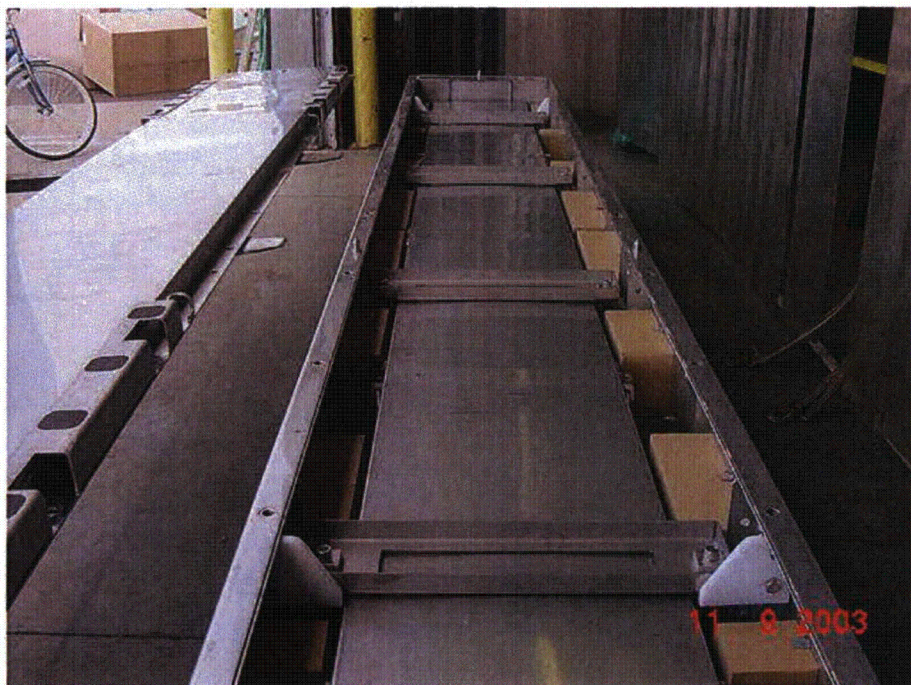


Figure 2-21 Inner Container Secured in Outer Container

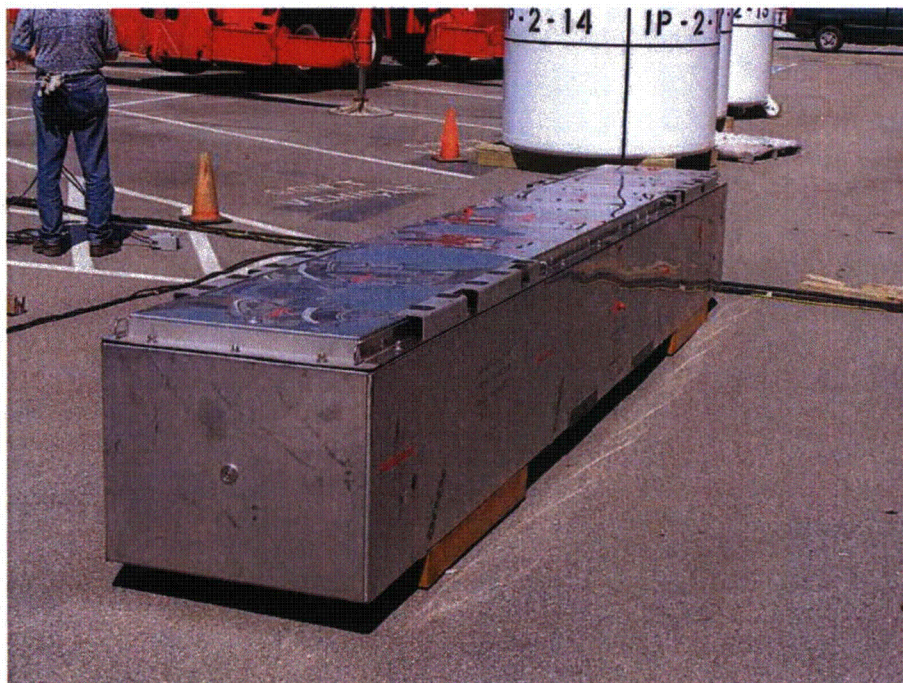


Figure 2-22 CTU 2 Prior to Testing

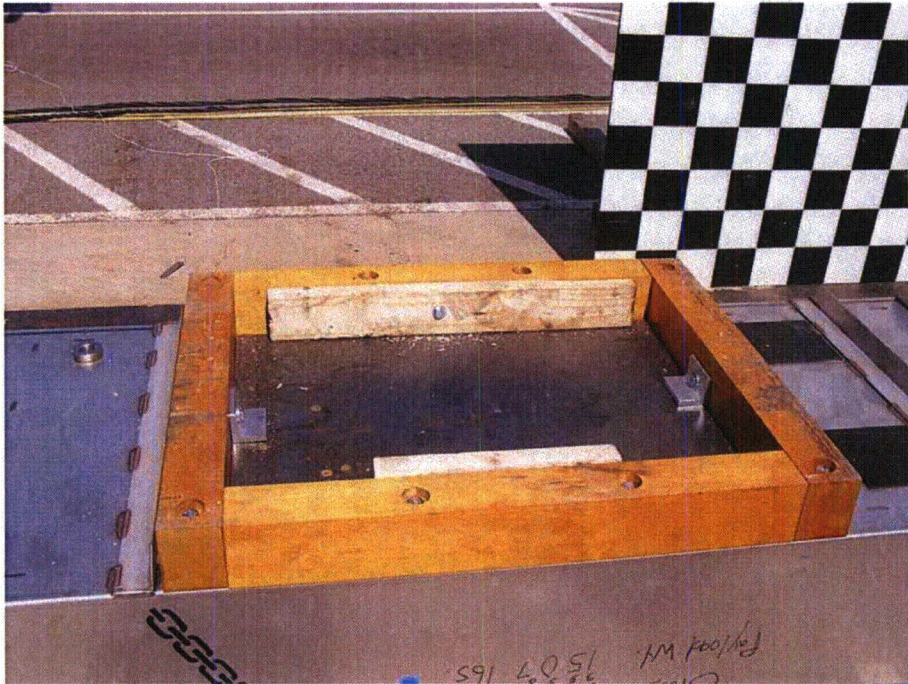


Figure 2-23 Addition of Tare Weight to CTU 1



Figure 2-24 Addition of Tare Weight to CTU 2



Figure 2-25 CTU 1 Positioned for 15° 9-m (30-foot) Slap-down Drop



Figure 2-26 Alignment for Oblique Puncture



Figure 2-27 Position for Puncture Test



Figure 2-28 Position for End Drop

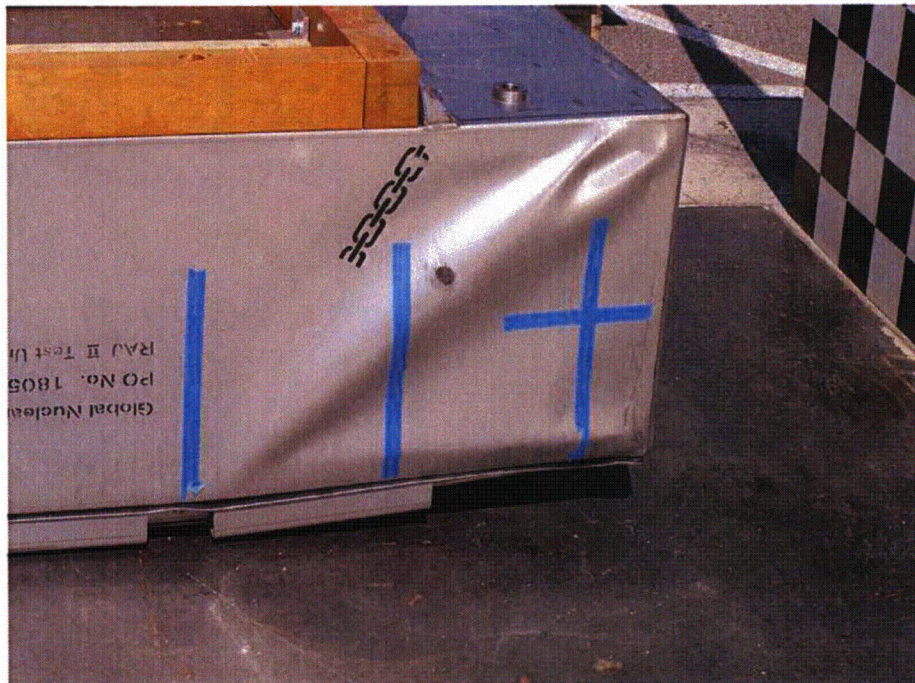


Figure 2-29 Primary Impact End Slap-down Damage



Figure 2-30 Secondary Impact End Damage



Figure 2-31 Puncture Damage

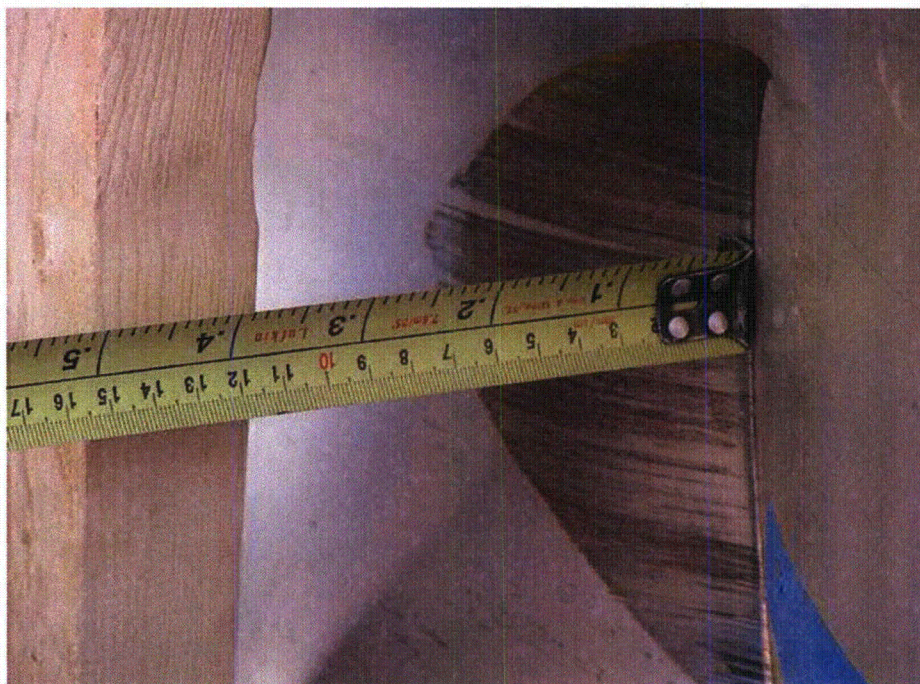


Figure 2-32 Close Up of Puncture Damage

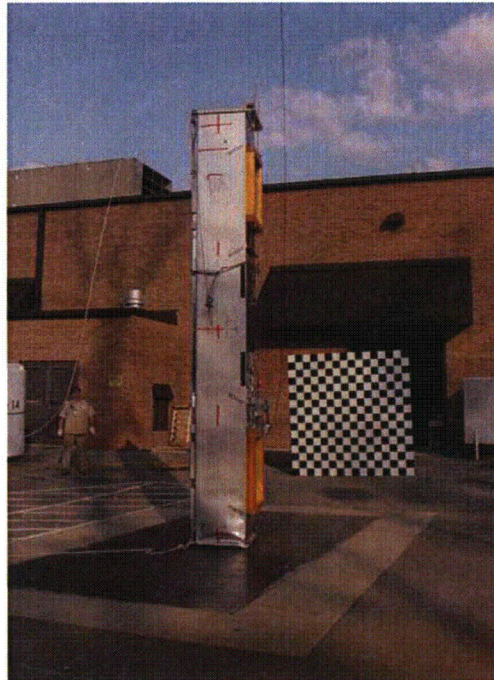


Figure 2-33 End Impact

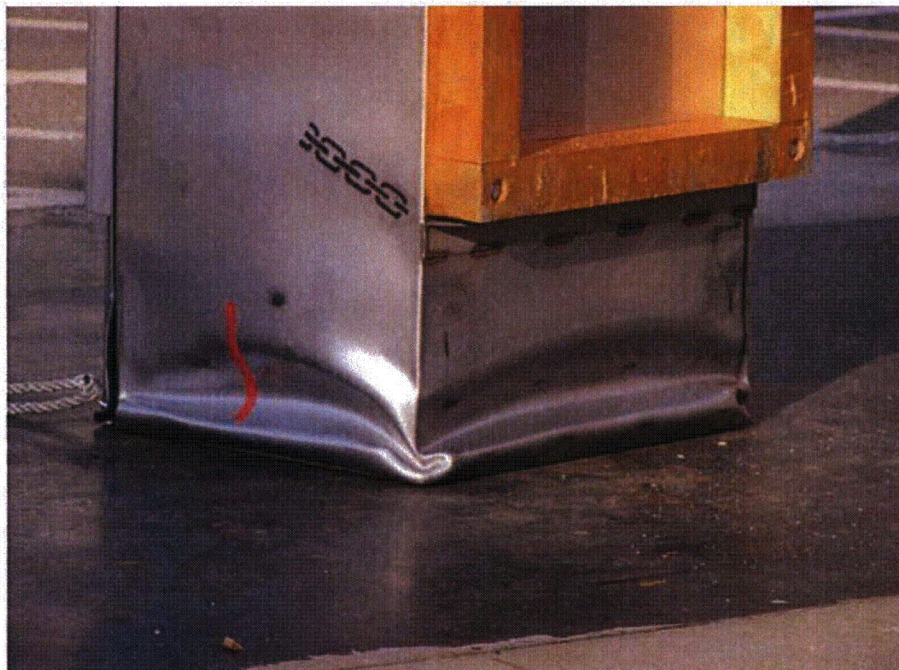


Figure 2-34 Damage from End Impact (Bottom and Side)



Figure 2-35 End Impact Damage (Top and Side)



Figure 2-36 Damage Inside Outer Container to CTU 1



Figure 2-37 Internal Damage to Outer Container CTU 1



Figure 2-38 Lid Crush on CTU 1

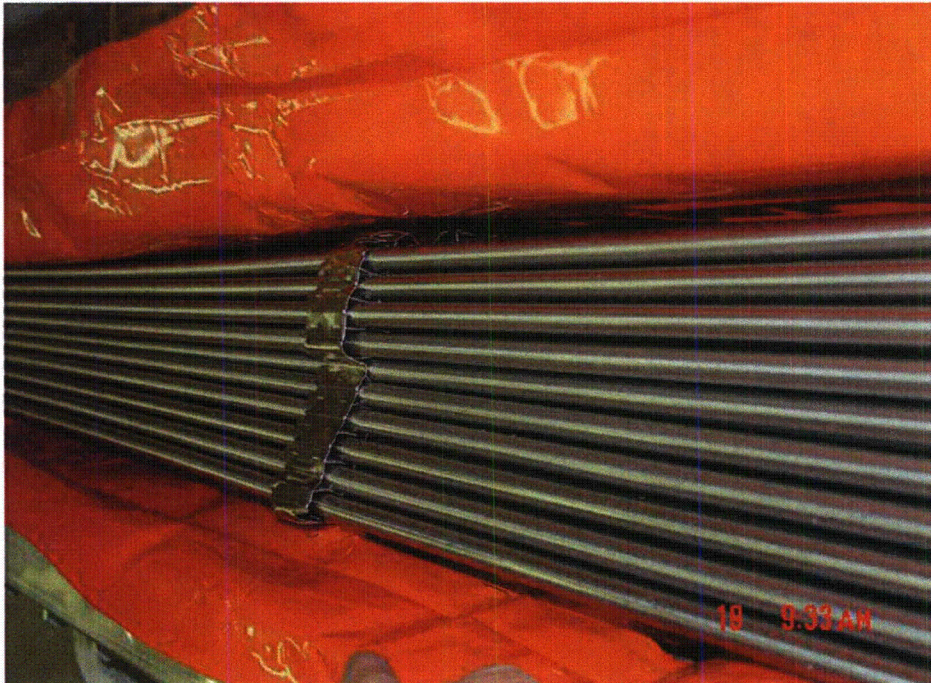


Figure 2-39 Damage to Fuel in CTU 1

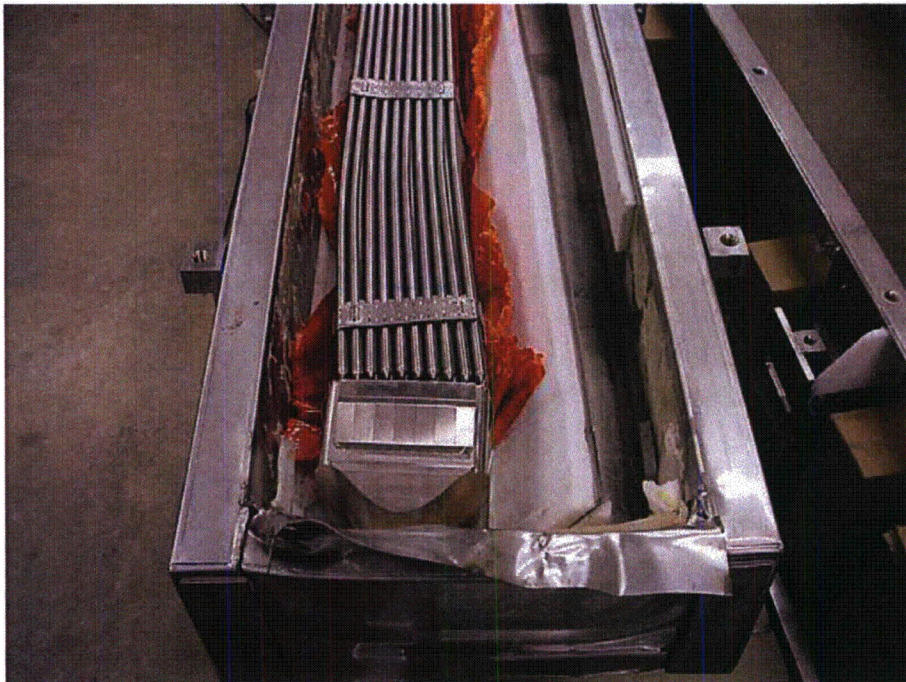


Figure 2-40 Internal Damage to CTU 2

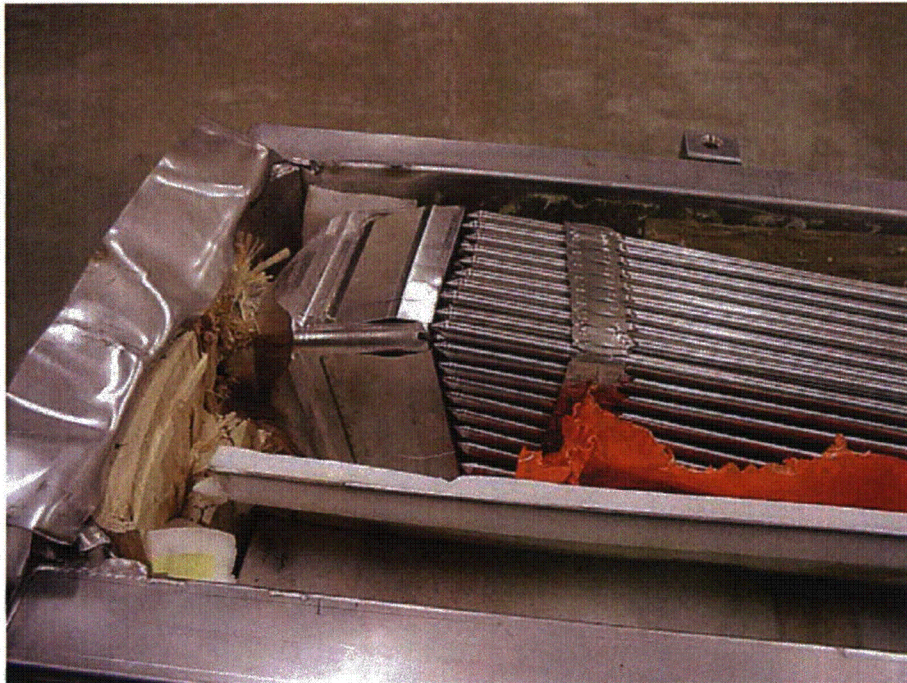


Figure 2-41 Fuel Damage CTU 2

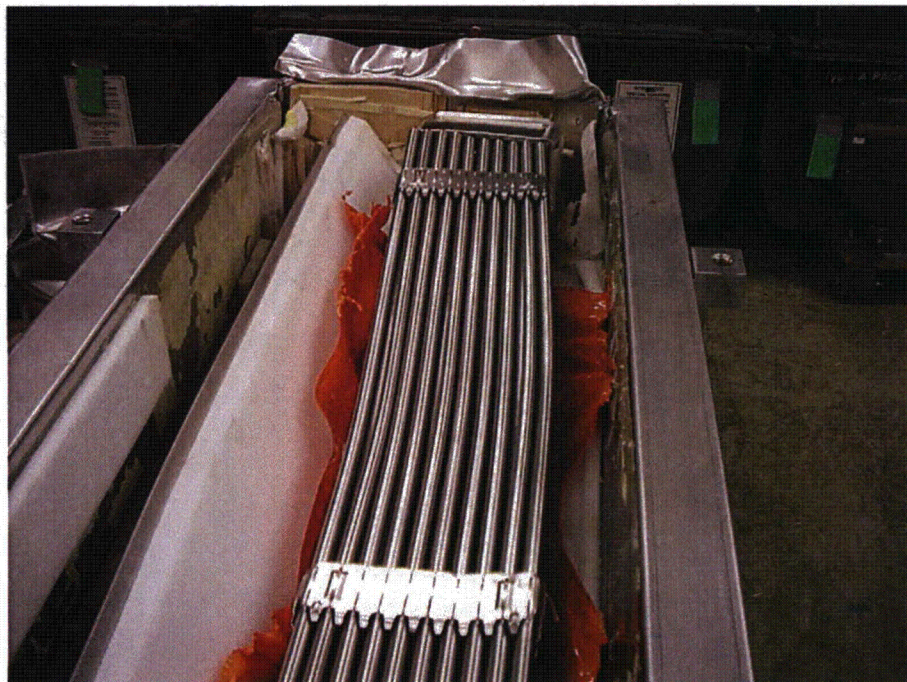


Figure 2-42 Fuel Prior to Leak Testing CTU 2

2.12.2. GNF-J Certification Tests

Normal conditions of transport (NCT) and hypothetical accident conditions (HAC) certification testing of the RAJ-II package was also performed by GNF-J as part of obtaining a Type AF certificate of compliance* in Japan. For the U.S. testing, the GNF-J certification tests were utilized to determine the worst-case test orientations for the certification tests identified in Appendix 2.12.1. This appendix summarizes the GNF-J RAJ-II certification tests.

2.12.2.1. Certification Test Units

Two certification test units (CTUs) were utilized for the GNF-J RAJ-II tests. Each CTU was fabricated in accordance with the Packaging General Arrangement Drawings found in Appendix 1.4.1, with the following exceptions:

1. The lateral wood bolsters on each end were not installed. Elimination of these wood bolsters is conservative for the free drops.
2. Maximum content weight was 560 kg (1,235 lbs), which results in a maximum package weight of 1,490 kg (3,285 lbs). This weight reduction is less than 8% lower than the maximum gross weight of the RAJ-II package, and will result in higher impact forces. The small difference in weight will have an insignificant effect on the free drop response of the package and/or fuel assembly.

One simulated fuel assembly and one dummy weight were utilized in each CTU to simulate the payload contents. Accelerometers were installed on the CTUs to measure and record each free drop impact. No accelerometers were used for the puncture drop tests.

2.12.2.2. Test Orientations

Since the RAJ-II package relies on the fuel cladding as the containment boundary, free drop and puncture drop orientations that could damage the fuel cladding and potentially breach the containment boundary should be included in the test series. In addition, orientations that could damage the package and/or the fuel assemblies such that an unsafe criticality geometry would exist should be included in the test series.

Free drop orientations that could result in this type of damage include:

1. Vertical drop on the package end – maximizes axial impact acceleration to a fuel assembly, potentially buckling and failing the fuel cladding (containment boundary).

* Global Nuclear Fuel - Japan (fka Japan Nuclear Fuel Co., Ltd), Application for Approval of Packaging, Type RAJ-II, STO-M00-034, dated September 26, 2000.

2. Horizontal drop of the package – maximizes lateral impact acceleration on a fuel assembly, potentially bending and failing the fuel cladding (containment boundary).
3. CG-over-corner of the package – maximizes deformation of outer container (OC).

All of these orientations were included in the free drop test series of the package. Puncture drop orientations that could potentially breach the containment boundary (cladding) include:

1. Horizontal puncture drop on the center of the package – maximizes puncture impact onto fuel pins and potentially shearing and failure of the fuel cladding (containment boundary).
2. Vertical puncture drop on the end of the package – maximizes puncture impact onto the fuel assembly

Because of the end internal structure and wood dunnage in the outer container, the puncture drop on the end will not result in any significant deformation of the fuel assembly or the inner container. Therefore, this puncture drop orientation is bounded by the horizontal puncture drop on the center of the package.

The free drop tests included NCT drops of 0.3 meters (1 foot) and 1.2 meters (4 feet) prior to performing the 9-meter (30-foot) HAC free drop on each CTU. The horizontal puncture drop test was only performed on CTU 2J.

Two certification test series were performed. Three free drop tests were performed on CTU 1J, and three free drop and one puncture drop tests were performed on CTU 2J. The test series for each CTU is summarized in Table 2-10. All drop tests were performed at ambient temperature.

2.12.2.3. Test Performance

Free drop and puncture testing was performed at two test facilities in Japan. At one facility, the drop pad consisted of a 32-mm (1.26-inch) thick steel plate that was embedded in a 1-meter (40-inch) thick concrete and steel support structure, with an overall length of 8 meters (26 feet). The other drop pad consisted of a 50-mm (1.97-inch) thick × 5-meter (16.4-feet) × 5-meter (16.4-feet) steel plate that was embedded in a 450-mm (12-inch) thick × 8.5-meter (27.9-feet) wide concrete and steel structure. The mass of each drop pad constituted an essentially unyielding surface for the CTUs, which weighed approximately 1,490 kg (3,285 lb).

2.12.2.3.1. *CTU 1J*

CTU 1J was tested for a total of six free drop tests at heights of 0.3 meters (1 foot), 1.2 meters (4 feet), and 9 meters (30 feet). Figures 2-43 through 2-48 sequentially photo-document the CTU 1J tests.

The maximum resultant accumulated deformation, ~163 mm (~6 inches) occurred in the OC body corner. This orientation resulted in the maximum impact acceleration of 203g. No failure of the cladding (containment boundary) occurred from this test series.

2.12.2.3.2. CTU 2J

The testing of CTU 2J focused on free drop orientations not addressed by the CTU 1J tests. In addition, a HAC puncture drop test and HAC thermal test were performed. A total of three free drop tests at heights of 0.3 meters (1 foot), 1.2 meters (4 feet), and 9 meters (30 feet) were performed. Figures 2-49 and 2-50 sequentially photo-document the CTU 2J tests. The maximum resultant accumulated deformation, ~163 mm (~6 inches) occurred in the OC body corner. This orientation resulted in the maximum impact acceleration of 146g. No failure of the cladding (containment boundary) occurred from this test series.

2.12.2.4. Test Summaries

Two 0.3-meter (1-foot), four 1.2-meter (4-foot), three 9-meter (30-foot) free drops, one 1-meter (40-inch) puncture drop, and one HAC thermal test were performed on two CTUs. The packages retained the fuel assemblies and protected the fuel. There was no visual damage or loss of fuel pellets from the simulated fuel assemblies from both CTUs. A summary of the test results is provided in Table 2 - 11.

Table 2-12 GNF-J CTU Test Series Summary

CTU	Drop Height, m (ft)	Test Description	Purpose
1J	0.3 (1)	Free drop, CG-over-bottom end lower corner	Normal operation impact on OC body corner.
	1.2 (4)	NCT free drop, CG-over-bottom end lower corner	Impart initial deformation in same orientation as subsequent HAC free drop
		NCT free drop, horizontal on OC lid	Impart initial deformation in same orientation as planned HAC free drop
		NCT free drop, vertical, bottom end	Impart initial deformation in same orientation as subsequent HAC free drop
	9 (30)	HAC free drop, CG-over-bottom end lower corner	Maximize OC body deformation; potentially fail fuel rod and breach cladding.
		HAC free drop, vertical, bottom end	Maximize axial impact loads on fuel assemblies, potentially buckle fuel rod and
2J	0.3 (1)	Free drop, CG-over-lid corner	Normal operation impact on OC lid/body corner
	1.2 (4)	NCT free drop, horizontal on lid	Impart initial deformation in same orientation as subsequent HAC free drop
	9 (30)	HAC free drop, horizontal on lid	Maximize lateral impact loads on fuel assemblies, potentially breaching cladding.
	1 (3.3)	HAC puncture drop, horizontal on OC lid	Impact directly on HAC free drop damage; attempt to rupture fuel cladding.
	N/A	HAC thermal test	Demonstrate thermal performance of package.

Table 2-13 GNF-J CTU Test Series Results

CTU	Drop Height, m (ft)	Test Description	Result
1J	0.3 (1)	Free drop, CG-over-bottom end lower corner	Combined deformation of ~40 mm (~1.6 inches) of bottom corner.
	1.2 (4)	NCT free drop, CG-over-bottom end lower corner	
		NCT free drop, horizontal on OC lid	No significant deformation.
		NCT free drop, vertical, bottom end	Impacted end deformed ~3.9 mm (~0.2 inches)
	9 (30)	HAC free drop, CG-over-bottom end lower corner	Impacted OC bottom corner deformed ~163 mm (~6 inches), OC lid corner ~101 mm (~4 inches). Maximum acceleration of 203g.
HAC free drop, vertical, bottom end		IC body/lid deformed ~2 - 81 mm (~0.08 - 3 inches) in length, U-shaped lifting bar on fuel assembly bent due to contact with wood end dunnage. Maximum acceleration of 58g.	
2J	0.3 (1)	Free drop, CG-over-lid corner	Combined deformation of ~2.9 mm (~0.1 inches) of lid corner.
	1.2 (4)	NCT free drop, horizontal on lid	
	9 (30)	HAC free drop, horizontal on lid	Impacted side deformed ~2 - 19 mm (~0.08 - 0.8 inches), localized weld failure of OC lid flange/OC lid sheet interface, no failure of OC lid bolts. Maximum acceleration of 146g.
	1 (3.3)	HAC puncture drop, horizontal on OC lid	~100 mm deep x ~2,000 mm (~4 inches x ~79 inches) wide indentation in OC lid, no breach of OC lid sheet.
	N/A	HAC thermal test	No failure of simulated fuel assembly cladding.

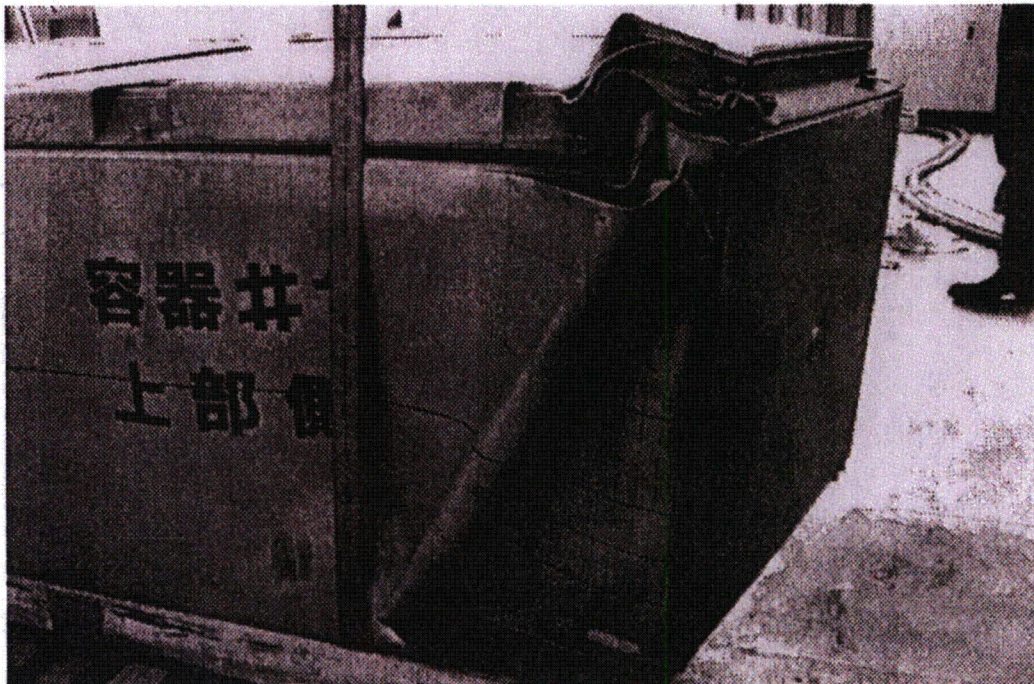


Figure 2-43 CTU 1J 9 m CG-Over-Bottom Corner Free Drop: View of Impacted Corner

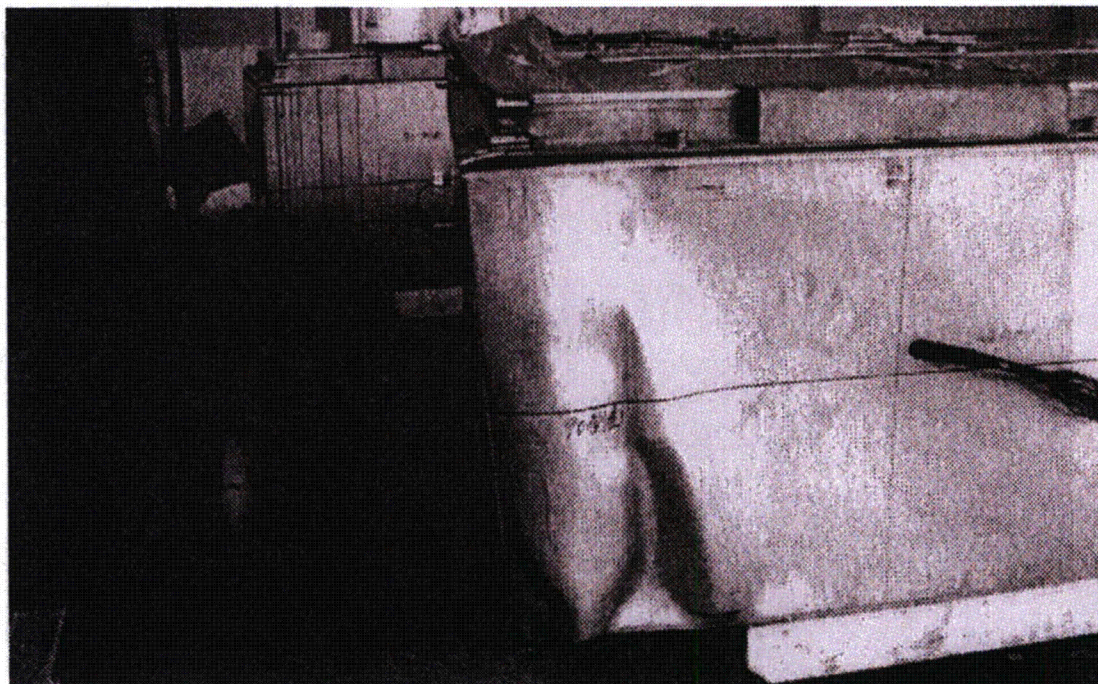


Figure 2-44 CTU 1J 9 m CG-Over-Bottom Corner Free Drop: View of Opposite Corner

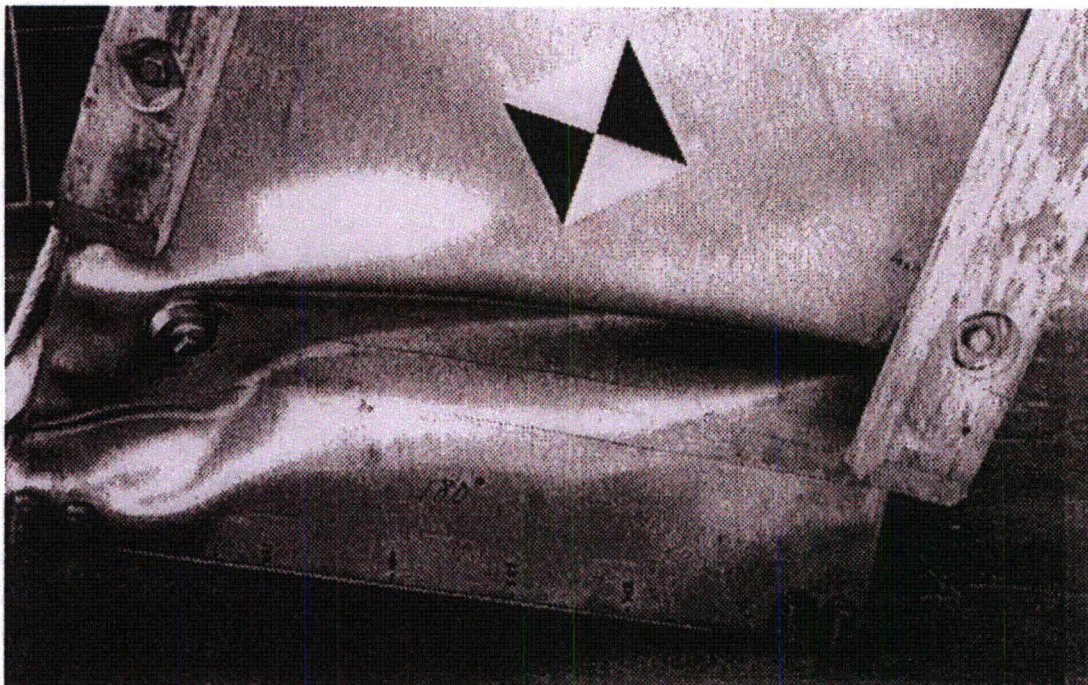


Figure 2-45 CTU 1J 9 m CG-Over-Bottom Corner Free Drop: View of Bottom

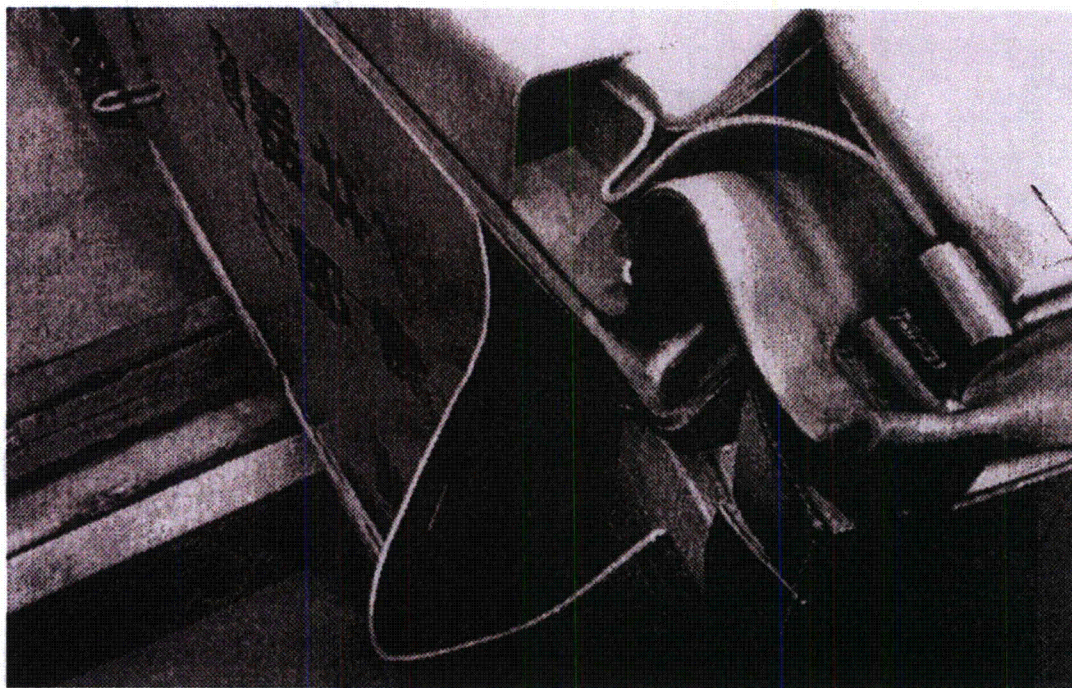


Figure 2-46 CTU 1J 9 m CG-Over-Bottom Corner Free Drop:
Close-up View of Top Corner

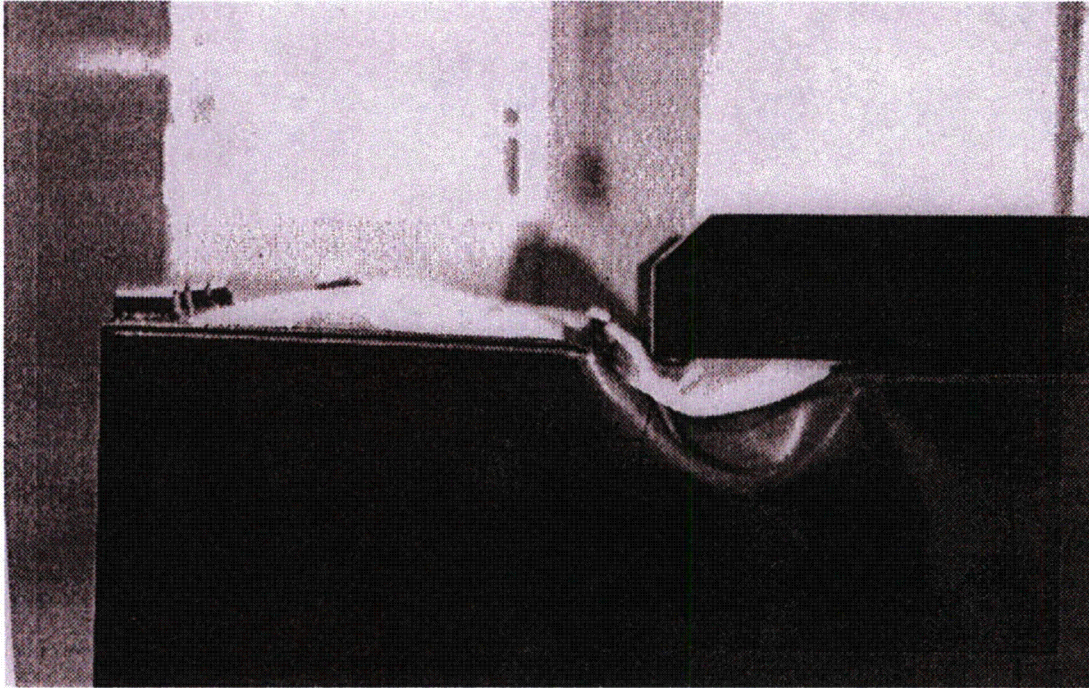


Figure 2-47 CTU 1J 9-m Vertical End Drop: Close-up Side View of Bottom Damage

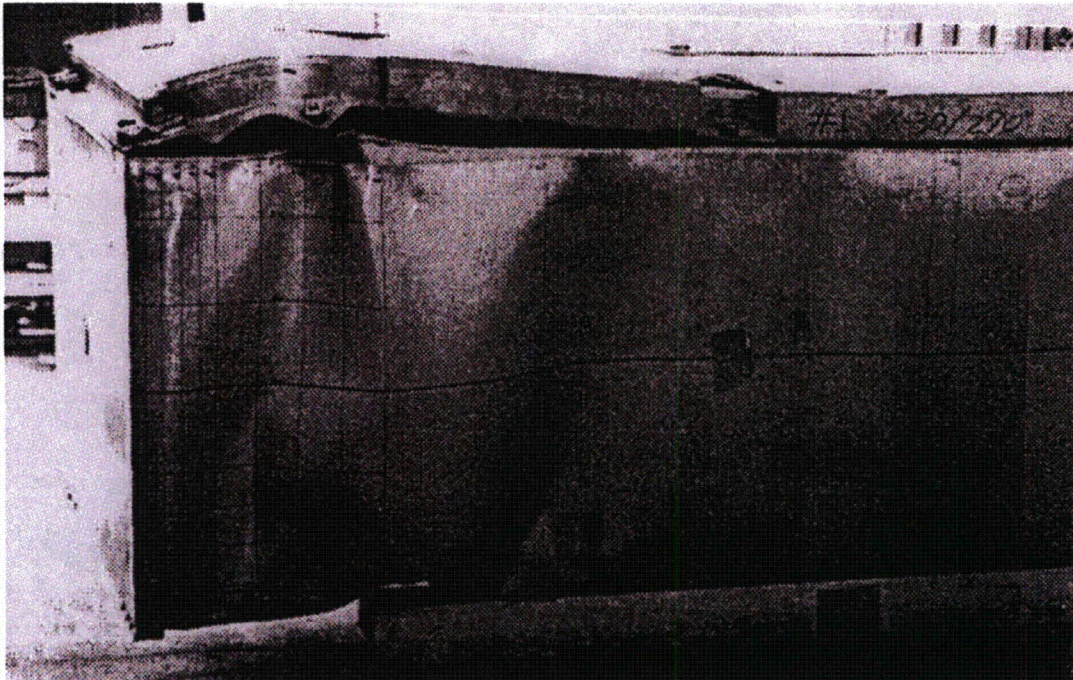


Figure 2-48 CTU 1J 9-m Vertical End Drop: Overall View of Damage

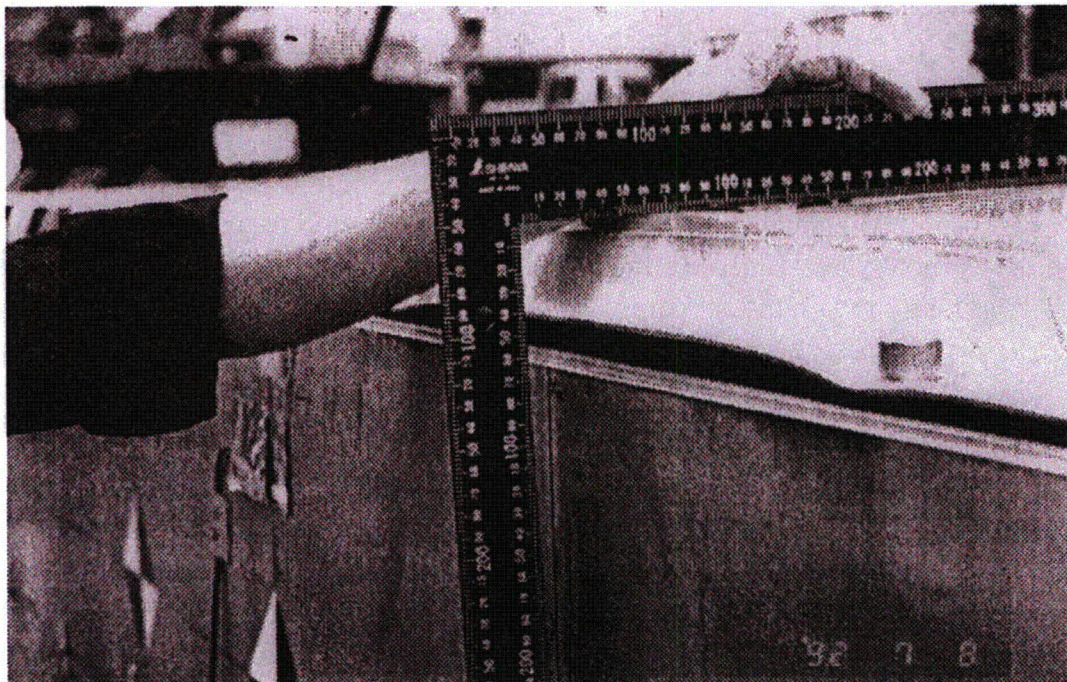


Figure 2-49 CTU 2J 9-m Horizontal Free Drop: Close-up Side View of Damage

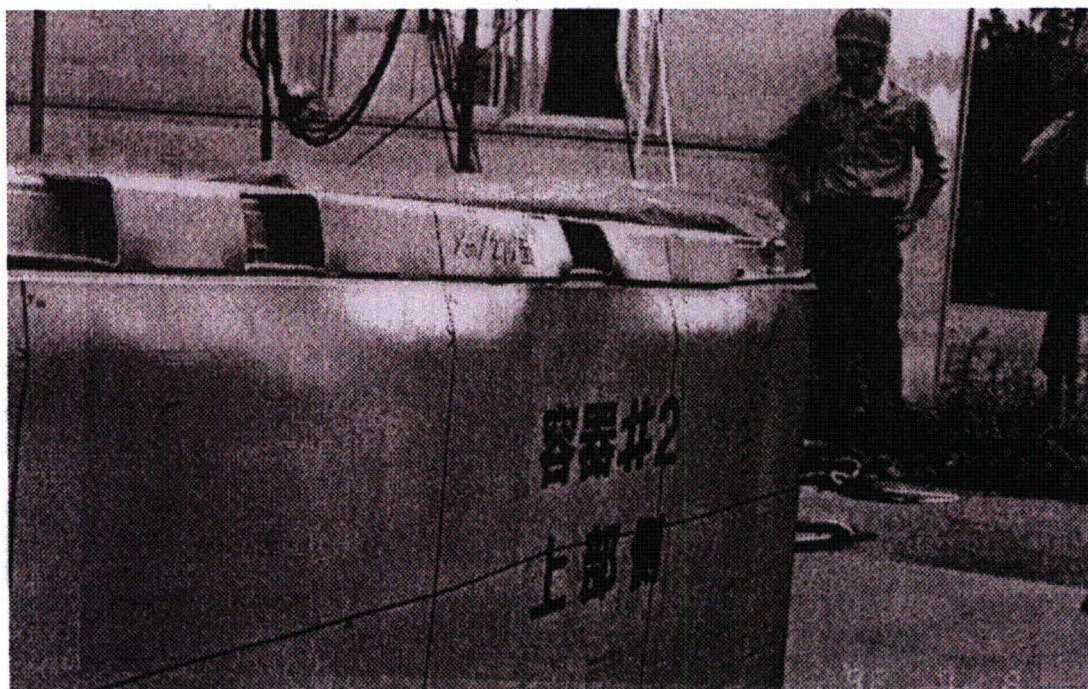


Figure 2-50 CTU 2J 9-m Horizontal Free Drop: Overall Side View of Damage

2.12.3. Outer Container Gasket Sealing Capability

The outer container for the TN-B1 packaging utilizes a 5 mm thick × 40 mm wide × 11,360 mm long, 50 shore durometer, solid natural rubber gasket. As shown in Appendix 1.4.1, Packaging General Arrangement Drawings, the gasket is attached to the flange of the outer container lid. The outer container lid is secured to the outer container body by twenty-four (24) M14 × 2, Type 304 stainless steel bolts, which are tightened to “wrench tight or as defined in user procedures”. Since a specific tightening torque is not specified, the maximum bolt tension will be based on the minimum yield strength of the stainless steel.

The maximum force, F_b , in each lid bolt will be:

$$F_b = S_y(A_t)$$

where: S_y = Minimum yield strength = 206.8 MPa (30.0 ksi) (Ref. Table 2-2)

A_t = Tensile area for M14 × 2 bolt = 115 mm² (0.1783 in²)

Substituting these values into the above equation yields a bolt force of 23,782 N (5,349 lb_f).

The total compressive force applied to the gasket, F_{gasket} , is then:

$$F_{\text{gasket}} = (24)F_b = (24)(23,782) = 570,768 \text{ N (128,376 lb}_f\text{)}$$

For the applied bolt force, the gasket compressive area, A_{gasket} , is 40 × 11,360 = 454,400 mm² (704.3 in²). Conservatively neglecting any deflection of the 4-mm thick lid flange between the lid bolts, the resultant compressive stress on the gasket is then:

$$\sigma_{\text{gasket}} = \frac{570,768}{454,400} = 1.256 \text{ MPa (182 psi)}$$

The shape factor, s , for the 5 × 40 gasket is:

$$s = \frac{\text{One Load Area}}{\text{Total Free Area}} = \frac{\text{Width}}{2(\text{Thickness})} = \frac{40}{10} = 4.0$$

From Figure 5-12 of Handbook of Molded and Extruded Rubber,* the percent compressive deflection of the 50-durometer gasket with $s = 4.0$ at 182 psi compressive stress is approximately 3%, or 0.15 mm (0.006 in), which is minimal.

* *Handbook of Molded and Extruded Rubber, Third Edition, Goodyear Tire & Rubber Company.*

To determine whether the gasket is compressed with the applied bolt force, the compression modulus and the linear spring rate for the gasket is computed. Equation 3-7 of Handbook of Molded and Extruded Rubber, the linear spring rate, K_L , for the rubber gasket is:

$$K_L = \frac{E_c (A)}{h}$$

where: E_c = Compression modulus

A = Compression area of gasket = 454,400 mm² (704.3 in²)

h = height of gasket = 5 mm (0.197 in)

The compression modulus is extracted from Figure 5-20 of the Handbook of Molded and Extruded Rubber for a shape factor "s" of 4.0 and an approximate compression of 3% for the 50 durometer gasket. From this figure, the compression modulus is interpolated to be 6,912 psi (47.7 MPa). The linear spring rate of the gasket is then:

$$K_L = \frac{6,912(704)}{0.197} = 24.7 \times 10^6 \text{ lb}_f / \text{in} \quad (4.33 \times 10^6 \text{ N/mm})$$

To compress the gasket 0.15 mm (0.006 in), the required force in the bolts is:

$$24F_{\text{bolt}} = K_L \Delta = 24.7 \times 10^6 (0.006) = 148,200 \text{ lb}_f \quad (659,266 \text{ N})$$

$$\Rightarrow F_{\text{bolt}} = 6,175 \text{ lb}_f \quad (27,648 \text{ N})$$

Since the resultant bolt force required to compress the gasket 3% is greater than the yield strength of the lid bolts, the gasket will not be compressed to the estimated 3% compression. To determine the estimated gasket compression with the maximum lid bolt force at yield strength (23,782 N [5,349 lb_f]), the linear spring rate will be computed for zero compression and then compared to the applied maximum force. From Figure 5-20 of the Handbook of Molded and Extruded Rubber for a shape factor "s" of 4.0, the compression modulus at zero compression will be:

$$E_c = 9,000(0.75) = 6,750 \text{ psi} \quad (46.5 \text{ MPa})$$

For zero compression and this compression modulus, the linear spring rate is:

$$K_L = \frac{6,750(704)}{0.197} = 24.1 \times 10^6 \text{ lb}_f / \text{in} \quad (4.23 \times 10^6 \text{ N/mm})$$

The resultant deformation of the gasket for this spring rate with the maximum bolt force is:

$$\Delta_{gasket} = \frac{24(F_{bolt})}{K} = \frac{24(23,782)}{4.23 \times 10^6} = 0.135 \text{ mm (0.005 in)}$$

This deformation is approximately 2.7% compression of the gasket. Prototypic seal testing in support of the TRUPACT-II package* has demonstrated that a pressure seal requires a minimum of 10% – 12% compression. Section 3.6, *Squeeze*, of the Parker O-ring Handbook† states that “*The minimum squeeze for all seals, regardless of cross-section should be about 0.2 mm (0.007 inches). The reason is that with a very light squeeze almost all elastomers quickly take 100% compression set.*” Based on these test results and the recommendations of Parker, the outer lid gasket will not form a pressure retaining seal.

* U. S. Department of Energy (DOE), *Safety Analysis Report for the TRUPACT-II Shipping Package*, USNRC Certificate of Compliance 71-9218, U.S Department of Energy, Carlsbad Field Office, Carlsbad, New Mexico.

† ORD 5700A/US, *Parker O-ring Handbook*, 2001, Parker Hannifin Corporation, Lexington, KY.

3. THERMAL EVALUATION

Provides an evaluation of the package to protect the fuel during varying thermal conditions.

3.1. DESCRIPTION OF THERMAL DESIGN

The TN-B1 package is designed to provide thermal protection as described in Subpart F of 10 CFR 71 for transport of two BWR fuel assemblies with negligible decay heat.

Compliance is demonstrated with 10 CFR 71 subpart F in the following subsections. The TN-B1 protects the fuel through the use of an inner and outer container that restricts the exposure of the fuel to external heat loads. The insulated inner container further restricts the heat input to the fuel through its insulation. The fuel requires very little thermal protection since similar fuel has been tested to the 800°C temperature without rupture.

Given negligible decay heat, the thermal loads on the package come solely from the environment in the form of solar radiation for Normal Conditions of Transport (NCT), as described in Section 3.4 or a half-hour, 800°C (1,475°F) fire for Hypothetical Accident Conditions (HAC), described in Section 3.5.

Specific ambient temperatures and solar heat loads are considered in the package thermal evaluations. Ambient temperatures ranging from -40°C to 38°C (-40°F to 100°F) are considered for NCT. The HAC fire event considers an ambient temperature of 38°C (100 F), with solar heat loading (insulation) before and after the HAC half-hour fire event.

Details and assumptions used in the analytical thermal models are described with the thermal evaluations.

3.1.1. *Design Features*

The primary features that affect the thermal performance of the package are 1) the materials of construction, 2) the inner and outer containers and 3) the thermal insulation of the inner container. The stainless sheet metal construction of the structural components of the inner and outer containers influences the maximum temperatures under normal conditions. The material also ensures structural stability under the hypothetical accident conditions as well as provides some protection to the fuel. Likewise the zirconium alloy cladding has also been proven to be stable at the high temperatures potentially seen during the Hypothetical Accident Conditions (HAC).

The multi walled construction of the single walled outer container and the double walled inner container reduces the heat transfer as well as provides additional stability. The multi walled construction also reduces the opportunity for the fire in the accident conditions to impinge directly on the fuel.

The thermal insulation also greatly reduces the heat transfer to the fuel from external sources. The insulation consists of alumina silicate around most of the package plus the use of wood on the ends that both provide some insulation as well as shock absorbing capabilities.

3.1.2. Content's Decay Heat

Since the contents are unirradiated fuel, the decay heat is insignificant.

3.1.3. Summary Tables of Temperatures

Since the decay heat load is negligible, the maximum NCT temperature of 171°F (77°C, 350 K) occurs on the package exterior, and the maximum HAC temperature of 1198°F (648°C, 921 K) occurs at the inner surface of the inner container at the end of the fire. These analyses demonstrate that the TN-B1 package provides adequate thermal protection for the fuel assembly and will maintain the maximum fuel rod temperature well below the fuel rod rupture temperature of 800+°C under all transportation conditions.

3.1.4. Summary Tables of Maximum Pressures

The maximum pressure within the containment, the fuel rods during normal conditions of transport is 1.33 MPa (192.9 psia).

The maximum pressure during the hypothetical accident conditions is 3.50 MPa (508 psia).

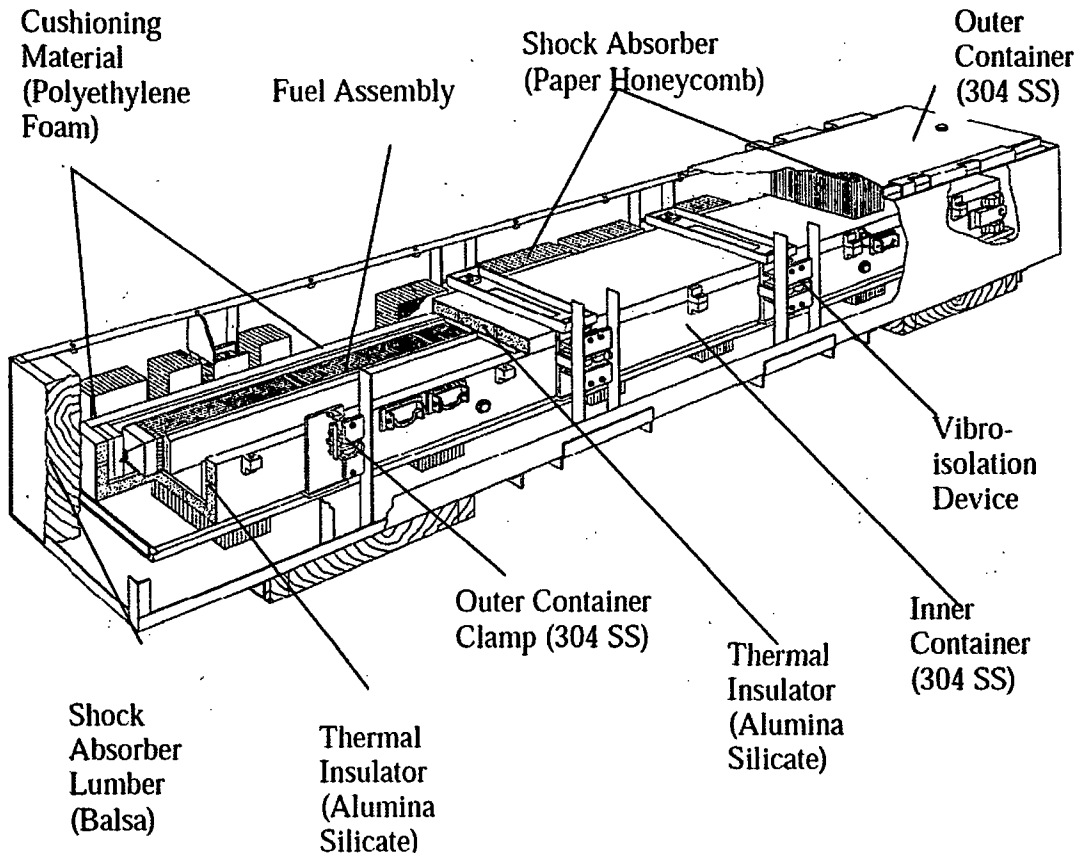


Figure 3-1 Overall View of TN-B1 Package



Security-Related Information
Figure Withheld Under 10 CFR 2.390

Figure 3-2 Transverse Cross-Sectional View of the Inner Container

3.2. MATERIAL PROPERTIES AND COMPONENT SPECIFICATIONS

3.2.1. *Material Properties*

The TN-B1 inner container is constructed primarily of Series 300 stainless steel, wood, and alumina silicate insulation. The void spaces within the inner container are filled with air at atmospheric pressure. The outer container is constructed of series 300 stainless steel, wood, and resin impregnated paper honeycomb. The thermal properties of the principal materials used in the thermal evaluations are presented in Table 3 - 1 and Table 3 - 2. Where necessary, the properties are presented as functions of temperature. Note that only properties for materials that constitute a significant heat transfer path are defined. A general view of the package is depicted in Figure 3-1. A sketch of the inner container transversal cross-section with the dimensions used in the calculation is presented in Figure 3-2.

For the Alumina Silicate, maximum values are specified because the maximum conductivity is the controlling parameter. This is because there is no decay heat in the payload and the only consideration is the material's ability to block of heat transfer to the fuel during the fire event.

Table 3-1 Material Properties for Principal Structural/Thermal Components

Material	Temperature, K	Thermal Conductivity, W/m-K	Specific Heat, J/kg-K	Density, kg/m ³	Notes
Wood	300	0.240	2,800	500	1
Series 300 Stainless Steel	300	15	477	7,900	2
	400	17	515		
	500	18	539		
	600	20	557		
	800	23	582		
	1,000	25	611		
Alumina Silicate Insulation	673	≤0.105	1,046 (Nominal)	250 (Nominal)	3
	873	≤0.151			
	1,073	≤0.198			4
	1,273	≤0.267			4

Notes:

- 1** The material specified for the wood spacers. The properties have been placed with typical values for generic softwood.
- 2** [Reference. 3.6.1.2. p.809, 811, 812, and 820]
- 3** The values shown are based on published data for Unifrax Duraboard LD [Reference 3.6.1.11] and include compensation for the possible variation in test data (see discussion in Section 3.2.1).
- 4** Values at higher temperatures than 1,000 K are linearly extrapolated.

Table 3-2 Material Properties for Air

Temperature (K)	Thermal Conductivity (W/m·K)	Density (kg/m ³)	Specific Heat (J/kg·K)	Coefficient of Kinematic Viscosity ν (m ² /s)	Prandtl Pr
300	0.0267	1.177	1005	15.66 E-06	0.69
310	0.0274	1.141	1005	16.54 E-06	0.69
320	0.0281	1.106	1006	17.44 E-06	0.69
330	0.0287	1.073	1006	18.37 E-06	0.69
340	0.0294	1.042	1007	19.32 E-06	0.69
350	0.030	1.012	1007	20.30 E-06	0.69
360	0.0306	0.983	1007	21.30 E-06	0.69
370	0.0313	0.956	1008	22.32 E-06	0.69
380	0.0319	0.931	1008	23.36 E-06	0.69
390	0.0325	0.906	1009	24.42 E-06	0.69
400	0.0331	0.883	1009	25.50 E-06	0.69
500	0.0389	0.706	1017	37.30 E-06	0.69
600	0.0447	0.589	1038	50.50 E-06	0.69
700	0.0503	0.507	1065	65.15 E-06	0.70
800	0.0559	0.442	1089	81.20 E-06	0.70
900	0.0616	0.392	1111	98.60 E-06	0.70
1000	0.0672	0.354	1130	117.3 E-06	0.70

Source: Reference 3.6.1.2, p.824

3.2.2. Component Specifications

None of the materials used in the construction of TN-B1 package, such as series 300 stainless steel and alumina silicate insulation, are sensitive to temperatures within the range of -40°C to 800°C (-40°F to 1,475 F) that spans the NCT and HAC environment. Stainless steel has a melting point above 1,400°C (2,550 F), and maximum service temperature of 427°C (800 F). Similarly, the ceramic fiber insulation has a maximum operating temperature of 1,300°C (2,372°F). Wood is used as dunnage and as part of the inner package wall in the TN-B1 package. Before being consumed in the HAC fire, the wood would insulate portions of the inner container from exposure to the flames. However, the HAC transient thermal analyses presented herein conservatively neglects the wood's insulating effect, and assumes that all of the wood is consumed in the fire generating heat for all of its total mass.

The temperature limit for the fuel assembly's rods is greater than 800°C (1,472°F), based on the pressure evaluation provided in Section 3.5.3.2.

3.3. GENERAL CONSIDERATIONS

3.3.1. Evaluation by Analysis

The normal conditions of transport thermal conditions are evaluated by closed form calculations. The details of this analysis and supporting assumptions are found in that evaluation. The evaluation finds the maximum temperature for the outside of the package due to the insulation and uses that temperature for the contents of the package.

The transient hypothetical accident conditions are evaluated using an ANSYS finite element model. The model does not take credit for the outer container or the wood used in the inner container. Details of the model and the supporting assumptions maybe found in Section 3.5.

3.3.2. Evaluation by Test

Thermal testing was performed on fuel rods to determine the ability of the cladding (primary containment) to withstand temperatures greater than 800°C. The testing was performed for a range of fuel rods of different diameters, clad thickness and internal pressure. Since some of the current fuel designs for use in the TN-B1 are outside the range of parameters tested, additional thermal analyses have been performed to demonstrate the fuel rod's ability to withstand the HAC fire. In these tests, the fuel rods were heated to various temperatures from 700°C to 900°C for periods over one hour to determine the rupture temperature and pressure of the fuel. It was found that the fuel cladding did not fail at 800°C the temperature of the hypothetical accident conditions. This temperature associated pressure and resulting

stress were used to provide the allowable conditions of the fuel which is used for containment.

3.3.3. Margins of Safety

For the normal condition evaluation the margins of safety are qualitative, based on comparisons to the much higher temperatures the fuel is designed for when it is in service in the reactors. There is no thermal deterioration of the packaging components at normal condition temperatures therefore no margins for the package components are calculated.

The margins of safety for the accident conditions are evaluated in Section 3.5 and are based on the testing discussed in Section 3.3.2.

3.4. THERMAL EVALUATION UNDER NORMAL CONDITIONS OF TRANSPORT

This section presents the results of thermal analysis of the TN-B1 package for the Normal Conditions of Transport (NCT) specified in 10 CFR 71.71. The maximum temperature for the normal conditions of transport is used as input (initial conditions) in the Hypothetical Accident Condition (fire event) analysis.

3.4.1. Heat and Cold

Per 10 CFR 71.71(c)(1), the maximum environmental temperature is 100°F (311 K), and per 10 CFR 71.71(c)(2), the minimum environmental temperature is -40°F (233 K).

Given the negligible decay heat of the fuel assembly, the thermal loads on the TN-B1 package come solely from the environment in the form of solar radiation for NCT as prescribed by 10 CFR 71.71(c)(1). As such, the solar heat input into the package is 800 g·cal/cm² for horizontal surfaces and 200 g·cal/cm² for vertical surfaces for a varying insolation over a 24-hour period).

3.4.1.1. Maximum Temperatures

For the analysis, the applied insolation is modeled transiently as sinusoidal over a 24-hour period, except when the sine function is negative (the insolation level is set to zero). The timing of the sine wave is set to achieve its peak at 12:00 PM and peak value of the curve is adjusted to ensure that the total energy delivered matched the regulatory values (800 g·cal/cm² for horizontal surfaces, 200 g·cal/cm² for vertical surfaces). As such, the total energy delivered in one day by the sine wave model is given by:

$$\int_{6-hr}^{18-hr} Q_{peak} \cdot \sin\left(\frac{\pi t}{12 \cdot hr} - \frac{\pi}{2}\right) dt = \left(\frac{24 \cdot hr}{\pi}\right) \times Q_{peak}$$

Using the expression above for the peak rate of insolation, the peak rates for top and side insolation may be calculated as follows:

Based on these inputs, the maximum NCT temperature on the inside surface of the inner container, as calculated in Appendix 3.6.3, is 350 K (77°C, 171°F).

Given negligible decay heat, the maximum accessible surface temperature of the TN-B1 package in the shade is the maximum environment temperature of 38°C (100°F), which is less than the 50°C (122°F) limit established in 10 CFR 71.43(g) for a non-exclusive use shipment.

3.4.1.2. Minimum Temperatures

The minimum environmental temperature that the TN-B1 package will be subjected to is -40°F, per 10 CFR 71.71(c)(2). Given the negligible decay heat load, the minimum temperature of the TN-B1 package is -40°F.

3.4.2. **Maximum Normal Operating Pressure**

The fuel rods are pressurized with helium to a maximum pressure of 1.145 MPa (absolute pressure (161.7 psia) helium at ambient temperature prior to sealing. Hence, the Maximum Normal Operating Pressure (MNOP) at the maximum normal temperature is:

$$MNOP = (P_1 \frac{T_{max}}{T_{ambient}} = 1.1145 \times \frac{350}{293} = 1.33 \text{ MPa} = 192.9 \text{ psia}$$

Since there is no significant decay heat and the fuel composition is stable, MNOP calculated above would not be expected to change over a one year time period.

3.4.3. **Maximum Thermal Stresses**

Due to the construction of the TN-B1, light sheet metal constructed primarily of the same material, 304 SS, there are no significant thermal stresses. The package is constructed so that there is no significant constraint on any component as it heats up and cools down. The fuel cladding which provides containment is likewise designed for thermal transients, greater than what is found in the normal conditions of transport. The fuel rod is allowed to expand in the package. The fuel within the cladding is also designed to expand without interfering with the cladding.

3.5. THERMAL EVALUATION UNDER HYPOTHETICAL ACCIDENT CONDITIONS

This section presents the results of the thermal analysis of the TN-B1 package for the Hypothetical Accident Condition (HAC) specified in 10 CFR 71.73(c) (4).

For the purposes of the Hypothetical Accident Conditions fire analysis, the outer container of the TN-B1 package is conservatively assumed to be not present during the fire. This allows the outer surface of the inner container to be fully exposed to the fire event. The wood used in the inner container is conservatively assumed to combust completely. By ignoring the outer container and applying the fire environment directly to the inner container, the predicted temperature of the fuel rods is bounded. To provide a conservative estimate of the worst-case fuel rod temperature, the fuel assembly and its corresponding thermal mass are not explicitly modeled as well as the polyethylene foam shock absorber. The maximum fuel rod temperature is conservatively derived from the maximum temperature of the inside surface of the inner stainless steel wall. The analysis considering the insulation and multi-layers of packaging is very conservative because as discussed in Section 3.3.2 the bare fuel has been demonstrated to maintain integrity when exposed to temperatures that equal those found in the hypothetical accident conditions.

Thermal performance of the TN-B1 package is evaluated analytically using a 2-D model that represents a transversal cross-section of the inner container (Figure 3-2) in the region containing the metallic and wood spacers. The 2-D inner container finite element model was developed using the ANSYS computer code [Reference 3.6.1.3]. ANSYS is a comprehensive thermal, structural and fluid flow analysis package. It is a finite element analysis code capable of solving steady state and transient thermal analysis problems in one, two or three dimensions. Heat transfer via a combination of conduction, radiation and convection can be modeled.

The solid entities were modeled in the present analysis with PLANE55 two-dimensional elements and the radiation was modeled using the AUX12 Radiation Matrix method. The developed ANSYS input file is included as Appendix 3.6.2.

The initial temperature distribution in the inner container prior to the HAC fire event is a uniform 375 K conservatively corresponding to the outer surface temperature of the inner container per the normal condition calculations presented in Appendix 3.6.3.

3.5.1. *Initial Conditions*

The environmental conditions preceding and succeeding the fire consist of an ambient temperature of 38 °C (311 K) and insulation per the normal condition thermal analysis. The solar absorptivity coefficient of the outer surface has been increased for the post-fire period to 1 to include changes due to charring of the surfaces during the fire event.

3.5.2. Fire Test Conditions

The Hypothetical Accident Condition fire event is specified per 10 CFR 71.73(c) (4) as a half-hour, 800°C (1,073 K) fire with forced convection. For the purpose of calculation, the value of the package surface absorptivity coefficient (0.8) is selected as the highest value between the actual value of the surface (0.42) and a value of 0.8 as specified in 10 CFR 71.73(c) (4).

A value of 1.0 for the emissivity of the flame for the fire condition is used in the calculation. The rationale for this is that 1.0 maximizes the heating of the package. This value exceeds the minimum value of 0.9 specified in 10 CFR 71.73(c) (4). The Hypothetical Accident Condition (HAC) fire event is specified per 10 CFR 71.73(c)(3) as a half-hour, 800°C (1,475°F) fire with forced convection and an emissivity of 0.9. The environmental conditions preceding and succeeding the fire consist of an ambient temperature of 100 °F and insulation per the NCT thermal analyses.

To model the combustion of the wood, the wood elements of the model are given a heat generation rate based on the high heat value of Western Hemlock of 3630 Btu/lb (8.442×10⁶ J/kg) from Reference 3.6.1.8, Section 7, Table 9. It is conservatively assumed that the entire mass of the wood will burn. Moreover, the wood will burn across its thinnest section from opposite faces. Using data burn rate data for redwood which has approximately the same density as hemlock [3.6.1.8], each face will burn 5 mm at a minimum rate of 0.543 mm/min [Reference 3.6.1.10] resulting in a 9.2 minute time of combustion. This conservatively results in the longest burn time for the hemlock, and the greatest effect on temperature. The resulting heat generation rate in the wood spacers is equal to:

$$\dot{Q} = (8.42 \times 10^6) \times (500 \text{ kg} / \text{m}^3) / (9.2 \text{ s} \times 60) = 7.63 \times 10^6 \text{ W/m}^3/\text{s}$$

3.5.2.1. Heat Transfer Coefficient during the Fire Event

During a HAC hydrocarbon fire, the heating gases surrounding the package will achieve velocities sufficient to induce forced convection on the surface of the package. Peak velocities measured in the vicinity of the surfaces were under 10 m/s [Reference 3.6.1.4].

The heat transfer coefficient takes the form [Reference 3.6.1.4, p. 369]:

$$h = k/D \cdot C \cdot (u \cdot D/u)^m \cdot Pr^{1/3}$$

Where:

- D: average width of the cross-section of the inner container (0.373 m)
- k: thermal conductivity of the fluid
- u: kinematic viscosity of the fluid

u: free stream velocity

C, m: constants that depend on the Reynolds number ($Re=u \cdot D/u$)

Pr: Prandtl number for the fluid

The property values of k, u and Pr are evaluated at the film temperature, which is defined as the mean of the wall and free stream fluid temperatures. At the start of the fire the wall temperature is 375 K (101.7°C, 215°F) and the stream fluid temperature is 1,073 K (1,475°F). The film temperature is therefore 710.5 K, and the property values for air at this temperature (interpolated from Table 3 - 2) are $k=0.0509$ W/m·K, $u=66.84E-06$ m²/s and $Pr=0.70$. Assuming a maximum stream velocity of 10 m/s this yields a Reynolds number of 55.8E03. At this value of Re, the constants C and n are 0.102 and 0.675 respectively [Reference 3.6.1.4, Table 7.3].

$$h = \frac{0.0509 \cdot 0.102 \cdot \left(10 \cdot \frac{0.373}{66.84 \times 10^{-6}}\right)^{0.675} \cdot (0.70)^{1/3}}{0.373}$$

$$h = 19.8 \text{ W/m}^2 \text{ K}$$

A value of 19.8 W/m²·K was conservatively used in the analysis of the regulatory fire.

3.5.2.2. Heat Transfer Coefficient during Post-Fire Period

During the post-fire period of the HAC, it is conservatively assumed that there is negligible wind and that heat is transferred from the inner container to the environment via natural convection. Natural heat transfer coefficients from the outer surface of the square inner container are calculated as follows.

Reference 3.6.1.4 recommends the following correlations for the Nusselt number (Nu) describing natural convection heat transfer to air from heated vertical and horizontal surfaces:

Vertical heated surfaces [Reference 3.6.1.4, p. 493]:

$$N_u = \left(0.825 + \frac{0.387 \times (Gr \times Pr)^{\frac{1}{6}}}{\left(1 + \left(0.492/n\right)^{9/16}\right)^{\frac{8}{27}}}\right)^2$$

For entire range of $Ra=Gr \times Pr$ (9)

Where:

Nu: Nusselt number

Gr: Grashof number

Pr: Prandtl number

Horizontal heated surfaces facing upward [Reference 3.6.1.4, p.498]:

$$Nu = 0.54 \times (Gr \times Pr)^{1/4} \text{ for } (10^4 < Gr \times Pr < 10^7) \quad (10)$$

$$Nu = 0.15 \times (Gr \times Pr)^{1/3} \text{ for } (10^7 < Gr \times Pr < 10^{11}) \quad (11)$$

and, for horizontal heated surfaces facing downward:

$$Nu = 0.27 \times (Gr \times Pr)^{1/4} \text{ for } (10^5 < Gr \times Pr < 10^{10}) \quad (12)$$

The correlations for the horizontal surfaces are calculated using a characteristic length defined by the relation $L=A/P$, where A is the horizontal surface area and P is the perimeter [Reference 3.6.1.4, p. 498]. The calculated characteristic length for the horizontal surfaces of the inner container is $L=0.209$ m ($A=2.14812$ m² and $P=10.278$ m).

The following convective heat transfer coefficients (Table 3 - 1) have been calculated using Eq. (5), (6), (9), (10), (11) and (12). The corresponding characteristic length used in calculating the Nusselt number for each surface is also used in Eq. 5 for calculating the heat transfer coefficient. The thermal properties of air have been evaluated at the mean film temperature $(= (T_s + T_{\text{ambient}})/2)$.

The effects of solar radiation are included during the post-fire period by specifying the equivalent heat flow for each node of the surfaces exposed to fire for an additional 3.5 hours, i.e. the fire starts at the time of the peak temperature in the inner container (8 hours after sunrise) and is 0.5 hours in duration. This results in an additional 3.5 hours of solar insolation. Using the peak rates calculated in section 3.4.1.1, the nodal heat flows at 2:30 PM are equal to:

$$q'_{top} = \frac{1,218 \frac{W}{m^2} \left(\sin \left(\frac{\pi \times (6 + 8.5)}{12} - \frac{\pi}{2} \right) \right) (0.459 \text{ m})}{(155 - 1)} = 2.88 \text{ W/m}$$

$$q'_{side} = \frac{305 \frac{W}{m^2} \left(\sin \left(\frac{\pi \times 14.5}{12} - \frac{\pi}{2} \right) \right) (0.281 \text{ m})}{(99 - 1)} = 0.69 \text{ W/m}$$

Where 0.459 m is the width of the inner container, 0.281 m is its height, and the model is 155 nodes in width by 99 nodes in height. For the remaining 3.5 hours of solar insolation, these heat fluxes are conservatively applied as bounding constant values rather than varying with time.

The solar absorptivity coefficient of the outer surface is conservatively assumed to be 1. The duration of the post-fire period has been extended to 12.5 hr to investigate the cool-down of the inner container.

3.5.3. Maximum Temperatures and Pressure

3.5.3.1. Maximum Temperatures

The peak fuel rod temperature, which is conservatively assumed to be the same as the inner wall temperature of the package, response over the course of the HAC fire scenario is illustrated in Figure 3-3. The temperature reaches its maximum point of 921 K or 648°C (1198 F) at the end of the fire or 1,800 seconds after the start of the fire. This peak temperature occurs at top corners of the inner wall.

The maximum temperature even when applied to the fuel directly is well below the maximum temperature the fuel can withstand. Similar fuel with no thermal protection has been tested in fire conditions at over 800°C (1,475°F) for more than 60 minutes without failures.

3.5.3.2. Maximum Internal Pressure

The maximum pressure for the fuel can be determined by considering that the fuel is pressurized initially with helium. As the fuel is heated, the internal pressure in the cladding increases. By applying the perfect gas law the pressure can be determined and the resulting stresses in the cladding can be determined. Since the temperatures can be well above the normal operating range of the fuel the cladding performance can best be determined by comparison to test data.

Similar fuel with similar initial pressures has been heated in an oven to over 800°C for over an hour without failures (Reference 3.6.1.6). The fuel that was tested in the oven was pressurized with 10 atmospheres of helium. When heated to the 800°C it had an equivalent pressure of:

$$P_{max} = (P_1) \frac{T_{max}}{T_{ambient}} = 1.1145 MPa \times \frac{1,073}{293} = 4.08 MPa = 592 psia$$

This results in an applied load to the cladding of 3.98 MPa or 577.3 psig. The fuel that was tested had an outer diameter of 0.4054 inch (10.30 mm). Since the fuel when tested to

850°C had some ruptures but did not rupture at 800°C when held at those temperatures for 1 hour, the stresses at 800°C are used as the conservative allowable stress. Both the tested fuel and the fuels to be shipped in the TN-B1 have similar zirconium cladding. The stress generated in the cladding of the test fuel is:

$$\rho = \frac{pr}{t} = \frac{3.98MPa \times 4.56mm}{0.584mm} = 31.1MPa = 4,510 \text{ psia}$$

Recognizing that the properties of the fuel cladding degrade as the temperature increases the above calculated stress is conservatively used as the allowable stress for the fuel cladding for the various fuels to be shipped. The fuel is evaluated at the maximum temperature the inner wall of the inner container sees during the Hypothetical Accident Condition thermal event evaluated above. Table 3 - 5 shows the maximum pressure for each type of fuel and the resulting stress and margin. The limiting design properties of the fuel, maximum cladding internal diameter, minimum cladding wall thickness and initial pressurization for each type of fuel are considered in determining the margin of safety. Positive margins are conservatively determined for each type of fuel demonstrating that containment would be maintained during the Hypothetical Accident events. The minimum cladding thickness does not include the thickness of the liner if used.

The results of the transient analysis are summarized in Table 3 - 4. The temperature evolution during the transient in three representative locations on the inner wall and one on the outer wall is included. The maximum temperature on the inner wall is 921 K (648°C, 1198°F) and is reached at the upper inner corners of the container, 1,800 seconds after the beginning of the fire. The graphic evolution of the temperatures listed in Table 3 - 4 is represented in Figure 3-3. Representative plots of the isotherms at various points in time are depicted in Figure 3-4 through Figure 3-7.

The temperatures and resulting pressures are within the capabilities of the fuel cladding as shown by test. Therefore the fuel cladding and closure welds maintain containment during the Hypothetical Accident Conditions.

The temperatures and resulting pressures are within the capabilities of the fuel cladding as shown by test. Therefore the fuel cladding and closure welds maintain containment during the Hypothetical Accident Conditions.

3.5.4. Accident Conditions for Fissile Material Packages for Air Transport

Approval for air transport is not requested for the TN-B1.

Table 3-3 Convection Coefficients for Post-fire Analysis

T_s (surface temperature)		T_{ambient}		H (vertical surface)	h (horizontal surface facing upward)	h (horizontal surface facing downward)
°F	K	°F	K	(W/m ² ·K)	(W/m ² ·K)	(W/m ² ·K)
150	338.71	100	311	4.68	5.19	2.34
200	366.48	100	311	5.61	6.34	2.74
250	394.26	100	311	6.18	7.05	2.99
300	422.04	100	311	6.60	7.55	3.17
350	449.82	100	311	6.90	7.92	3.30
400	477.59	100	311	7.13	8.18	3.41
600	588.71	100	311	7.64	8.74	3.67
900	755.37	100	311	8.00	9.07	3.89
1,375	1,019.26	100	311	8.25	9.17	4.09

**Table 3-4 Calculated Temperatures for Different Positions on the Walls of
the Inner Container Walls**

Time (s)	Inner Wall Temperature (top right corner) (K)	Inner Wall Temperature (bottom) (K)	Inner Wall Temperature (top) (K)	Outer Wall Temperature (K)
0.1	375	375	375	377
911	750	667	546	1,062
1,800	921	821	696	1,067
1,900	918	823	710	807
2,000	905	817	723	686
2,200	868	797	742	583
2,600	803	761	760	509
3,268	723	715	758	463
4,280	639	662	727	437
27,973	354	335	369	378
45,000	349	324	358	377

Table 3-5 Maximum Pressure

Parameter	Units	8 X 8 Fuel	9 X 9 Fuel	10 X 10 Fuel
Initial Pressure	MPa absolute	0.608	1.1145	1.1145
Fill temperature	°C	20	20	20
Temperature during HAC	°C	648	648	648
Outside Diameter Maximum	mm	12.5	11.46	10.52
	inches	.492	.4512	.4142
Minimum Allowable Cladding Thickness	inches	0.0268	0.0224	0.0205
	mm	.68	0.570	0.520
Cladding Inside Diameter Maximum	mm	11.14	10.32	9.48
	inches	.439	.406	.373
Pressure @ HAC	MPa(absolute)	1.91	3.50	3.50
	Psia	277	508	508
Applied Pressure @ HAC	MPa	1.81	3.40	3.40
	Psig	262	493	493
Stress Pr/t	MPa	14.82	30.8	31.0
	Psi	2149	4,467	4,498
Margin	(allowed stress/ actual stress)-1	1.10	0.01	0.003
Max allowed cladding	Inside Radius/Thickness	20.20	9.14	9.14

Note: Table values for cladding thickness and diameters are for example purposes and represent current limiting fuel designs. However, all fuel to be shipped must have a maximum pre-pressure times the maximum Inside Radius/Thickness product of $9.14 \times 1.1145 \text{ MPa} = 10.18653 \text{ MPa}$ or less. Thus, all products must meet the maximum product of allowed pressure multiplied by Inside Radius/Thickness of 10.18653 MPa .

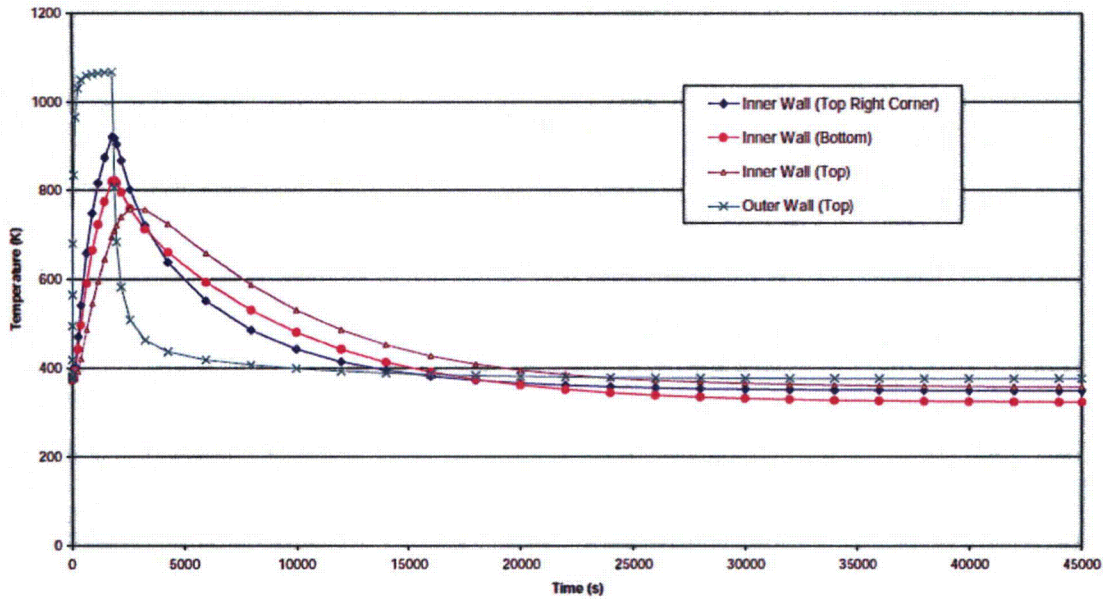


Figure 3-3 Calculated Temperature Evolution During Transient

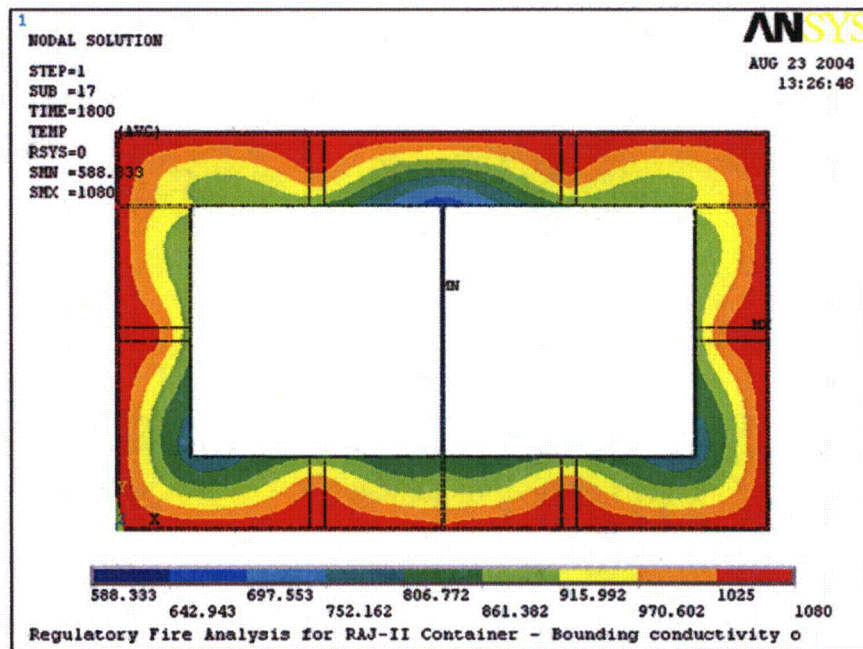


Figure 3-4 Calculated Isotherms at the End of Fire Phase (1,800 s)

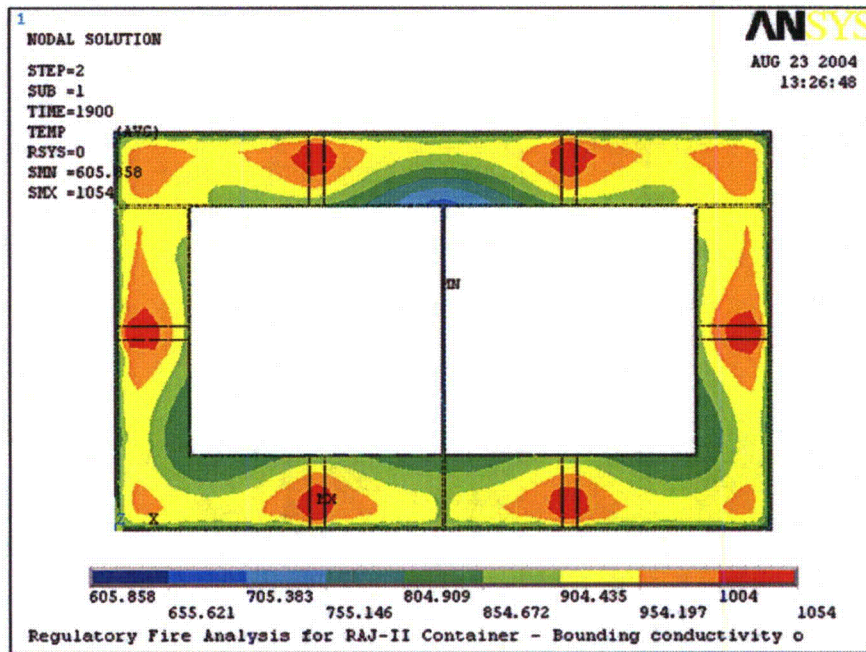


Figure 3-5 Calculated Isotherms at 100s After the End of Fire

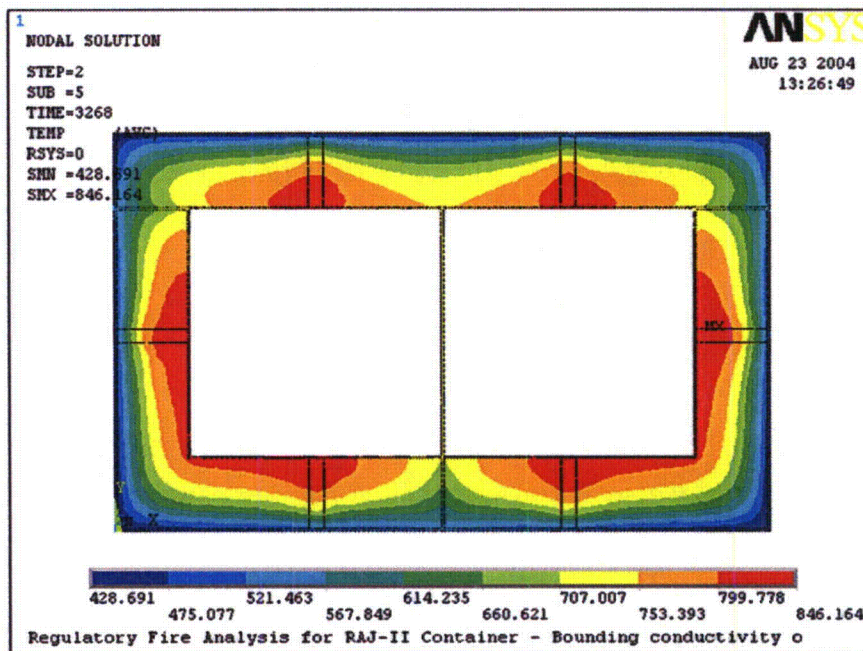


Figure 3-6 Calculated Isotherms at 1,468 s After the End of Fire

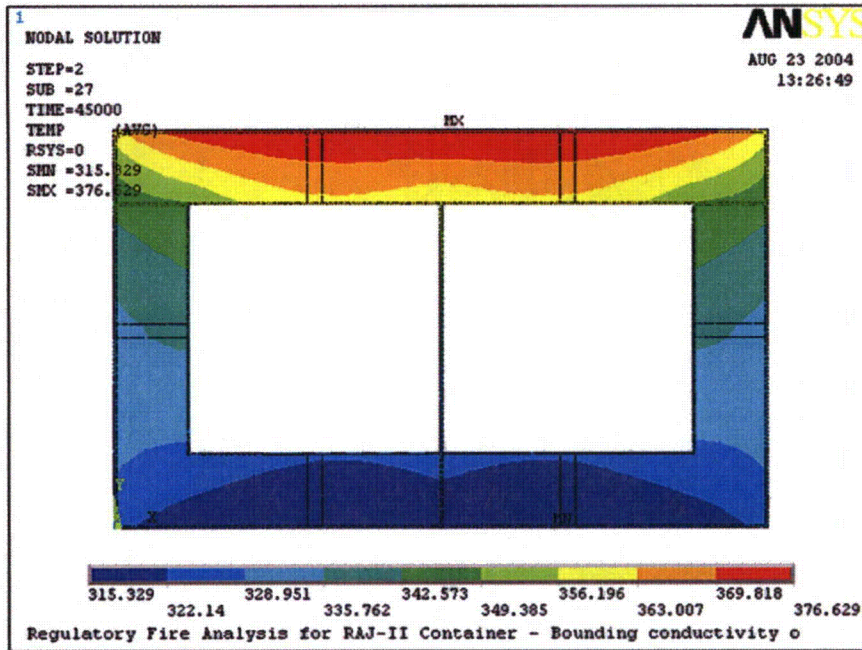


Figure 3-7 Calculated Isotherms at 12 hr After the End of Fire



3.6. APPENDIX

3.6.1. *References*

- 3.6.1.1. 10 CFR 71, Packaging and Transportation of Radioactive Material
- 3.6.1.2. Mills, A.F., Heat Transfer, Irwin, Inc., Homewood, Illinois, 1992
- 3.6.1.3. ANSYS Finite Element Computer Code, Version 5.6, ANSYS, Inc., 2000
- 3.6.1.4. McCaffery, B.J., Purely Buoyant Diffusion Flames – Some Experimental Results, Report PB80-112113, U.S. National Bureau of Standards, Washington, D.C., 1979
- 3.6.1.5. Incropera, F.P., Dewitt, D.P., Fundamentals of Heat and Mass Transfer, John Wiley and Sons, Inc., New York, New York, 1996
- 3.6.1.6. GNF-2 Fuel Rod Response to An Abnormal Transportation Event (proprietary)(30 Minute Fire)
- 3.6.1.7. Handbook of Heat Transfer, Warren M. Rohsenow, James P. Hartnett, McGraw Hill book company.
- 3.6.1.8. Standard Handbook for Mechanical Engineers, Baumeister , Marks, McGraw Hill book company, Seventh edition.
- 3.6.1.9. Thermal Properties of Paper, PTN149, Charles Green, Webster New York, 2002 (<http://www.frontiernet.net/~charmard/>).
- 3.6.1.10. Tran, H.C., and White, R. H., Burning Rate of Solid Wood Measured in a Heat Release Calrimeter, Fire and Materials, Vol. 16, pp 197-206, 1992.
- 3.6.1.11. “Pactec Specification: Regarding Global Nuclear Fuel Specification for Alumina Silicate for use in the RAJ-II Shipping container,” Unifrax Corporation, 6/3/04.

3.6.2. ANSYS Input File Listing

Listing of the ANSYS input file (file: model_fl_heat.inp)

finl	K,4,0.0015,0.0015,0,
/clear	K,5,0.136,0.0015,0,
/filnam,model_fl_heat,	K,6,0.146,0.0015,0,
/outp,model_fl_heatout,out	K,7,0.2285,0.0015,0,
/PREP7	K,8,0.2305,0.0015,0,
/TITLE, Regulatory Fire Analysis for RAJ-II Container - Bounding conductivity of Alumina	K,9,0.313,0.0015,0,
/UNITS,SI	K,10,0.323,0.0015,0,
/SHOW,JPEG	K,11,0.4575,0.0015,0,
!* !*set element types	K,12,0.459,0.0015,0,
!* ET,1,PLANE55,1	K,13,0.0015,0.0515,0,
ET,2,LINK32	K,14,0.0515,0.0515,0,
ET,3,MATRIX50,1	K,15,0.136,0.0515,0,
!* !* define keypoints	K,16,0.146,0.0515,0,
!* K,1,0,0,0,	K,17,0.2285,0.0515,0,
K,2,0.459,0,0,	K,18,0.2305,0.0515,0,
K,3,0,0.0015,0,	K,19,0.313,0.0515,0,
	K,20,0.323,0.0515,0,
	K,21,0.4075,0.0515,0,
	K,22,0.4575,0.0515,0,
	K,23,0.0515,0.0525,0,
	K,24,0.0525,0.0525,0,



K,25,0.2285,0.0525,0,

K,26,0.2305,0.0525,0,

K,27,0.4065,0.0525,0,

K,28,0.4075,0.0525,0,

K,29,0.0525,0.0705,0,

K,30,0.0705,0.0705,0,

K,31,0.2105,0.0705,0,

K,32,0.2285,0.0705,0,

K,33,0.2305,0.0705,0,

K,34,0.2485,0.0705,0,

K,35,0.3885,0.0705,0,

K,36,0.4065,0.0705,0,

K,37,0.0015,0.1335,0,

K,38,0.0515,0.1335,0,

K,39,0.4075,0.1335,0,

K,40,0.4575,0.1335,0,

K,41,0.0015,0.1435,0,

K,42,0.0515,0.1435,0,

K,43,0.4075,0.1435,0,

K,44,0.4575,0.1435,0,

K,45,0.0705,0.1975,0,

K,46,0.2105,0.1975,0,

K,47,0.2485,0.1975,0,

K,48,0.3885,0.1975,0,

K,49,0.0525,0.2155,0,

K,50,0.060,0.2115,0,

K,51,0.066,0.2055,0,

K,52,0.2175,0.2055,0,

K,53,0.2235,0.2115,0,

K,54,0.2285,0.2155,0,

K,55,0.2305,0.2155,0,

K,56,0.2355,0.2115,0,

K,57,0.2415,0.2055,0,

K,58,0.393,0.2055,0,

K,59,0.399,0.2115,0,

K,60,0.4065,0.2155,0,

K,61,0.,0.2275,0,

K,62,0.0015,0.2275,0,

K,63,0.0515,0.2275,0,

K,64,0.0525,0.2275,0,

K,65,0.4065,0.2275,0,

K,66,0.4075,0.2275,0,

K,67,0.4575,0.2275,0,

K,68,0.459,0.2275,0,

K,69,0.,0.2285,0,

K,70,0.0525,0.2285,0,

K,71,0.06,0.2285,0,

K,72,0.2235,0.2285,0,



K,73,0.2285,0.2285,0,	SAVE
K,74,0.2305,0.2285,0,	!*
K,75,0.2355,0.2285,0,	!* define material properties
K,76,0.399,0.2285,0,	!*
K,77,0.4065,0.2285,0,	!*
K,78,0.459,0.2285,0,	!* STAINLESS STEEL (SS304)
K,79,0.,0.2295,0,	!*
K,80,0.0015,0.2295,0,	MP,DENS,1,7900
K,81,0.136,0.2295,0,	MPTEMP,1,300,400,500,600,800,1000
K,82,0.146,0.2295,0,	MPDATA,kxx,1,1,15,17,18,20,23,25
K,83,0.313,0.2295,0,	MPDATA,c,1,1,477,515,539,557,582,611
K,84,0.323,0.2295,0,	!*
K,85,0.4575,0.2295,0,	!* THERMAL INSULATOR
K,86,0.459,0.2295,0,	!*
K,87,0.,0.2795,0,	MP,DENS,2,260
K,88,0.0015,0.2795,0,	MP,C,2,1046
K,89,0.136,0.2795,0,	MPTEMP
K,90,0.146,0.2795,0,	MPTEMP,1,673,873,1073,1273
K,91,0.313,0.2795,0,	MPDATA,KXX,2,1,0.105,0.151,0.198,0.267 IMAX VALUES
K,92,0.323,0.2795,0,	!*
K,93,0.4575,0.2795,0,	!*
K,94,0.459,0.2795,0,	!* WOOD (generic softwood)
K,95,0.,0.281,0,	!*
K,96,0.459,0.281,0,	!*



UIMP,3,NUXY, , , ,	FITEM,2,12
UIMP,3,ALPX, , , ,	FITEM,2,11
UIMP,3,REFT, , , ,	FITEM,2,10
UIMP,3,MU, , , ,	FITEM,2,9
UIMP,3,DAMP, , , ,	FITEM,2,8
UIMP,3,DENS, , , 500,	FITEM,2,7
UIMP,3,KXX, , , 0.24,	FITEM,2,6
UIMP,3,C, , , 2800,	FITEM,2,5
UIMP,3,ENTH, , , ,	FITEM,2,4
UIMP,3,HF, , , ,	FITEM,2,3
UIMP,3,EMIS, , , ,	A,P51X
UIMP,3,QRATE, , , ,	FLST,2,7,3
UIMP,3,VISC, , , ,	FITEM,2,3
UIMP,3,SONC, , , ,	FITEM,2,4
UIMP,3,MURX, , , ,	FITEM,2,13
UIMP,3,MGXX, , , ,	FITEM,2,37
UIMP,3,RSVX, , , ,	FITEM,2,41
UIMP,3,PERX, , , ,	FITEM,2,62
I*	FITEM,2,61
I* define areas	A,P51X
I*	FLST,2,5,3
FLST,2,12,3	FITEM,2,4
FITEM,2,1	FITEM,2,5



FITEM,2,14	FITEM,2,19
FITEM,2,13	FITEM,2,18
A,P51X	A,P51X
FLST,2,4,3	FLST,2,4,3
FITEM,2,5	FITEM,2,9
FITEM,2,6	FITEM,2,10
FITEM,2,16	FITEM,2,20
FITEM,2,15	FITEM,2,19
A,P51X	A,P51X
FLST,2,4,3	FLST,2,5,3
FITEM,2,6	FITEM,2,10
FITEM,2,7	FITEM,2,11
FITEM,2,17	FITEM,2,22
FITEM,2,16	FITEM,2,21
A,P51X	FITEM,2,20
FLST,2,4,3	A,P51X
FITEM,2,7	FLST,2,7,3
FITEM,2,8	FITEM,2,11
FITEM,2,18	FITEM,2,12
FITEM,2,17	FITEM,2,68
A,P51X	FITEM,2,67
FLST,2,4,3	FITEM,2,44
FITEM,2,8	FITEM,2,40

A,P51X	FITEM,2,19
FLST,2,5,3	FITEM,2,20
FITEM,2,13	FITEM,2,21
FITEM,2,14	FITEM,2,28
FITEM,2,23	FITEM,2,27
FITEM,2,38	FITEM,2,26
FITEM,2,37	FITEM,2,25
A,P51X	FITEM,2,24
FLST,2,8,3	FITEM,2,23
FITEM,2,23	A,P51X
FITEM,2,24	FLST,2,8,3
FITEM,2,29	FITEM,2,25
FITEM,2,49	FITEM,2,26
FITEM,2,64	FITEM,2,33
FITEM,2,63	FITEM,2,55
FITEM,2,42	FITEM,2,74
FITEM,2,38	FITEM,2,73
A,P51X	FITEM,2,54
FLST,2,14,3	FITEM,2,32
FITEM,2,14	A,P51X
FITEM,2,15	FLST,2,8,3
FITEM,2,16	FITEM,2,27
FITEM,2,17	FITEM,2,28



FITEM,2,43	A,P51X
FITEM,2,66	FLST,2,4,3
FITEM,2,65	FITEM,2,41
FITEM,2,60	FITEM,2,42
FITEM,2,36	FITEM,2,63
A,P51X	FITEM,2,62
FLST,2,5,3	A,P51X
FITEM,2,21	FLST,2,4,3
FITEM,2,22	FITEM,2,43
FITEM,2,40	FITEM,2,44
FITEM,2,39	FITEM,2,67
FITEM,2,28	FITEM,2,66
A,P51X	A,P51X
FLST,2,4,3	SAVE
FITEM,2,37	FLST,2,6,3
FITEM,2,38	FITEM,2,61
FITEM,2,42	FITEM,2,62
FITEM,2,41	FITEM,2,63
A,P51X	FITEM,2,64
FLST,2,4,3	FITEM,2,70
FITEM,2,39	FITEM,2,69
FITEM,2,40	A,P51X
FITEM,2,44	FLST,2,6,3



FITEM,2,66	FITEM,2,79
FITEM,2,67	A,P51X
FITEM,2,68	FLST,2,4,3
FITEM,2,78	FITEM,2,79
FITEM,2,77	FITEM,2,80
A,P51X	FITEM,2,88
FLST,2,18,3	FITEM,2,87
FITEM,2,69	A,P51X
FITEM,2,70	FLST,2,4,3
FITEM,2,71	FITEM,2,80
FITEM,2,72	FITEM,2,81
FITEM,2,73	FITEM,2,89
FITEM,2,74	FITEM,2,88
FITEM,2,75	A,P51X
FITEM,2,76	FLST,2,4,3
FITEM,2,77	FITEM,2,81
FITEM,2,78	FITEM,2,82
FITEM,2,86	FITEM,2,90
FITEM,2,85	FITEM,2,89
FITEM,2,84	A,P51X
FITEM,2,83	FLST,2,4,3
FITEM,2,82	FITEM,2,82
FITEM,2,81	FITEM,2,83



FITEM,2,90	FITEM,2,89
A,P51X	FITEM,2,90
FLST,2,4,3	FITEM,2,91
FITEM,2,83	FITEM,2,92
FITEM,2,84	FITEM,2,93
FITEM,2,92	FITEM,2,94
FITEM,2,91	FITEM,2,96
A,P51X	FITEM,2,95
FLST,2,4,3	A,P51X
FITEM,2,84	SAVE
FITEM,2,85	I*
FITEM,2,93	I* glue all areas
FITEM,2,92	I*
A,P51X	FLST,2,31,5,ORDE,2
FLST,2,4,3	FITEM,2,1
FITEM,2,85	FITEM,2,-31
FITEM,2,86	AGLUE,P51X
FITEM,2,94	I*
FITEM,2,93	/PNUM,KP,0
A,P51X	/PNUM,LINE,0
SAVE	/PNUM,AREA,1
FLST,2,10,3	/PNUM,VOLU,0
FITEM,2,87	/PNUM,NODE,0



/PNUM,SVAL,0

/NUMBER,0

!*

/PNUM,ELEM,0

/REPLOT

!* APLOT

FLST,5,14,5,ORDE,10

FITEM,5,1

FITEM,5,-2

FITEM,5,6

FITEM,5,10

FITEM,5,12

FITEM,5,-15

FITEM,5,21

FITEM,5,-24

FITEM,5,30

FITEM,5,-31

ASEL,S,,P51X

/REPLOT

FLST,5,14,5,ORDE,10

FITEM,5,1

FITEM,5,-2

FITEM,5,6

FITEM,5,10

FITEM,5,12

FITEM,5,-15

FITEM,5,21

FITEM,5,-24

FITEM,5,30

FITEM,5,-31

CM,_Y,AREA

ASEL,,,P51X

CM,_Y1,AREA

CMSEL,S,_Y

!*

CMSEL,S,_Y1

AATT, 1,, 1, 0

CMSEL,S,_Y

CMDELE,_Y

CMDELE,_Y1

!* ALLSEL,ALL

FLST,5,11,5,ORDE,11

FITEM,5,3

FITEM,5,5

FITEM,5,7

FITEM,5,9



FITEM,5,11	I*
FITEM,5,16	CMSEL,S,_Y1
FITEM,5,19	AATT, 2, , 1, 0
FITEM,5,-20	CMSEL,S,_Y
FITEM,5,25	CMDELE,_Y
FITEM,5,27	CMDELE,_Y1
FITEM,5,29	I* ALLSEL,ALL
ASEL,S, , ,P51X	FLST,5,6,5,ORDE,6
FLST,5,11,5,ORDE,11	FITEM,5,4
FITEM,5,3	FITEM,5,8
FITEM,5,5	FITEM,5,17
FITEM,5,7	FITEM,5,-18
FITEM,5,9	FITEM,5,26
FITEM,5,11	FITEM,5,28
FITEM,5,16	ASEL,S, , ,P51X
FITEM,5,19	FLST,5,6,5,ORDE,6
FITEM,5,-20	FITEM,5,4
FITEM,5,25	FITEM,5,8
FITEM,5,27	FITEM,5,17
FITEM,5,29	FITEM,5,-18
CM,_Y,AREA	FITEM,5,26
ASEL, , , ,P51X	FITEM,5,28
CM,_Y1,AREA	CM,_Y,AREA



ASEL, , , P51X	CHKMSH,'AREA'
CM_Y1,AREA	CMSEL,S,_Y
CMSEL,S,_Y	!*
!*	AMESH,_Y1
CMSEL,S,_Y1	!*
AATT, 3, , 1, 0	CMDELE,_Y
CMSEL,S,_Y	CMDELE,_Y1
CMDELE,_Y	CMDELE,_Y2
CMDELE,_Y1	!*
!*	/PNUM,KP,0
ALLSEL,ALL	/PNUM,LINE,0
SAVE	/PNUM,AREA,0
!*	/PNUM,VOLU,0
!* mesh the areas	/PNUM,NODE,0
!*	/PNUM,TABN,0
ALLSEL,ALL	/PNUM,SVAL,0
APLOT	/NUMBER,0
SMRT,10	!*
FLST,5,31,5,ORDE,2	/PNUM,MAT,1
FITEM,5,1	/REPLOT
FITEM,5,-31	ALLSEL,ALL
CM_Y,AREA	!* select nodes on the outer surfaces
ASEL, , , P51X	NSEL,S,LOC,X,0,.0001

NSEL,A,LOC,Y,0.,0.0001	EMIS,1,0.8,
NSEL,A,LOC,Y,0.2809,0.281	STEF,5.67e-08,
!* define element for outer surface	GEOM,1,0,
!* TYPE, 2	SPACE,50000,
MAT, 1	!* VTYPE,0,20,
NPLOT	MPRINT,0
esurf	WRITE,rad
!* !* create space node	!* ALLSEL,ALL
N,50000,0.3,0.5,0,...	FINISH
!* select the nodes and elements that	/PREP7
!* make up the radiation surfaces	!* !* TYPE, 3
ESEL,S,TYPE,,2	MAT, 1
NSLE,R	REAL,
NSEL,S,LOC,X,0.,0.0001	ESYS, 0
NSEL,A,LOC,X,0.4589,0.459	SECNUM,
NSEL,A,LOC,Y,0.,0.0001	TSHAP,LINE
NSEL,A,LOC,Y,0.2809,0.281	!* SE,rad, , ,0.0001,
ESLN,R	ESEL,S,TYPE,,2
NSEL,a,node,,50000	
FINISH	
!* define radiation matrix	



SAVE

!* Define effective heat transfer coefficients for

!* post-fire (vert-20,horiz-up-25, horiz-down-35) MPTEMP

MPTEMP,1,338.71,366.48,394.26,422.04,449.82,477.59,

MPTEMP,7,588.71,755.37,1019.26,

MPDATA,HF,20,1,4.68,5.61,6.18,6.60,6.90,7.13,

MPDATA,HF,20,7,7.64,8.00,8.25,

MPDATA,HF,25,1,5.19,6.34,7.05,7.55,7.92,8.18,

MPDATA,HF,25,7,8.74,9.07,9.17,

MPDATA,HF,35,1,2.34,2.74,2.99,3.17,3.30,3.41,

MPDATA,HF,35,7,3.67,3.89,4.09,

MPLIST

SAVE

FINISH

/SOLU

!* setup convection coefficients for fire case

ALLSEL,ALL

NSEL,S,LOC,X,0.,0.0001

NSEL,A,LOC,X,0.4589,0.459

NSEL,A,LOC,Y,0.,0.0001

NSEL,A,LOC,Y,0.2809,0.281

SF,ALL,CONV,19.8,1073

NSEL,ALL

!.....

!* Test Heat Generation modelling wood burning

ASEL,S,MAT,,3

ESLA,S

/GO

!*

*DIM,burning,TABLE,5,1,0,TIME

!*

BFE,ALL,HGEN, , %burning%

!*

!*****BFA,ALL,HGEN, %burning%

*SET,BURNING(1,0,1) , 0.0

*SET,BURNING(2,0,1) , 0.1

*SET,BURNING(3,0,1) , 0.2

*SET,BURNING(4,0,1) , 552.2

*SET,BURNING(5,0,1) , 552.3

*SET,BURNING(1,1,1) , 0.0

*SET,BURNING(2,1,1) , 0.0

*SET,BURNING(3,1,1) , 7.63e6

*SET,BURNING(4,1,1) , 7.63e6

*SET,BURNING(5,1,1) , 0.0

ALLSEL,ALL

SAVE



```

|.....
|.....
D,50000,TEMP, 1073
    
```

```

|.....
|.....
TUNIF,375,          IREVISÉ FOR NEW NCT
NUMBER (IC OUTER SHELL)
    
```

```

|.....
|.....
SAVE
    
```

```

|*
|* set up run parameters for fire case
    
```

```

|*
ANTYPE,4
    
```

```

|*
TRNOPT,FULL
    
```

```

LUMPM,0
    
```

```

|*
TIME,1800
    
```

```

AUTOTS,-1
    
```

```

DELTIM,0.1,0.1,600,1
    
```

```

KBC,1
    
```

```

|*
TSRES,ERASE
    
```

```

|*
    
```

```

|*
LSWRITE,2,

|*

|* change boundary conditions for post fire case

|* ALLSEL,ALL

NSEL,S,LOC,X,0.000,0.0001

NSEL,A,LOC,X,0.4589,0.459

SF,ALL,CONV,-20, 311

ALLSEL,ALL

NSEL,S,LOC,Y,0.0,0.0001

SF,ALL,CONV,-35, 311

ALLSEL,ALL

NSEL,S,LOC,Y,0.2809,0.281

SF,ALL,CONV,-25, 311

ALLSEL,ALL

D,50000,TEMP,311

|*

|* apply solar heat flux

|*

ALLSEL,ALL

|* select vertical lines and nodes on the left side

nse|,s,loc,x,0

IFLST,5,4,4,ORDE,4
    
```



IFITEM,5,18

IFITEM,5,76

IFITEM,5,94

IFITEM,5,97

ILSEL,S,,P51X

INSL,S,1

IFLST,2,97,1,ORDE,9

IFITEM,2,12

IFITEM,2,17

IFITEM,2,56

IFITEM,2,70

IFITEM,2,72

IFITEM,2,447

IFITEM,2,-521

IFITEM,2,2039

IFITEM,2,-2055

/GO

!*

F,all,HEAT,0.69

ALLSEL,ALL

!* select lines and nodes on the right side

nsl,s,loc,x,.459,.460

IFITEM,5,35

IFITEM,5,77

IFITEM,5,86

IFITEM,5,108

ILSEL,S,,P51X

INSL,S,1

IFLST,2,97,1,ORDE,9

IFITEM,2,3

IFITEM,2,27

IFITEM,2,57

IFITEM,2,63

IFITEM,2,78

IFITEM,2,795

IFITEM,2,-869

IFITEM,2,2240

IFITEM,2,-2256

/GO

!*

F,all,HEAT,0.69

!* select nodes on upper surface

ALLSEL,ALL

NSEL,S,LOC,Y,0.2809,0.281



IFITEM,2,79	/SOLU
IFITEM,2,-80	/STATUS,SOLU
IFITEM,2,2257	LSSOLVE,2,3,1
IFITEM,2,-2409	FINISH
/GO	SAVE
!*	/POST26
F,all,HEAT,2.88	!*
ALLSEL,ALL	!* plot temperature evolution at specified nodes
!* set up run parameters for post fire	!*
TIME,14400 lwas 9000	!*
AUTOTS,-1	!* Inner wall, top right corner
DELTIM,0.5,0.1,2000,1	NSOL,2,58,TEMP, ,inn_wtr
KBC,1	!*
!*	!*
TSRE S,ERASE	!* inner wall, bottom mid position
!*	NSOL,3,1185,TEMP, ,inn_wbm
TINTP,0.005, , ,-1,0.5,-1	!*
!*	!*
OUTRES,ALL,ALL,	!* inner wall, top mid position
TIME,45000	NSOL,4,1720,TEMP, ,inn_wtm
DELTIM,100,10,2000,1	!*
LSWRITE,3,	!*
SAVE	!* outer wall, top mid position



```

!*
!*
PLVAR,2,3,4,5,, , , , ,
PRVAR,2,3,4,5,,
FINISH
!* plot Isothermes at certain moments in time
/POST1
SET,LIST,2
SET, , , 1, , , , 17,
/EFACE,1
!*
PLNSOL,TEMP, ,0,
FINISH
/POST1
SET, , , 1, , , , 18,
/EFACE,1
!*
PLNSOL,TEMP, ,0,
SET, , , 1, , , , 20,
/EFACE,1
!*
PLNSOL,TEMP, ,0,
SET, , , 1, , , , 22,

```

```

!*
PLNSOL,TEMP, ,0,
SET, , , 1, , , , 30,
/EFACE,1
!*
PLNSOL,TEMP, ,0,
SET, , , 1, , , , 43,
/EFACE,1
!*
PLNSOL,TEMP, ,0,
SET,PREVIOUS
FINISH

|*****NEW
allsel
/post1

Tmax=0
TimeMAX=0
nmax=0

nsel,s,loc,x,0.0525,.4065,
nsel,r,loc,y,0.0525,.2285,

```



nplot	*endif
*GET, ncount, NODE, 0, count	set,next
cm,lcnodes,node	*enddo
set,1,1	tmax=tmax
*do,t,1,46	nmax=nmax
tmaxn=0	timemax=timemax
cmsel,s,lcnodes	allsel
*do,i,1,ncount	/show,term
nodei=node(0,0,0)	/post1,
*get,temp1,node,node1,temp	! Reverse Video
*if,temp1,gt,tmaxn,then	/rgb,index,100,100,100,0
tmaxn=temp1	/rgb,index,80,80,80,13
nmaxn=nodei	/rgb,index,60,60,60,14
*endif	/rgb,index,0,0,0,15
nsel,u,,node1	set,1,17
*enddo	p1nsol,temp
*if,tmaxn,gt,tmax,then	/image,save,fig3-4(1800),wmf
tmax=tmaxn	set,2,1
nmax=nmaxn	/replot
	/image,save,fig3-5(1900),wmf

```

/replot

/image,save,fig3-6(3268),wmf

set,last

/replot

/image,save,fig3-7(45000),wmf

|*****NEW

|/EXIT,ALL
    
```

3.6.3. NCT Transient Analysis

The transient analysis uses a one dimensional model of the vertical face of the packaging (thinner part of the packaging) as described in the figure below:

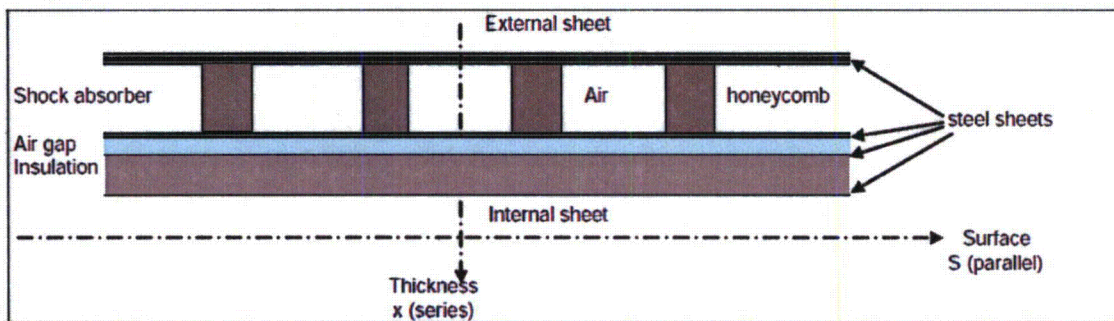


Figure 3-8 Vertical Face Model

The heat flux is set as a sine wave function:

$$Q = \pi/2 \times 800 \sin(\omega \theta) \quad 0 < (\omega \theta) < \pi$$

$$Q = 0 \quad \pi < (\omega \theta) < 2\pi$$

With: Q = heat energy in g-cal/cm²

$$\omega = 2\pi / 24 \text{ pulsation}$$

θ = time in hour

Note that the peak value of $(\pi/2 \times 800)$ complies with 10CFR 71.71(c)(1), conservatively assuming the highest value of 800 g-cal/cm² for the insolation.

$$\int_0^{24 \text{ hr}} Q d\theta = 800 \text{ g-cal/cm}^2$$

Assuming that at each time step, the external surface of the package achieves steady state conditions, the energy balance between the solar heat load, and the convection and radiation exchanges (see section 3.4.1.1), results time dependant solution for the external surface temperature.

The result is plotted on the Figure 3.6.3-1 (blue curve) and is close to a sine wave function. Indeed, when calculating the energy balance equation, it appears that the convention term represents 65% of the exchange, and the radiation term 35%. As the convection term is linearly proportional to the external temperature, this curve is nearly proportional to the solar heat load.

Assume that the external temperature is a sine function with respect to time as follows (and as plotted on Figure 3.6.3-1):

$$T_s = T_{\text{avg}} + T^+ \sin(\omega \theta)$$

$$\text{With: } T_{\text{avg}} = 420 \text{ K} \quad (\text{maximum value of the blue curve})$$

$$T^+ = (420 - 311) = 109 \text{ K}$$

The system is thus modeled as a one dimensional model of conduction, with a sinusoidal wave temperature on the external surface as a boundary condition.

Using equation 4-22 of the "Handbook of Heat Transfer", Reference 3.6.1.7, the heat equation through a layer of material leads to a temperature of:

$$T(x,\theta) = T_{avg} + T^+ \exp(-L x/d) \sin[L(2 L Fo - x/d)]$$

Using the reference's notation, it becomes:

$$T(x,\theta) = T_{avg} + T^+ \exp[-(\omega/2\alpha)^{1/2} x] \sin[\omega \theta - (\omega/2\alpha)^{1/2} x]$$

With:

- $\alpha = K / \rho C =$ thermal diffusivity,
- $K =$ conductivity of material,
- $\rho =$ density of material,
- $C =$ specific heat of the material,
- $x =$ thickness thru the material.

Through each layer of material "i" in the TN-B1 packaging, the temperature of the external surface is so decreased by a factor η and lagged by a factor φ :

$$\eta_i = \exp[-(\omega/2\alpha_i)^{1/2} x_i]$$

$$\varphi_i = (\omega/2\alpha_i)^{1/2} x_i$$

Table 3.6.3-1 summarizes the material properties for each component layer through the thickness of the model.

Equivalent properties of material

The thermal properties (K, ρ , C) of a material equivalent to materials of a system are following the rules:

$$\text{Material in series } K = \frac{e_T}{\sum_i \frac{e_i}{K_i}}$$

$$\text{Material in parallel } K = \frac{1}{S_T} \sum_i S_i K_i$$

$$\text{Material in series } \rho C = \frac{\sum_i \rho_i C_i e_i}{e_T}$$

$$\text{Materials in parallel } \rho C = \frac{\sum_i \rho_i C_i S_i}{S_T}$$

The maximum temperature of the cavity surface of the packaging resulting from solving the one dimensional model occurs at ten hours into the cycle and is equal to 350 K. The maximum temperature on the outer surface of the inner container occurs at 8 hours and is equal to 375K. Temperatures are summarized on Table 3.6.3-2.

Table 3-6 Material properties

Component	Material	Thickness x (m)	Surface S (m)	Conductivity K (W/m-K)	Density r (kg/m ³)	Specific heat C (J/kg-K)	Diffusivity a (m ² /s)
OC outer sheet	steel	0.004	-	15	7900	477	3.981E-06
Honeycomb ¹	paper	-	0.084 ¹	0.13595	700 ¹	1531 ¹	3.932E-07
	air	-	0.916 ¹	0.0267	1.177	1005	
Shock absorbers	honeycomb	0.108	0.64	0.0359	60	1522	1.737E-06
	air		3.186	0.0267	1.177	1005	
OC inner sheet	steel	0.001	-	15	7900	477	3.981E-06
Air gap	air	0.01	-	0.0267	1.177	1005	2.257E-05
IC outer sheet	steel	0.0015	-	15	7900	477	3.981E-06
IC insulation	Alumina	0.048	-	0.09	250	1046	3.442E-07
IC inner sheet	steel	0.001	-	15	7900	477	3.981E-06

- ¹ The honeycomb is assumed to be a combination of paper and air in a parallel system (see below). The proportion of paper and air is determined by the ratio of the densities:

$$\text{Honeycomb density} = 60 \text{ kg/m}^3$$

$$\text{Paper density} = 700 \text{ kg/m}^3 \quad 8.4\%$$

$$\text{Air density} = 1.177 \text{ kg/m}^3 \quad 91.6\%$$

Thermal properties of resin impregnated kraft paper (density, conductivity, specific heat) are conservatively assumed to correspond to that of ordinary paper according to Reference 3.6.1.9.

Table 3-7 NCT Temperatures Through the Package Thickness

Time (hour)	Surface temp sin wave Ts	T thru OC Outer	T thru Honeycomb and	T thru OC Inner	T thru Air Gap	T thru IC Inner Shell	T thru Alumina Silicate
0	311	311	311	311	311	311	311
0.5	325	324	311	311	311	311	311
1	339	338	311	311	311	311	311
1.5	353	351	311	311	311	311	311
2	366	364	312	312	311	311	311
2.5	377	376	321	320	320	319	311
3	388	386	329	329	328	327	311
3.5	397	396	337	337	336	335	311
4	405	404	345	345	343	343	312
4.5	412	410	352	352	350	350	317
5	416	415	358	358	357	356	322
5.5	419	418	364	364	362	362	327
6	420	419	368	368	367	367	332
6.5	419	418	372	372	371	370	336
7	416	415	375	375	373	373	340
7.5	412	411	376	376	375	375	343
8	405	405	377	376	376	375	346
8.5	397	397	376	376	375	375	348
9	388	388	374	374	373	373	349
9.5	377	378	371	371	371	371	350
10	366	366	367	367	367	367	350
10.5	353	353	362	362	362	362	350
11	339	340	357	357	357	357	349
11.5	325	326	350	350	350	350	347
12	311	312	343	343	343	343	344
12.5	311	311	335	335	336	336	342
13	311	311	327	327	328	328	338
13.5	311	311	318	319	319	320	334
14	311	311	311	311	311	311	330
14.5	311	311	311	311	311	311	325
15	311	311	311	311	311	311	320
15.5	311	311	311	311	311	311	315
16	311	311	311	311	311	311	311
16.5	311	311	311	311	311	311	311

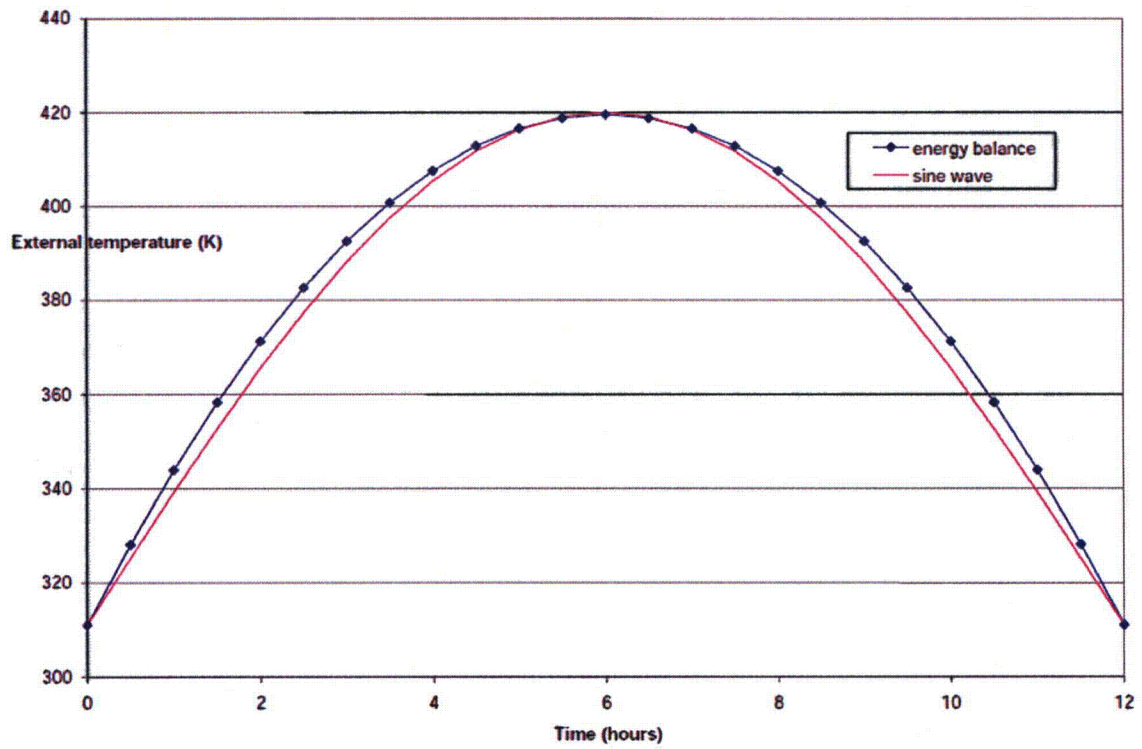


Figure 3-9 Comparison Between Energy Equation Solution with a Sine Wave Equation

4. CONTAINMENT

4.1. DESCRIPTION OF THE CONTAINMENT SYSTEM

4.1.1. *Containment Boundary*

TN-B1 container is limited to use for transporting low enriched uranium, nuclear reactor fuel assemblies and rods. The radioactive material is bound in sintered ceramic pellets having very limited solubility and has minimal propensity to suspend in air. The pellets are sintered at temperatures greater than 1,600°C. These pellets are further sealed into zirconium alloy cladding to form the fuel rod portion of each assembly. The primary containment boundary for the TN-B1 package is the fuel cladding. Design and fabrication details for this cladding are provided in Section 1.2.3. The containment system includes the ceramic sintered pellet, clad in zirconium tubes which are contained in a stainless steel box which is contained in another stainless steel box.

There are no penetrations in the fuel cladding when shipped. The fuel cladding after loading with the pellets is pressurized with helium and end plugs are welded on to close the rod. These welds are designed to withstand the rigorous operating environment of a nuclear reactor. The fuel is leak tested to demonstrate that it is leak tight ($<1 \times 10^{-7}$ atm-cc/s).

4.1.2. *Special Requirements for Plutonium*

This section is not applicable since the package is not being used for plutonium shipments.

4.2. GENERAL CONSIDERATIONS

4.2.1. *Type A Fissile Packages*

The Type A fissile package is constructed, and prepared for shipment so that there is no loss or dispersal of the radioactive contents and no significant increase in external surface radiation levels and no substantial reduction in the effectiveness of the packaging during normal conditions of transport. The fissile material is bound as a ceramic pellet and contained in a zirconium fuel rod. These rods are leak tested prior to shipment to assure their integrity. Chapter 6.0 demonstrates that the package remains subcritical under normal and hypothetical accident conditions.

4.2.2. *Type B Packages*

The Type B fissile package is constructed, and prepared for shipment so that there is no loss or dispersal of the radioactive contents and no significant increase in external surface

radiation levels and no substantial reduction in the effectiveness of the packaging during normal conditions of transport.

The package satisfies the quantified release rate of 10 CFR 71.51 by having a release rate less than $10^{-6} A_2/\text{hr}$ as demonstrated below.

$$A_2 = 0.17 \text{ Ci, therefore } 10^{-6} A_2 = 1.7 \times 10^{-7} \text{ Ci/hr}$$

The mass density of UO_2 in an aerosol from NUREG/CR-6487, page 17 is $9 \times 10^{-6} \text{ g/cm}^3$. Specific Activity of fuel material is $1.4 \times 10^{-5} \text{ Ci/g UO}_2$ (550kg $\text{UO}_2/7.7 \text{ Ci}$).

Leak rate at $1 \times 10^{-7} \text{ atm-cm}^3/\text{s}$ ($3.6 \times 10^{-4} \text{ cm}^3/\text{hr}$) is equal to $1 \times 10^{-6} \text{ atm-cm}^3/\text{s}$ ($3.6 \times 10^{-3} \text{ cm}^3/\text{h}$) when pressurized to 10 atm. Assuming that the pressure is further increased due to temperature the leak rate is assumed to increase by an additional factor of 10 so that it is equal to $3.6 \times 10^{-2} \text{ cm}^3/\text{h}$.

$$\begin{aligned} \text{Release rate} &= 3.6 \times 10^{-2} \text{ cm}^3/\text{hr} \times 1.4 \times 10^{-5} \text{ Ci/g UO}_2 \times 9 \times 10^{-6} \text{ g/cm}^3 \\ &= 4.5 \times 10^{-12} \text{ Ci/h} \end{aligned}$$

Much less than the $1.7 \times 10^{-7} \text{ Ci/hr}$ limit.

4.3. CONTAINMENT UNDER NORMAL CONDITIONS OF TRANSPORT (TYPE B PACKAGES)

The nature of the contained radioactive material and the structural integrity of the fuel rod cladding including the closure welds are such that there will be no release of radioactivity under normal conditions of transport. The welded close containment boundary is not affected by any of the normal conditions of transport as demonstrated in the previous chapters. The pressurization that could be seen by the containment boundary is far below the normal conditions the fuel experiences while in service.

4.4. CONTAINMENT UNDER FOR HYPOTHETICAL ACCIDENT CONDITIONS (TYPE B PACKAGES)

The sintered pellet form of the radioactive material and the integrity of the fuel rod cladding are such that there will be no substantial release of radioactivity under the Hypothetical Accident Conditions. Before and after the accident condition testing the rods were helium leak tested demonstrating leak tightness. Similar fuel rods have been tested at temperatures and resulting pressures that will be seen by fuel shipped in the TN-B1.

10 CFR 71.51 requires that no escape of other radioactive material exceeding a total amount A_2 in 1 week, and no external radiation dose rate exceeding 10 mSv/h (1 rem/h) at 1 m (40 in) from the external surface of the package. The following qualitative assessment demonstrates that the performance requirement of 10 CFR 71.51(a)(2) will be satisfied.

Table 1-4 shows the calculated A_2 for the mixture of the maximum radionuclide content in the package is 0.17 Ci. The total radioactivity in the package using the maximum isotopic values is 7.7 Ci. The mass of UO_2 equivalent to an activity of 7.7 Ci is 550 kg (275 kg UO_2 /assembly x 2 assemblies) which yields a mass to activity ratio of 71.4 kg UO_2 /Ci. The mass equivalent A_2 is therefore 2.1 kg UO_2 .

Following the drop test, fuel rods were leak tested and shown to have a very low leak rate of He at a rate of $5.5 \times 10^{-6} \text{ cm}^3/\text{s}$. Over one week this is equal to 3.3 cm^3 ($5.5\text{E-}6 \text{ cm}^3/\text{s} \times 6.05\text{E}5 \text{ s/wk} = 3.3 \text{ cm}^3$). Conservatively assuming that the density of the radioactive material is $10\text{g}/\text{cm}^3$ and using the A_2 mass above of 2,100 g of UO_2 , the UO_2 would have a volume of 210 cm^3 . This is much greater than the volume leaked. This calculation is extremely conservative since the UO_2 would predominantly stay in a ceramic form and not be available for dispersion.

Test fuel rods as described in Section 2.0 have been baked at 800°C for over 30 minutes and did not leak.

Additionally, the large mass, 2,100 g, of material required to exceed the A_2 would require a catastrophic failure of the rod, significant leak of the inner and outer container.

Dose rates are less than the 10mSv/hr under any condition because of the low specific activity and low abundance of gamma emitters in the fuel.

Based on this evaluation, it is demonstrated that the package meets the containment requirements of 10 CFR 71.51

4.5. LEAKAGE RATE TESTS FOR TYPE B PACKAGES

During manufacturing each fuel rod is He leak tested to demonstrate that it is leak tight ($<1 \times 10^{-7} \text{ atm-cc/s}$). There are no leak rate requirements for the inner and outer packaging.

4.6. APPENDIX

None